ARMY RESEARCH LABORATORY

Hydrocode Simulation of Flexilinear Shaped Charge Jet Penetration Into an Explosive Filled Cylinder

George A. Gazonas
Steven B. Segletes
Carl V. Paxton
Joseph W. Gardiner

ARL-TR-976

March 1996

NOTICES

REPORT DOCUMENTATION PAGE

Form Approved
OMB No. 0704-0188

1. AGENCY USE ONLY *(Leave blank)*

2. REPORT DATE
March 1996

3. REPORT TYPE AND DATES COVERED
Final, April 1994–April 1995

4. TITLE AND SUBTITLE
Hydrocode Simulation of Flexilinear Shaped Charge Jet Penetration Into an Explosive Filled Cylinder

5. FUNDING NUMBERS
4G015413R6

6. AUTHOR(S)
George A. Gazonas, Steven B. Segletes, Carl V. Paxton, and Joseph W. Gardiner

7. PERFORMING ORGANIZATION NAME(S) AND ADDRESS(ES)
U.S. Army Research Laboratory
ATTN: AMSRL-WT-PD
Aberdeen Proving Ground, MD 21005-5066

8. PERFORMING ORGANIZATION REPORT NUMBER
ARL-TR-976

9. SPONSORING/MONITORING AGENCY NAME(S) AND ADDRESS(ES)

10. SPONSORING/MONITORING AGENCY REPORT NUMBER

11. SUPPLEMENTARY NOTES

12a. DISTRIBUTION/AVAILABILITY STATEMENT
Approved for public release; distribution is unlimited.

12b. DISTRIBUTION CODE

13. ABSTRACT *(Maximum 200 words)*

This report presents the results of a combined numerical and experimental investigation of the penetration of a flexilinear shaped demolition charge into an explosive-filled, thin-walled aluminum cylinder. Computations and experiments were conducted using both CompB and LX-14 as the explosive fill in the aluminum cylinder. The 225 grains per foot (gpf) flexilinear shaped charge (FLSC) was composed of CH-6 high explosive encased in a seamless lead sheath liner. The numerical computations were conducted before the experiments using the Eulerian hydrocode CTH. The explosives encased in the cylinder were expected to detonate near the surface of the cylinder due to either a jet tip impact mechanism, or a liner "slap" mechanism. The hydrocode simulations show that neither of these mechanisms will initiate a detonation in the explosives in the geometry considered. However, minor decomposition occurred in the CompB simulation on the cylinder's symmetry axis. The LX-14 simulation predicts complete detonation of the explosive after initiation on the axis of the cylinder. The detonation initiates by superposition of shock waves as they converge upon the cylinder's symmetry axis. The simulations are qualitatively verified by experiments insofar as the CompB explosive did not detonate, whereas the LX-14 explosive did detonate.

14. SUBJECT TERMS
flexilinear shaped charge, CTH, hydrocode modeling, CompB, LX-14, detonation

15. NUMBER OF PAGES
93

16. PRICE CODE

17. SECURITY CLASSIFICATION OF REPORT	18. SECURITY CLASSIFICATION OF THIS PAGE	19. SECURITY CLASSIFICATION OF ABSTRACT	20. LIMITATION OF ABSTRACT
UNCLASSIFIED	UNCLASSIFIED	UNCLASSIFIED	UL

INTENTIONALLY LEFT BLANK.

ACKNOWLEDGMENTS

This work was supported by the Naval Explosive Ordnance Disposal (NAVEOD) Technology Center, Indian Head, MD, under U.S. Army Research Laboratory (ARL) XO/WO/JO 4G015-413-R6. The authors would like to acknowledge the overall assistance of Mr. Atul Patel and Mr. Richard Gold of NAVEOD with regards to the flexilinear shaped charge demolition problem. Thanks also go to Mr. Todd Bjerke (ARL) and Mr. Richard Gold for their constructive reviews.

INTENTIONALLY LEFT BLANK.

TABLE OF CONTENTS

		Page
	ACKNOWLEDGMENTS	iii
	LIST OF FIGURES	vii
1.	INTRODUCTION	1
2.	COMPUTATIONS	3
2.1	Computational Results	5
3.	EXPERIMENTS	10
4.	CONCLUSIONS	11
5.	REFERENCES	13
	APPENDIX A: COMPB SIMULATION INPUT DECK	15
	APPENDIX B: COMPB COMPUTATIONAL RESULTS	25
	APPENDIX C: LX-14 SIMULATION INPUT DECK	51
	APPENDIX D: LX-14 COMPUTATIONAL RESULTS	61
	DISTRIBUTION LIST	87

INTENTIONALLY LEFT BLANK.

LIST OF FIGURES

Figure		Page
1.	Photograph of the flexilinear shaped charge	1
2.	Critical dimensions of the FLSC	2
3.	Axisymmetric problem geometry, a) FLSC centered 0.5 in (12.7 mm) above bare explosive (indirect impact configuration), and b) FLSC centered over encased explosive (direct impact configuration)	3
4.	Axisymmetric geometry used in FLSC computations	4
5.	Cross section through the FLSC	4
6.	Adiabatic flow stress vs. equivalent plastic strain for aluminum (7075-T6), copper, and lead at ambient temperature and pressure	6
7.	Hugoniot for copper, aluminum, and lead	6
8.	Hypothetical leading edge of jet tip as it cuts through explosive cross section from 10 μs through 35 μs after initiation	7
9.	Detonation scenarios by jet tip impact, and liner "slap"	8
10.	Critical impact velocity as a function of projectile diameter	9
11.	Photograph of test configuration (Figure 3a) showing FLSC surrounding aluminum cylinder	10
12.	Photograph of crater on interior wall of RHA test fixture formed by impact from thin copper disk	11

INTENTIONALLY LEFT BLANK.

1. INTRODUCTION

Military demolition operations use a variety of shaped charge geometries (e.g., cylindrical, linear, curvilinear, and flexilinear) for the clearance of obstacles and barriers, the destruction of facilities and materiel, the construction of roads and trenches, and in land clearance and quarrying. The flexilinear shaped charge (FLSC) is commonly used in explosive ordnance disposal (EOD) as a means to sever the projectile from the body of an explosive-filled warhead. In this study, the Navy was interested in determining if the CTH hydrocode predictions of possible "go" or "no-go" detonation scenarios are verified by experiment. The FLSC used in this study consists of a continuous core, filled with CH-6 explosive, that is encased in a seamless lead sheath. The FLSC is available in 4-ft lengths with a density designation that ranges from 20 to 600 grains per foot (gpf). The density designation for the FLSC used in this study is 225 gpf (see Figure 1).

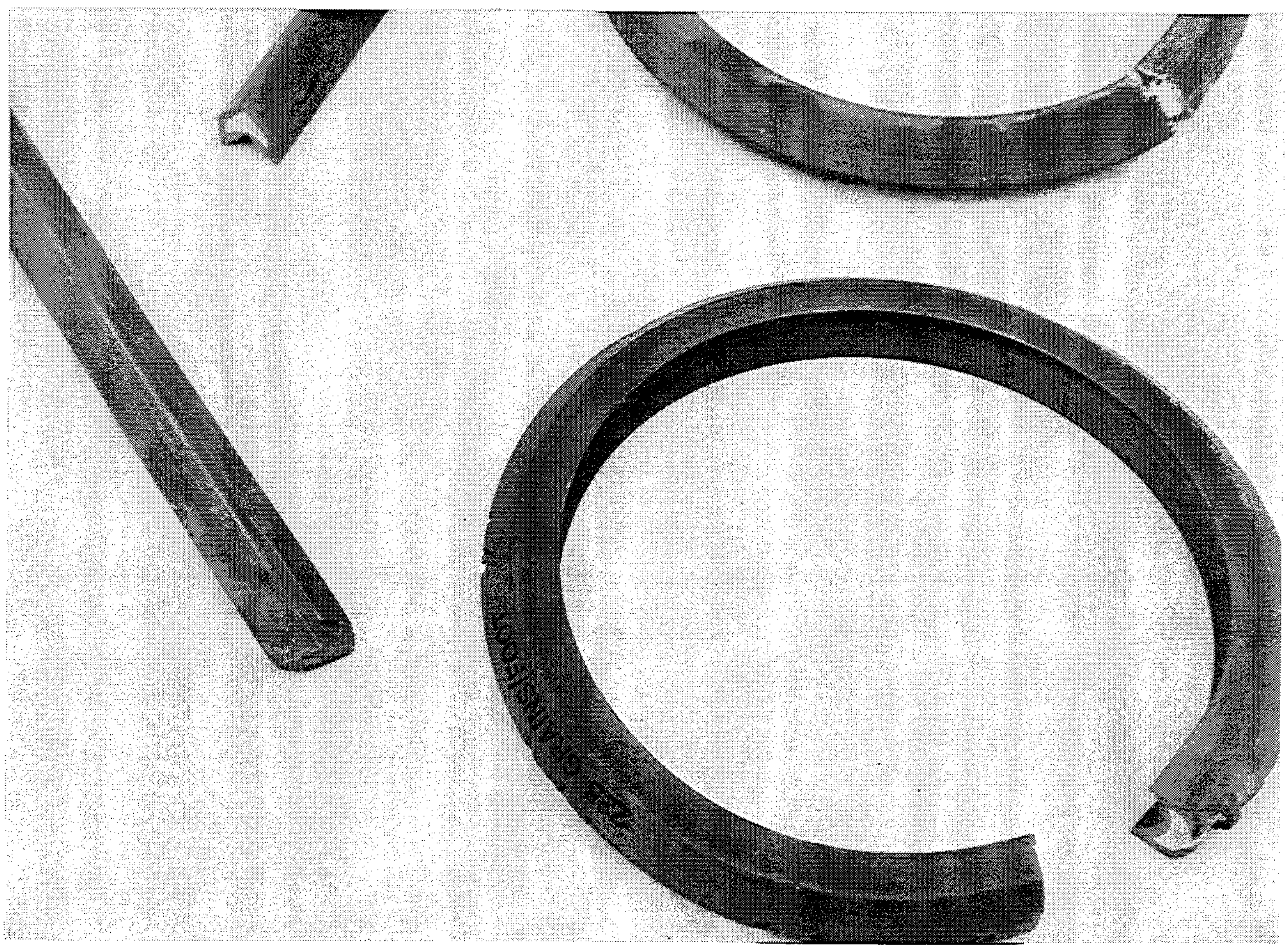

Figure 1. Photograph of the flexilinear shaped charge.

The FLSC is typically wrapped around the warhead and detonated at a single point using a blasting cap. The detonation wave travels around the circumference of the warhead and forms an inwardly directed shaped charge jet which severs the warhead into two pieces. The nominal dimensions of the FLSC used in this study (Figure 2) are: A = 90°, B = 0.240 in (6.1 mm), C = 0.480 in (12.2 mm), D = 0.450 in (11.43 mm), and E = 48.00 in (1,219.2 mm) (see Department of the Navy EODB/Department of the Army TM/U.S. Air Force TO 60A-2-1-51 1992).

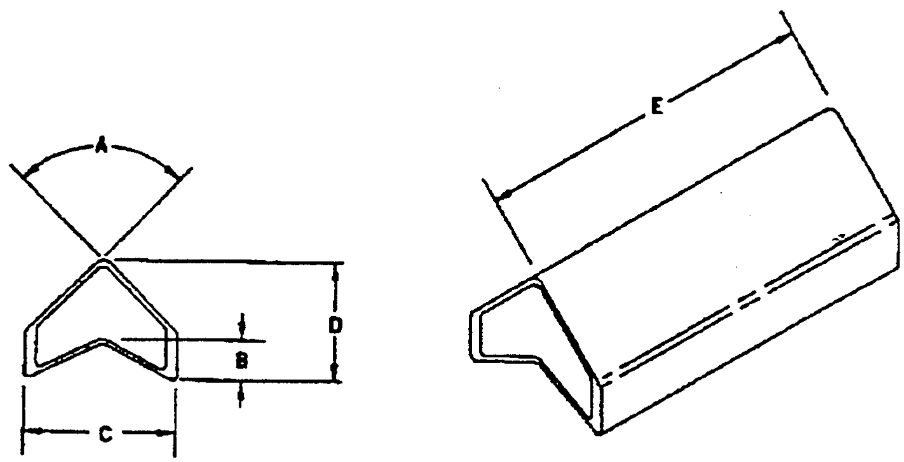

Figure 2. Critical dimensions of the FLSC (Department of the Navy EODB/Department of the Army TM/U.S. Air Force TO 60A-2-1-51 1992).

The Eulerian hydrocode CTH (McGlaun et al. 1988) is used in this study to model the penetrative and detonative performance of the FLSC as it collides into a thin-walled aluminum cylinder filled with either CompB and LX-14 high explosive (HE). Numerical simulations were conducted first, followed by experiments, in an attempt to evaluate the predictive capability of the hydrocode. Two different problem geometries were considered and are illustrated in Figure 3. In the first problem (Figure 3a), we want to determine if the explosive will detonate by impact from flying lead liner fragments. In the second problem (Figure 3b), the FLSC axis is centered directly over the explosive, which is encased in a thin-walled aluminum cylinder, and capped by thin copper discs (endcaps). In the second problem, we expected the explosive to detonate due to, 1) impact by the small diameter, high-velocity shaped charge jet tip, or 2) impact by the large-diameter, low-velocity liner. However, the hydrocode computations show that the LX-14 explosive detonates through shock-wave superposition at a location on the center axis of

the model. This prediction is qualitatively supported by experiment. Neither the hydrocode nor the experiment produced a detonation in the CompB model problem.

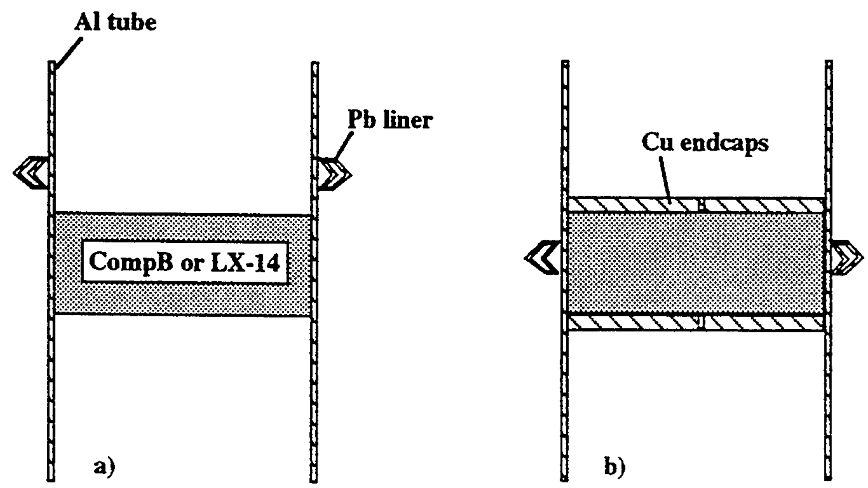

Figure 3. Axisymmetric problem geometry, a) FLSC centered at 0.5 in (12.7 mm) above bare explosive (indirect impact configuration), and b) FLSC centered over encased explosive (direct impact configuration).

2. COMPUTATIONS

Computations are performed using the Eulerian hydrocode, CTH (McGlaun et al. 1988), that has been primarily used in the analysis of problems involving large material distortions. We employed a two-dimensional, axisymmetric Eulerian description of the material body (Figure 4), wherein computational cells are fixed in space and quantities such as mass, momentum, and energy flux across cell boundaries. The Eulerian mesh density consisted of 200 and 182 cells in the x- and y-directions, respectively. The aluminum cylinder that encases the explosive is 6 in (152 mm) long, 3⅞ in (98.4 mm) in outer diameter, and is 1/16 in (1.59 mm) thick. The HE fill consists of cast CompB or pressed LX-14, 1 in (25.4 mm) thick, and 3¾ in (95.25 mm) in diameter. The copper endcaps are ⅜ in (9.5 mm) thick. Although the nominal dimensions for the FLSC are given in the introduction, the actual dimensions used in the simulation are obtained by digitizing an enlarged photograph of an FLSC (Figure 5). The input deck for

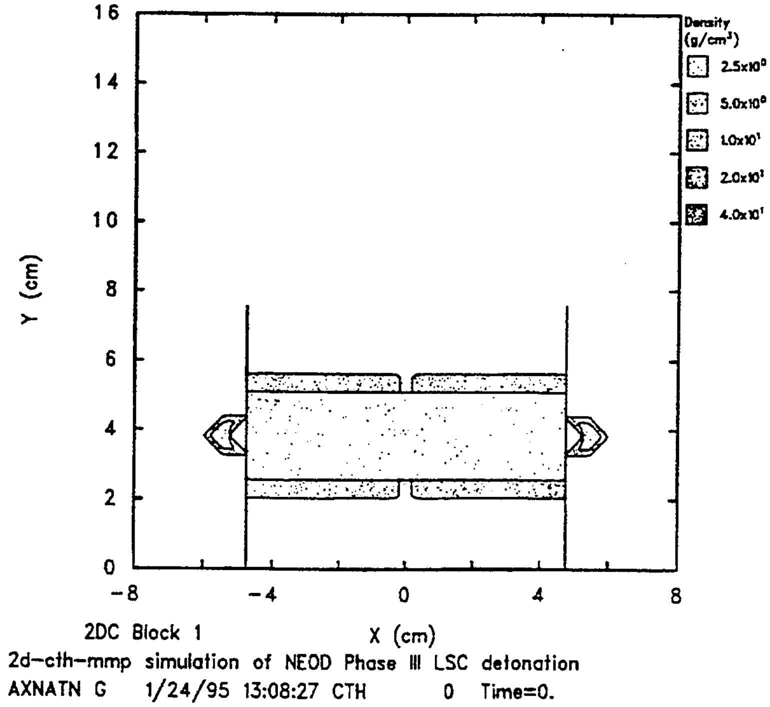

Figure 4. Axisymmetric geometry used in FLSC computations.

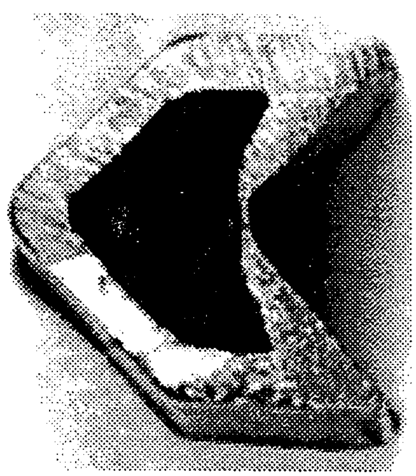

Figure 5. Cross section through the FLSC.

the CompB explosive-filled cylinder model appears in Appendix A, with corresponding computational results in Appendix B. The input deck for the LX-14 explosive-filled cylinder model appears in Appendix C, with corresponding computational results in Appendix D.

The distortional behavior of the aluminum cylinder (7075-T6), lead FLSC liner, and copper endcaps is modeled using the rate-independent version of the Steinberg-Guinan-Lund viscoplastic constitutive model (CTH material models 1, 4, and 5 respectively) (Steinberg and Lund 1989). The adiabatic yield stress vs. plastic strain for the metals is illustrated in Figure 6. The dilatational behavior of the metals is modeled with the Mie-Grüneisen equation of state (EOS) (Figure 7). The CompB and LX-14 HE are modeled using the Mie-Grüneisen EOS for the undetonated explosive, while the explosive detonation products are described with the SESAME EOS in conjunction with the history variable reactive burn (HVRB) model (see Kerley 1995). The coefficients for the various material models can be found in Appendix A and Appendix C input decks.

2.1 Computational Results. The axisymmetric nature of the model necessitates a simultaneous detonation of the FLSC around the periphery of the cylinder. This feature of the model differs from how the experiment is performed, since, in the experiment, the FLSC is detonated at one end, and the detonation wave travels unidirectionally around the circumference of the cylinder (Figure 8). The hypothetical location of the jet tip as it cuts through explosive cross section is determined by calculating the radius, r, or distance of the jet tip from the cylinder's symmetry axis defined as,

$$r = r_o - v_e \left(t - t_d - r_o \theta / v_f \right) , \tag{1}$$

in which t is time, t_d is the estimated delay time required for the liner to impact the aluminum casing (approximately 5 μs), r_o is the radius of the cylinder (0.049174 m), θ is the cylindrical coordinate ($0 < \theta < 2\pi$), and v_e and v_f are the jet tip cutting velocity (~1,700 m/s) and detonation wave velocity (7,800 m/s) in the explosive respectively. The locus of points in the x,y-coordinate system plotted in Figure 8 is obtained by substituting Equation 1 into the familiar equations for converting cylindrical coordinates to Cartesian coordinates,

$$\begin{aligned} x &= r \cos(\theta) \\ y &= r \sin(\theta) \ . \end{aligned} \tag{2}$$

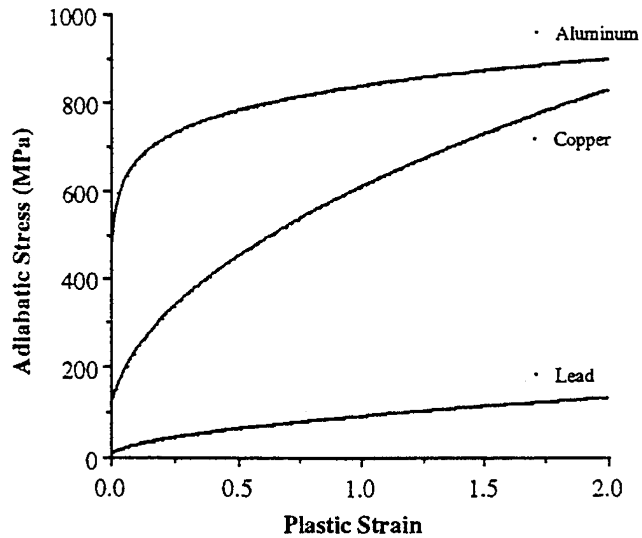

Figure 6. Adiabatic flow stress vs. equivalent plastic strain for aluminum (7075-T6), copper, and lead at ambient temperature and pressure.

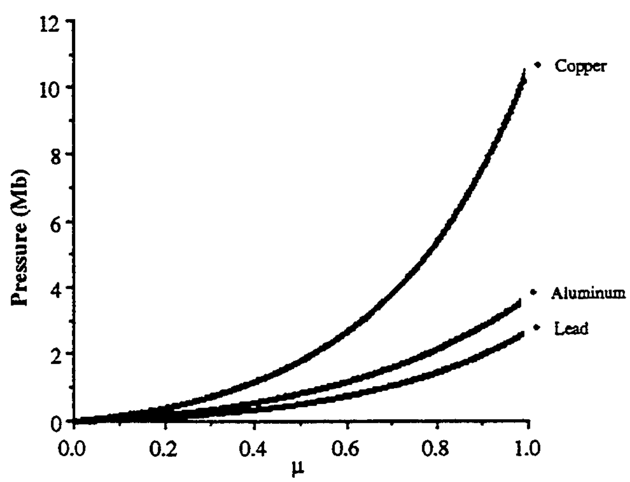

Figure 7. Hugoniot for copper, aluminum, and lead.

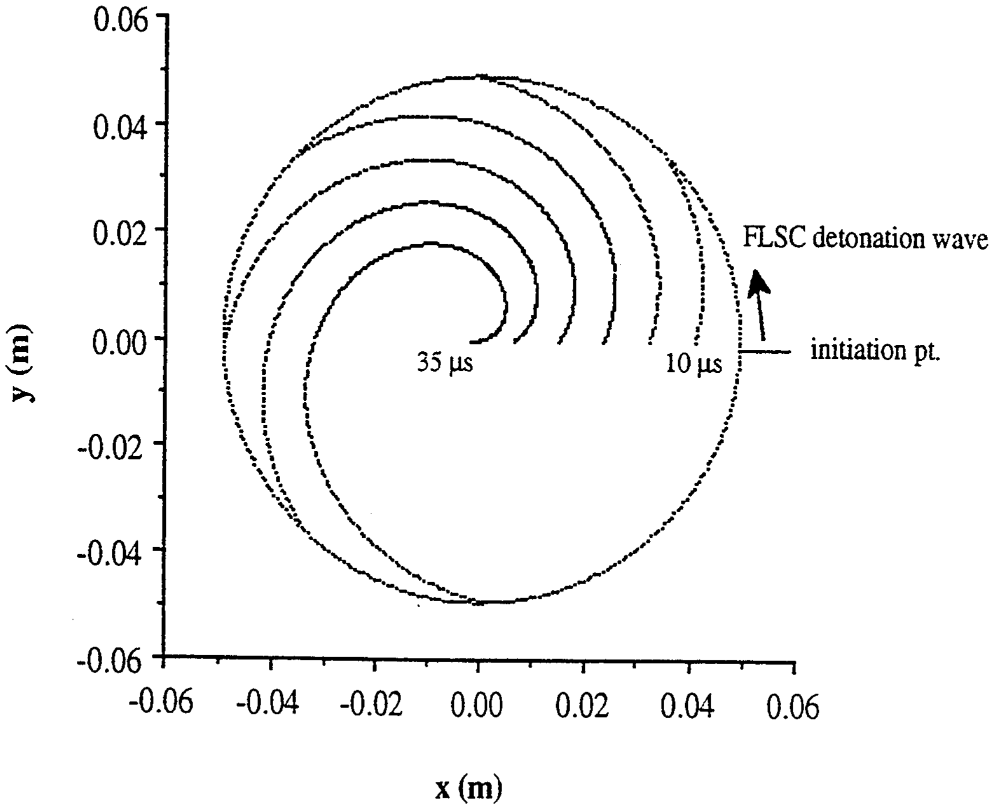

Figure 8. Hypothetical leading edge of jet tip as it cuts through explosive cross section from 10 µs through 35 µs after initiation.

The spiral nature of the leading edge profile is a result of the fact that the detonation wave velocity in the FLSC is much greater than the jet tip cutting velocity (i.e., v_f = 7,800 m/s > v_e = 1,700 m/s in Figure 8). One can estimate the time, t_c, it takes for the detonation wave to travel around the circumference of the cylinder, by knowing the CH-6 detonation velocity, v_e, and length, l, of the FLSC. The travel time is estimated at, $t_c = l/v_e$ = 0.31 m/7,800 m/s = 40 µs. The plot shows that the leading edge of the jet tip in the experiment is not symmetrically disposed about the cylinder axis, and since the axisymmetric computations indicate that the detonation wave reaches the center axis of the cylinder in only 17 µs (Appendix A), only the very short time (t < 17 µs) results of the computational model should be compared with experiment.

The hydrocode simulations predict that neither the CompB or LX-14 explosive will detonate in the indirect impact model configuration (Figure 3a). Experiments conducted at Range 16 with this configuration corroborate the hydrocode predictions. However, with the direct impact configuration (Figure 3b), we believed the explosives would detonate by shock initiation either by 1) direct shaped charge jet impact, or 2) a liner "slap" impact (Figure 9). The hydrocode computations show, however,

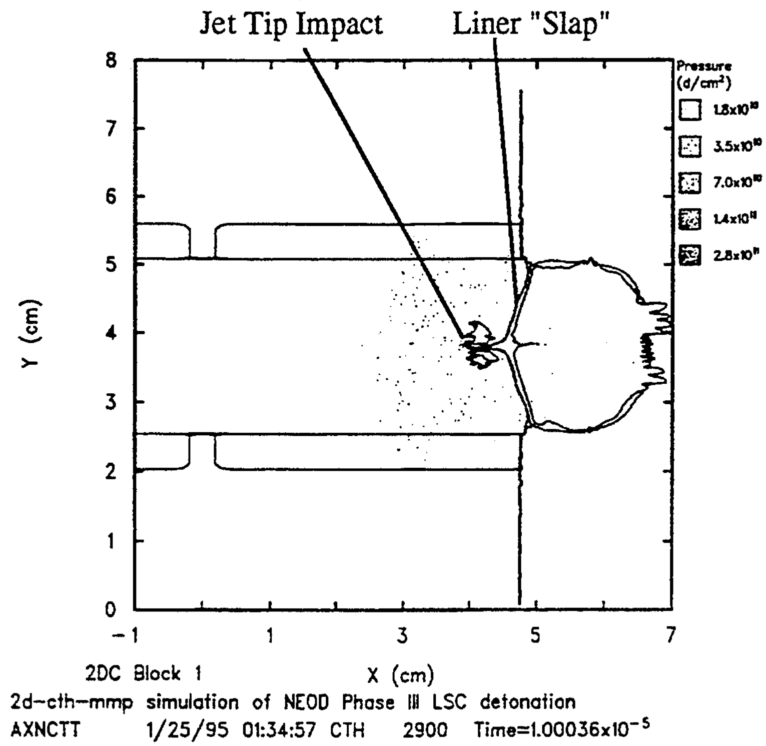

Figure 9. Detonation scenarios by jet tip impact and liner "slap."

that CompB explosive does not detonate under these impact conditions. Furthermore, using the v^2*d = constant criterion for explosive detonation, we see that both the jet tip and liner "slap" impact scenarios plot below the critical value necessary for detonation (see Figure 10 modified from Starkenberg et al. 1984). The empirical Jacobs-Roslund formula is plotted as the solid line in Figure 10, and all combinations of projectile velocity and diameter that fall above this line should result in detonation for CompB explosive. Points that fall below the Jacobs-Roslund line predict no detonation for CompB explosive.

The CTH computational results for CompB and in Appendix B where quantities such as pressure, density, and a history-dependent reaction variable (Kerley 1995) which tracks chemical decomposition (detonation) of the explosive are plotted at 5 μs intervals for a total of 25 μs. The reaction variable is normally scaled between 0 and 1; however, we increase this limit to 2, to provide for a better visual presentation of the data. The CompB simulations do not reveal any chemical decomposition of the explosive beneath the jet tip or impacting liner. However, some decomposition is visible along the center axis of the model, as a result of the superposition of shock wave fronts at this location. The zone of decomposition remains localized, however, and does not follow the expanding shock wave as it reflects

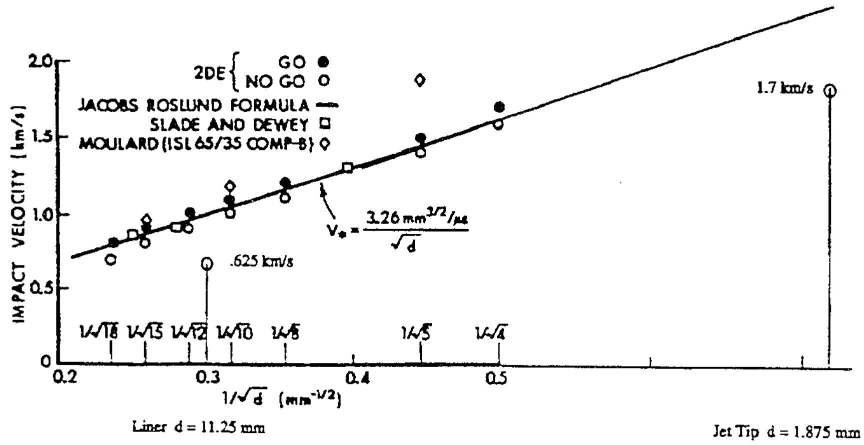

Figure 10. Critical impact velocity as a function of projectile diameter (modified from Figure 14) (Starkenberg et al. 1984).

off the cylinder axis (see Appendix B plots at 25 μs). We can infer then, that if a detonation were to occur in such an experiment, it would probably initiate as a result of shock wave superposition at an interior point of the body, and not as a result of impact by the jet tip or liner.

The CTH computational results for LX-14 are in Appendix D. A Jacobs-Roslund plot similar to that found for CompB is not available for LX-14 explosive (Starkenberg 1995). However, since LX-14 explosive is considerably more sensitive to impact than CompB explosive (Montesi and Bauldler 1990), we expected LX-14 to detonate by either the jet tip impact or liner "slap" mechanisms mentioned earlier. The results are somewhat different than anticipated, however, since the LX-14 detonation initiates on the center axis of the cylinder, and all the explosive detonates after 25 μs. Recall that minor decomposition of CompB explosive is predicted to occur along the cylinder's symmetry axis.

Based upon the results of the hydrocode simulations, we infer that neither the CompB or LX-14 explosives will detonate as a result of either jet tip or liner impact. We further infer that LX-14 will fully detonate as a result of the superposition of shock waves at a point interior to the body, yet the CompB will not.

3. EXPERIMENTS

Both direct and indirect FLSC impact configurations were investigated and are illustrated in Figure 3. The indirect impact configuration (Figure 3a) consists of the FLSC centered 0.5 in (12.7 mm) above the bare explosive. The direct impact configuration (Figure 3b) consists of the FLSC centered over the aluminum-covered explosive and capped with thin copper disks. The copper disks are inserted into both ends of the aluminum cylinder and are manually press-fit onto the explosive surface. A small hole is predrilled into each copper disk to allow entrained air to escape as the disk is pressed into position. The FLSC is wrapped around the aluminum cylinder and is detonated at one end using a thin wafer of Detasheet. The detonation wave travels unidirectionally around the cylinder forming an inwardly directed jet which cuts into the explosive fill. The cylinder is horizontally positioned on a meter high styrofoam stand within a rectangular "explosion-proof" test fixture whose walls are constructed of 2-in (50.8 mm)-thick plates of rolled-homogeneous armor (RHA). A photograph of the indirect impact test configuration appears in Figure 11.

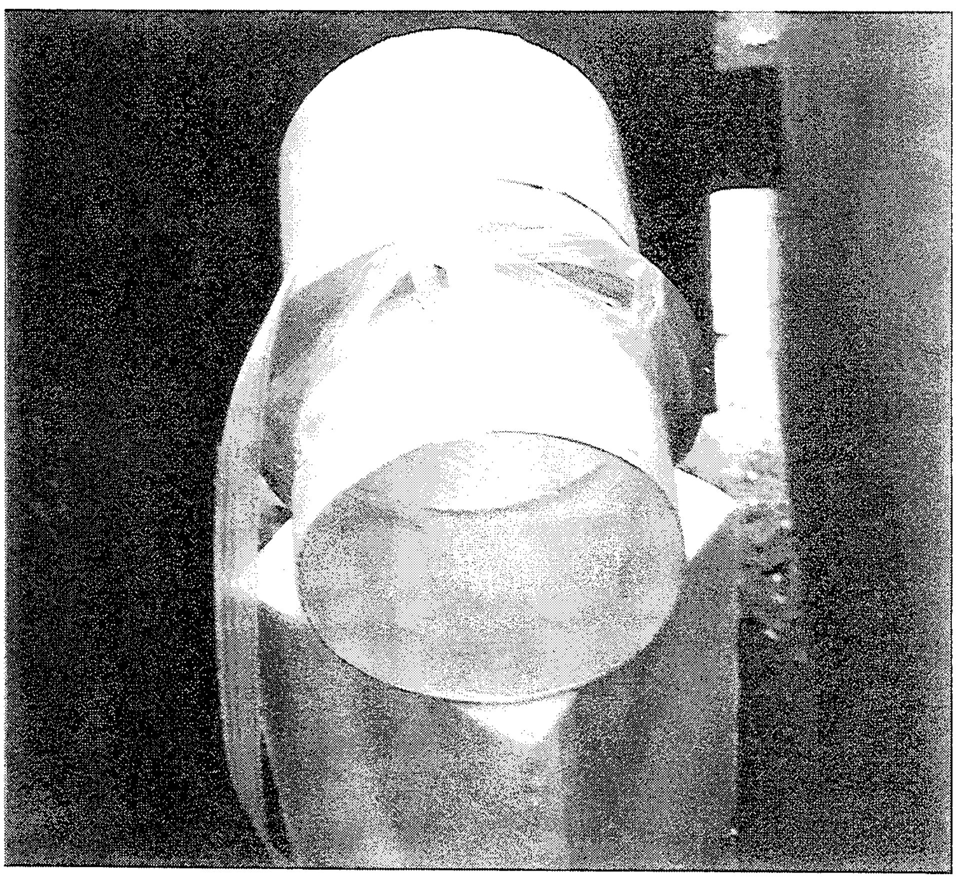

Figure 11. Photograph of test configuration (Figure 3a) showing FLSC surrounding aluminum cylinder.

Detonation did not occur with either explosive using the indirect impact test configuration. The direct impact test on CompB also did not reveal any evidence of detonation. However, the direct impact test on LX-14 produced a violent detonation that propelled the copper disks outward, forming a crater on the interior wall of the RHA test fixture (Figure 12). It could not be ascertained where the detonation initiated in the experiment since radiography was not used in the test series. However, based upon the hydrocode results, we surmise that the detonation initiated as a result of the superposition of shock waves at a point interior to the body.

Figure 12. Photograph of crater on interior wall of RHA test fixture formed by impact from thin copper disk.

4. CONCLUSIONS

CTH hydrocode simulations predict that detonation in both CompB and LX-14 explosives, encased in thin-walled, aluminum cylinders, will not initiate as a result of either direct impact by a 225 gpf FLSC jet tip, or by liner "slap" mechanisms. The CTH hydrocode predicts that detonation will initiate in the LX-14 explosive by shock wave superposition along the symmetry axis of the HE-filled cylinder. Some minor decomposition of CompB is also predicted to occur along the cylinder's symmetry axis, but detonation does not occur. Experiments conducted on HE-filled, thin-walled cylinders qualitatively verify the hydrocode predictions insofar as experiments that involve CompB did not detonate, whereas

experiments on LX-14 did detonate. The precise location of where the LX-14 detonation initiated could not be detected, as radiography was not used in this test series. We surmise that the LX-14 detonation initiated at a point interior to the body as a result of the superposition of shock waves. The actual detonation most likely initiated at a point not on the cylinder axis, since the experiment is fundamentally nonaxisymmetric. Radiography and a fully three-dimensioned CTH simulation could be used to verify this inference in future work.

5. REFERENCES

Department of the Navy EODB/Department of the Army TM/U.S. Air Force TO 60A-2-1-51, 1992.

Kerley, G. I. "BCAT User's Manual and Input Instructions, Version 1.05." Sandia National Laboratory, Albuquerque, NM, 1995.

McGlaun, J. M., F. J. Zeigler, S. L. Thompson, L. N. Kmetyk, and M. G. Elrick. "CTH-User's Manual and Input Instructions." Sandia National Laboratory Report SAND88-0523, Albuquerque, NM, April 1988.

Montesi, L. J., and B. A. Bauldler. "Qualification Test Results of LX-14 Explosive." Naval Surface Warfare Center, NAVSWC TR-88-296, Dahlgren, VA, 1990.

Starkenberg, J., Y. Huang, and A. Arbuckle. "Numerical Modeling of Projectile Impact Shock Initiation of Bare and Covered Composition-B." U.S. Army Ballistic Research Laboratory Report, ARBRL-TR-02576, Aberdeen Proving Ground, MD, August 1984.

Starkenberg, J. Personal communication. U.S. Army Research Laboratory, Aberdeen Proving Ground, MD, July 1995.

Steinberg, D. J., and C. M. Lund. "A Constitutive Model for Strain Rates From 10^{-4} to 10^{6} s^{-1}." Journal of Applied Physics, vol. 65, no. 4, 1989.

INTENTIONALLY LEFT BLANK.

APPENDIX A:

COMPB SIMULATION INPUT DECK

INTENTIONALLY LEFT BLANK.

```
*
*eor*cgenin
*
2d-cth-mmp simulation of NEOD Phase III LSC detonation
*
control
 ep
 mmp
endcontrol
*
mesh
 block  geometry 2dc  type e
  x0=0.0
   x1  n=70  w=4.747  dxl=0.0055
   x2  n=3   w=0.0155 rat=1
   x3  n=110 w=1.252  dxf=0.0055
   x4  n=17  w=1.5    dxf=0.021
  endx
  y0=0.0
   y1  dyf 0.15    dyl 0.05    w 2.54
   y2  dyf 0.05    dyl 0.0055  w 1.27
   y3  dyf 0.0055  dyl 0.05    w 1.27
   y4  dyf 0.05    dyl 0.15    w 2.54
  endy
  xact=4.76,5.95
  yact=3.24,4.40
 endblock
endmesh
*
insertion of material
 block 1
*
  package 'AL Case - 1'
   material 1
   numsub 50
   pressure 1.0e6
   insert box
    x1  4.747    x2  4.76250
    y1  0.000    y2  15.24000
   endinsert
  endpackage
*
  package 'HE Patty - 1'
   material 2
   numsub 50
```

```
   pressure 1.0e6
   insert box
    x1  0.000    x2  4.74700
    y1  2.540    y2  5.08000
   endinsert
  endpackage
*
  package 'HE LSC - 1'
   material 3
   numsub 50
*   G. Kerley told me (12/1/94) that RDX @o=1.70 g/cc detonates at
*   T=3560K=0.30678eV; Po=13.8GPa.  This calculation was done with BCAT
*   or PANDA. Specifying the insert at this temp is equivalent to
*   detonating the whole mass at time=0.
   temperature 0.30678
   insert uds
    point   5.24615  3.81328
    point   5.24615  3.77718
    point   5.24615  3.71811
    point   5.23957  3.66561
    point   5.21983  3.60982
    point   5.20009  3.56716
    point   5.16719  3.51465
    point   5.14087  3.46543
    point   5.13758  3.44902
    point   5.14416  3.42933
    point   5.15403  3.41948
    point   5.17706  3.41292
    point   5.20338  3.41620
    point   5.25273  3.41620
    point   5.30538  3.41620
    point   5.35473  3.41620
    point   5.39421  3.42276
    point   5.42382  3.43589
    point   5.44685  3.45230
    point   5.48304  3.48183
    point   5.52253  3.51465
    point   5.56859  3.56388
    point   5.63768  3.63607
    point   5.69361  3.69186
    point   5.73639  3.73452
    point   5.75284  3.75749
    point   5.75613  3.77390
    point   5.75942  3.80344
    point   5.75613  3.82969
    point   5.75613  3.84938
    point   5.72652  3.88548
```

```
    point   5.67058  3.95111
    point   5.61465  4.00362
    point   5.51595  4.10535
    point   5.45672  4.15457
    point   5.43040  4.17755
    point   5.40737  4.19395
    point   5.37118  4.20052
    point   5.29551  4.21364
    point   5.20667  4.22021
    point   5.16390  4.22021
    point   5.13429  4.22021
    point   5.12113  4.21036
    point   5.11784  4.19724
    point   5.12113  4.18411
    point   5.13100  4.17098
    point   5.14087  4.14473
    point   5.15732  4.11191
    point   5.18035  4.07253
    point   5.20338  4.03643
    point   5.22641  3.99377
    point   5.23628  3.95439
    point   5.23957  3.91173
    point   5.24286  3.87563
    point   5.24286  3.83625
    point   5.24615  3.81656
  endinsert
endpackage
package 'Lead LSC - 1'
  material 4
  numsub 50
  pressure 1.0e6
  insert uds
    point   5.19022  3.81000
    point   5.19351  3.79031
    point   5.19351  3.76078
    point   5.18693  3.74437
    point   5.17706  3.73452
    point   5.13100  3.68202
    point   5.06519  3.60982
    point   4.93359  3.47527
    point   4.80527  3.34401
    point   4.77895  3.31775
    point   4.77237  3.31119
    point   4.76579  3.29478
    point   4.76579  3.27509
    point   4.77237  3.25868
    point   4.78553  3.24556
```

point	4.80198	3.24227
point	4.82172	3.24227
point	4.87437	3.24227
point	5.12113	3.24556
point	5.29880	3.24227
point	5.33828	3.24556
point	5.39092	3.25212
point	5.43369	3.26196
point	5.46659	3.28494
point	5.52911	3.34072
point	5.66071	3.47199
point	5.79232	3.60326
point	5.91405	3.72468
point	5.93051	3.75093
point	5.94038	3.77390
point	5.94696	3.79359
point	5.94696	3.81656
point	5.94367	3.83625
point	5.93380	3.85266
point	5.92392	3.86579
point	5.89760	3.89532
point	5.83838	3.95767
point	5.76600	4.02659
point	5.70348	4.08894
point	5.63439	4.15457
point	5.55872	4.23333
point	5.46988	4.33178
point	5.45014	4.35147
point	5.43369	4.36788
point	5.41395	4.37444
point	5.38763	4.37773
point	5.30867	4.38101
point	5.20009	4.38101
point	5.03229	4.38429
point	4.84804	4.38757
point	4.80198	4.39085
point	4.78224	4.38101
point	4.77237	4.37116
point	4.76908	4.35804
point	4.76908	4.34819
point	4.77237	4.33178
point	4.78224	4.31537
point	4.81843	4.27928
point	4.88424	4.21036
point	4.95991	4.12504
point	5.05203	4.02987
point	5.11126	3.96424

```
    point  5.15403  3.92486
    point  5.17377  3.89204
    point  5.18693  3.86579
    point  5.19022  3.83953
    point  5.19022  3.81656
   endinsert
  endpackage
*
  package 'Cu Damper - Bottom'
   material 5
   numsub 50
   pressure 1.0e6
   insert box
    x1  0.258    x2  4.747
    y1  2.032    y2  2.540
   endinsert
  endpackage
*
  package 'Cu Damper - Top'
   material 5
   numsub 50
   pressure 1.0e6
   insert box
    x1  0.258    x2  4.747
    y1  5.080    y2  5.588
   endinsert
  endpackage
*
 endblock
endinsertion
*
eos
*
* Aluminum Mie-Grüneisen
 mat1  mgrun  eos=7075-t6_al  feos='/b/scheffle/cth/MGR_data'
     ro=2.804    cs=0.5200E6  s=1.360    go=2.20   cv=1.07E11
*
* Comp B Patty
*  Parameters estimated to be roughly halfway between RDX and TNT.
*  RP and R0 made identical per advice of G. Kerley, to avoid bug.
 MAT2  SESAME  EOS=8311  FEOS='/b/scheffle/cth/sesame'
     RP=1.75  R0=1.75  CS=2.55E5  S=1.99  G0=1.0  CV=1.35E11
     TYP=2.0  PR=9.0E10  ZR=3.00  MR=1.5  PI=0.5E10
     RMAX=5.0  RMIN=0.01  TMAX=5.0  PT=1.0E13
** CEQ(I),I=1,40
**  8.3110E+03  0.0000E+00  1.0000E+00  1.7500E+00  2.5680E-02
```

```
** 0.0000E+00 -5.0519E+06 1.0000E+00 1.3500E+11 1.0000E-02
** 5.0000E+00 6.6333E-01 3.2835E-01 1.9371E-01 1.8038E-01
** 3.2767E+00 -1.9307E+12 4.4248E+12 1.3500E+09 2.0000E+00
** 5.0000E+00 1.5000E+00 3.0000E+00 9.0000E+10 7.0359E+10
** 2.5500E+05 1.9900E+00 5.0000E+09 1.7200E+00 9.6333E+00
** 0.0000E+00 0.0000E+00 0.0000E+00 0.0000E+00 0.0000E+00
** 0.0000E+00 0.0000E+00 0.0000E+00 5.1220E+01 9.9985E+01
*
* CH-6 (RDX=HMX) HE as LSC charge
 mat3 SESAME EOS=8012 FEOS='/b/scheffle/cth/sesame'
     RP=1.70 R0=1.70
*
* Lead (6% Antimony) Mie-Gru (modified from Library data)
 mat4 mgrun eos=lead_s feos='/b/scheffle/cth/MGR_data'
     ro=10.9    cs=0.2006E6 s=1.429    go=2.74    cv=1.5512E10
* Copper Mie-gruneisen
 mat5 mgrun eos=copper feos='/b/scheffle/cth/MGR_data'
     ro=8.930    cs=3.940E5  s=1.489    go=1.99    cv=4.56E10
endeos
*
* heburn option not needed, with predetonated sesame option
**heburn
**endheburn
epdata
 vpsave
* Library 7075-T6 Al.
 matep 1 steinberg-guinan='7075-T6_ALUMINUM' fvp='/b/scheffle/cth/VP_data'
     poisson 0.16
 r0st=2.804   tm0st=0.105127 atmst=1.70 gm0st=2.20
 ast=6.52E-12 bst=7.148680  nst=0.10  c1st=0.00
 c2st=0.00    g0st=0.267E+12 btst=965.0 eist=0.00    ypst=0.00
 ukst=0.00    ysmst=0.00     yast=0.00  y0st=4.2E+09 ymst=8.1E+09
* Library Lead
 matep 4 steinberg-guinan='LEAD' fvp='/b/scheffle/cth/VP_data'
     poisson 0.43
 r0st=11.34   tm0st=0.065489 atmst=2.20 gm0st=2.74
 ast=11.63E-12 bst=13.461800 nst=0.52  c1st=0.00
 c2st=0.00    g0st=8.6E+10   btst=110.0 eist=0.00   ypst=0.00
 ukst=0.00    ysmst=0.00     yast=0.00  y0st=8.0E+07 ymst=1.0E+09
*
 matep 5 steinberg-guinan='COPPER' fvp='/b/scheffle/cth/VP_data'
     poisson 0.32
 r0st=8.93    tm0st=0.154244 atmst=1.50 gm0st=2.02
 ast=2.83E-12 bst=4.375085  nst=0.45  c1st=0.00
 c2st=0.00    g0st=0.477E+12 btst=36.0  eist=0.00   ypst=0.00
 ukst=0.00    ysmst=0.00     yast=0.00  y0st=1.2E+09 ymst=6.4E+09
*
```

```
 mix 3
endep
*
*
*eor*cthin
*
 2d-cth-mmp NEOD Phase III LSC detonation
*
control
 tstop=40.e-6
* cpshift=900.
* rdumpf=3600
* ntbad 1000000
endcontrol
restart
 cycle=6832
 file='rs04h'
 newfile=all
endrestart
*
cellthermo
 mmp
endcell
*
convct
 convect=1
 nofrag=2
 interface=high
endc
*
discard
 material 3  density -0.01  pressure 5.0e6  ton 7.0e-6
endd
*
edit
 shortt
  tim=0.  dt=10000.
 ends
 longt
  tim=0.  dt=10000.
 endl
 plott
  time=0.  dtfreq=5.0e-6
 endp
endedit
*
mindt
```

```
 time=0.     dtmin=1.0e-13
endm
*
fracts
 stress
 pfrac1=-8.1E9
 pfrac3=-1.0E9
 pfmix =-5.0E6
 pfvoid=-5.0E6
endf
*
boundary
 bhydro
   block=1
     bxbot 0
     bxtop 2
     bybot 2
     bytop 2
   endb
 endh
endb
*
*eor*pltin
*
units cgsev
*
nlegend=off
*
time,0.0e-6,rest
color table 4
units cgsk
limits x=-7.0,7.0,1 y=0.0,14.0,1
flegend=d
*2dplot,dots=density=2.,mirror,if

2dplot,materials,mirror
limits x=3.0,7.0,1 y=1.0,5.0,1
rbands, b1=1e6, b2=1e10, c1=256, c2=236, skip=-2
flegend=b
2dplot,materials
nlegend=on
2dplot bands=pressure, if
rbands, b1=0.0, b2=0.1, c1=256, c2=236, skip=-2
2dplot bands=hvb2, if
END OF FILE
```

APPENDIX B:

COMPB COMPUTATIONAL RESULTS

INTENTIONALLY LEFT BLANK.

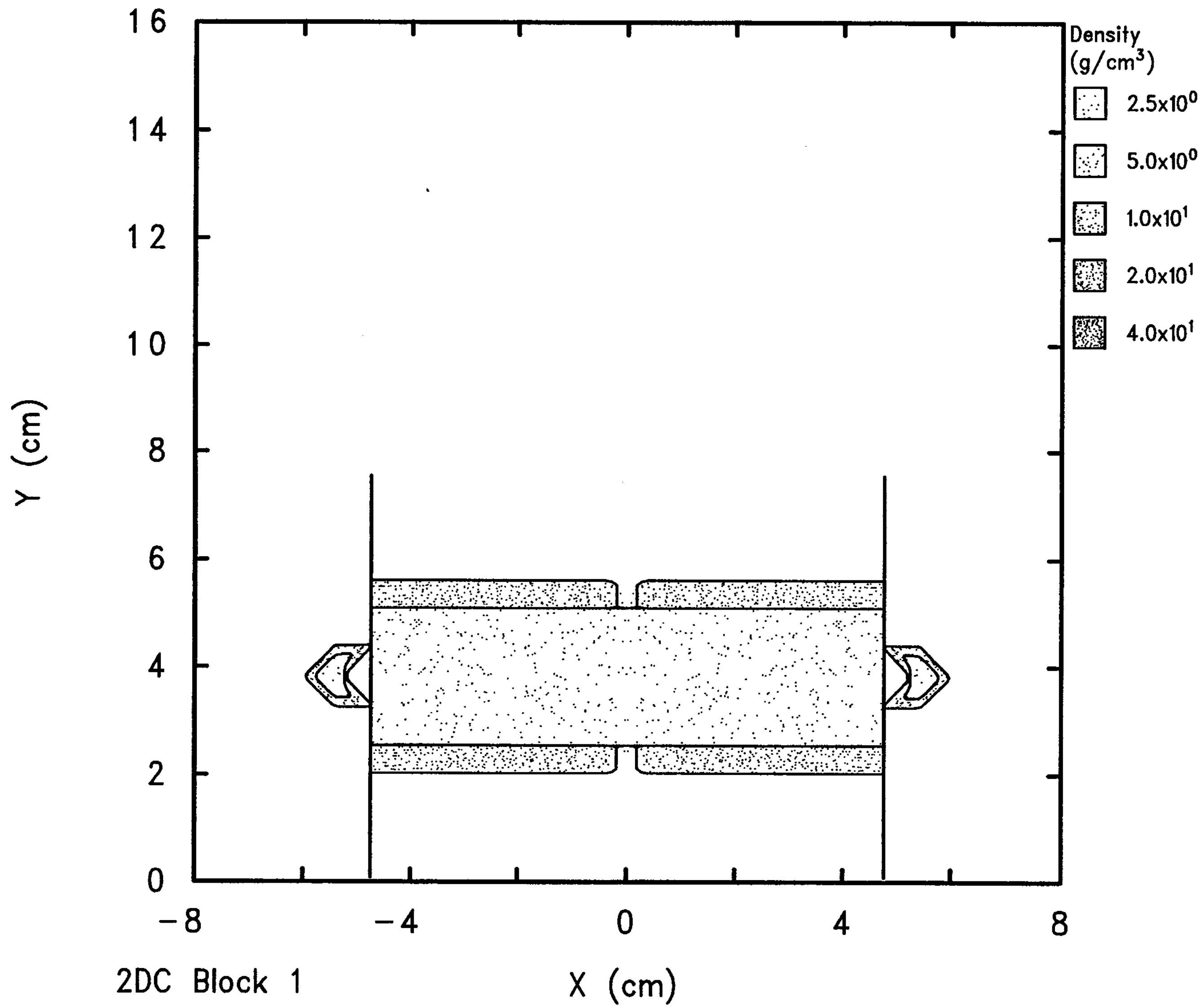

2d−cth−mmp simulation of NEOD Phase III LSC detonation
AXNATN G 1/24/95 13:08:27 CTH 0 Time=0.

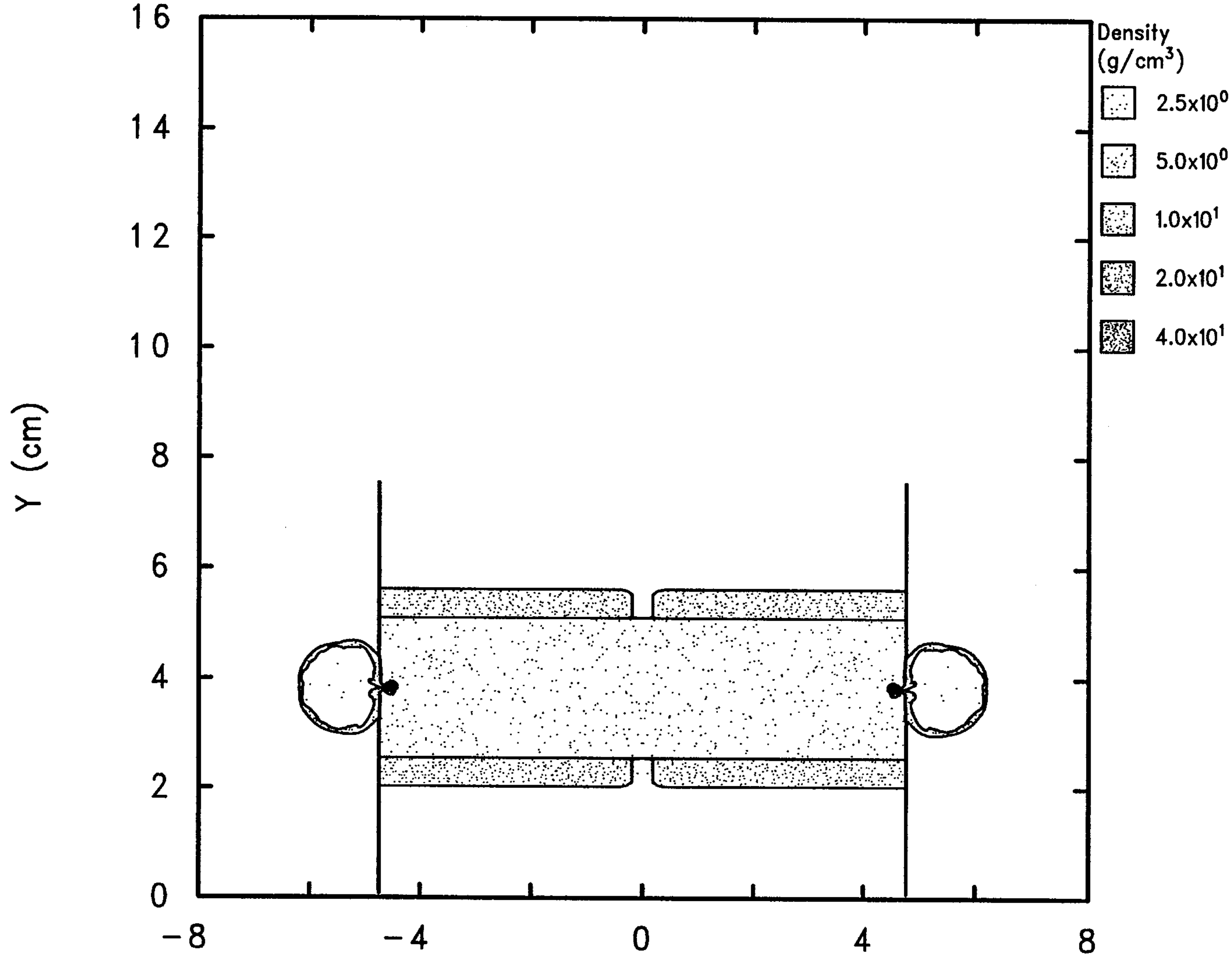

2DC Block 1

2d-cth-mmp simulation of NEOD Phase III LSC detonation

AXNCTT 1/24/95 19:45:27 CTH 1513 Time=5.00175×10^{-6}

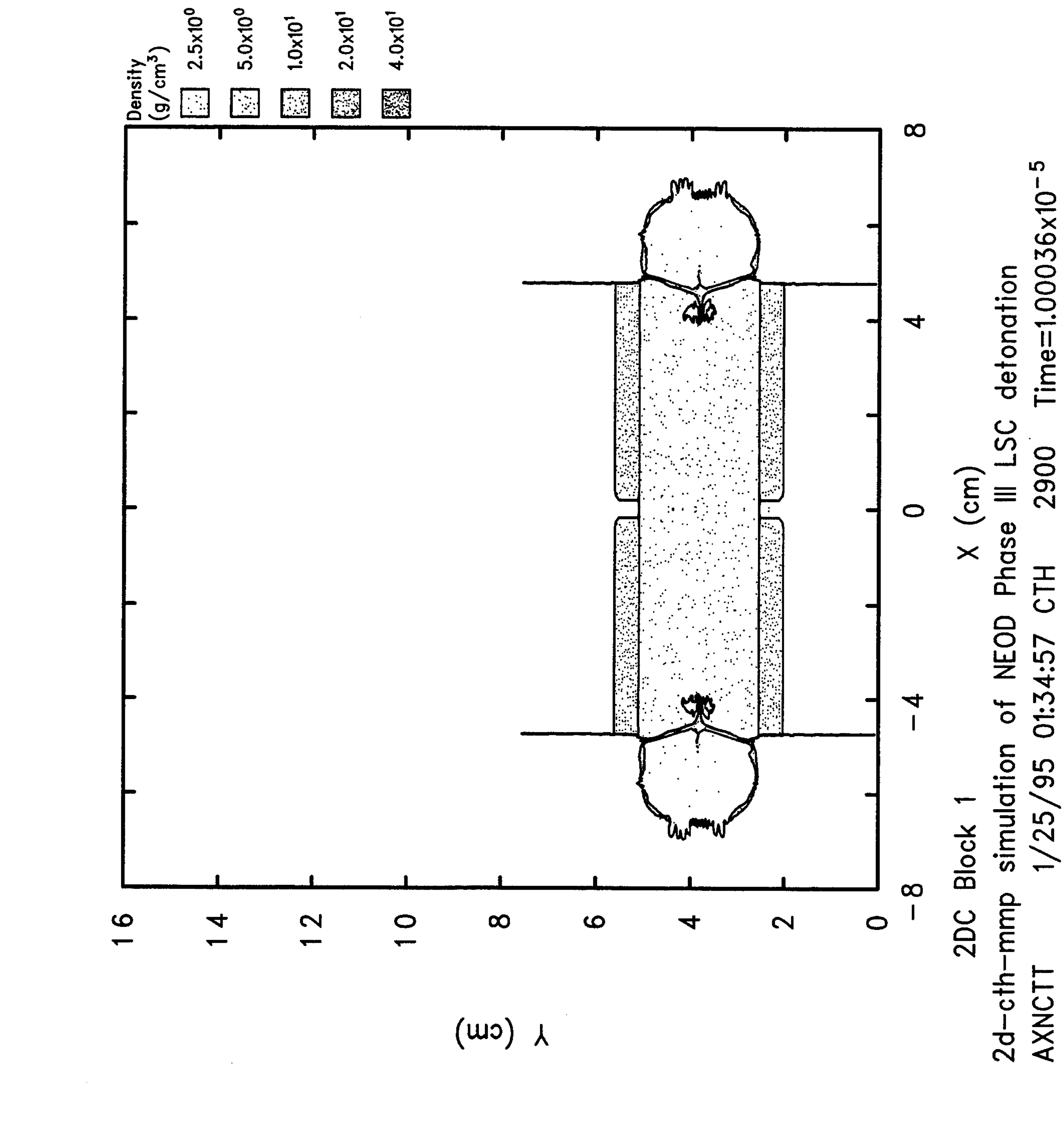
Density (g/cm^3)
2.5x10^0
5.0x10^0
1.0x10^1
2.0x10^1
4.0x10^1
Y (cm)
X (cm)
2DC Block 1
2d-cth-mmp simulation of NEOD Phase III LSC detonation
AXNCTT 1/25/95 01:34:57 CTH 2900 Time=1.00036x10^{-5}

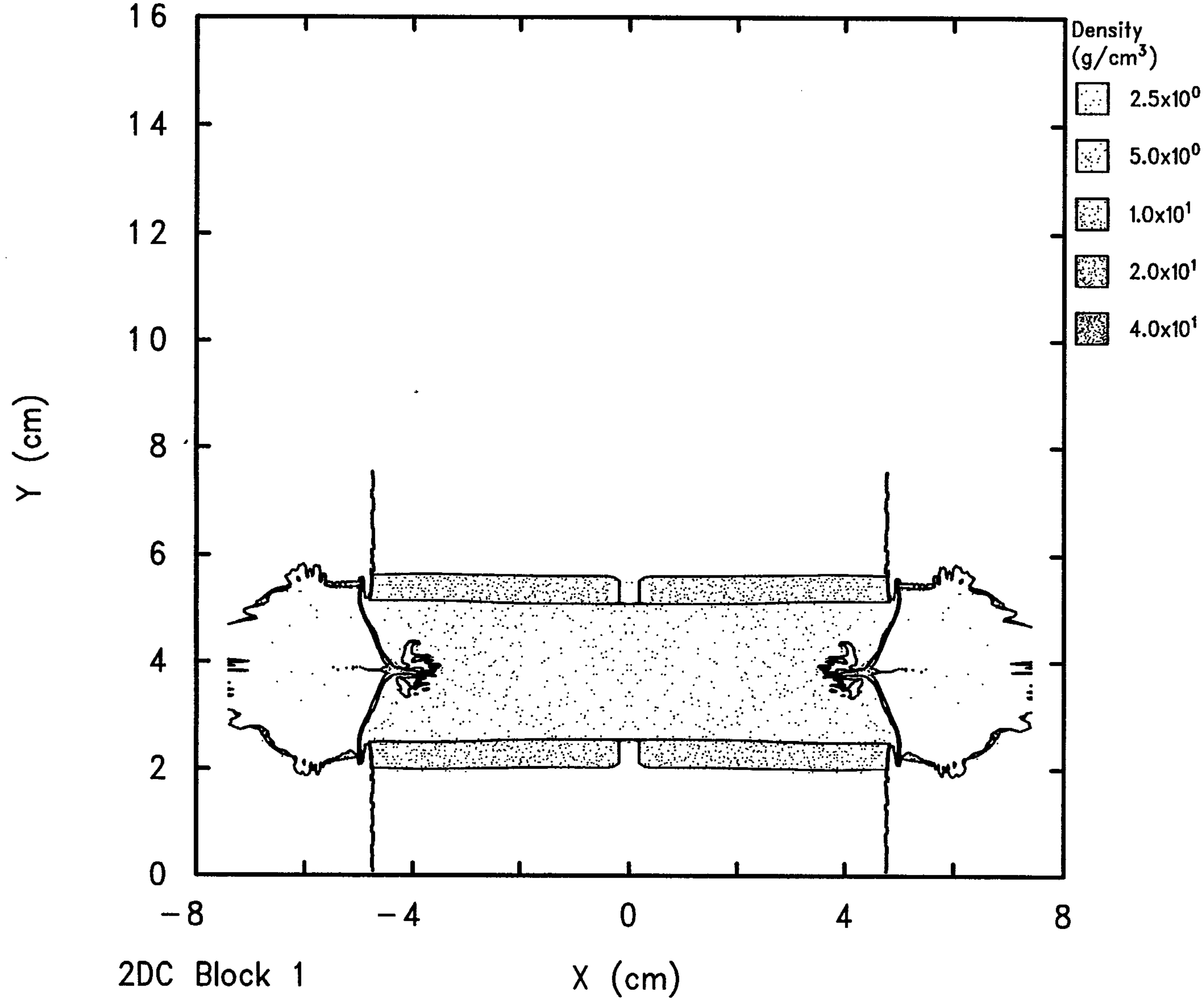

2DC Block 1

2d–cth–mmp simulation of NEOD Phase III LSC detonation

AYJAMT 1/25/95 10:03:14 CTH 4258 Time=1.50031×10^{-5}

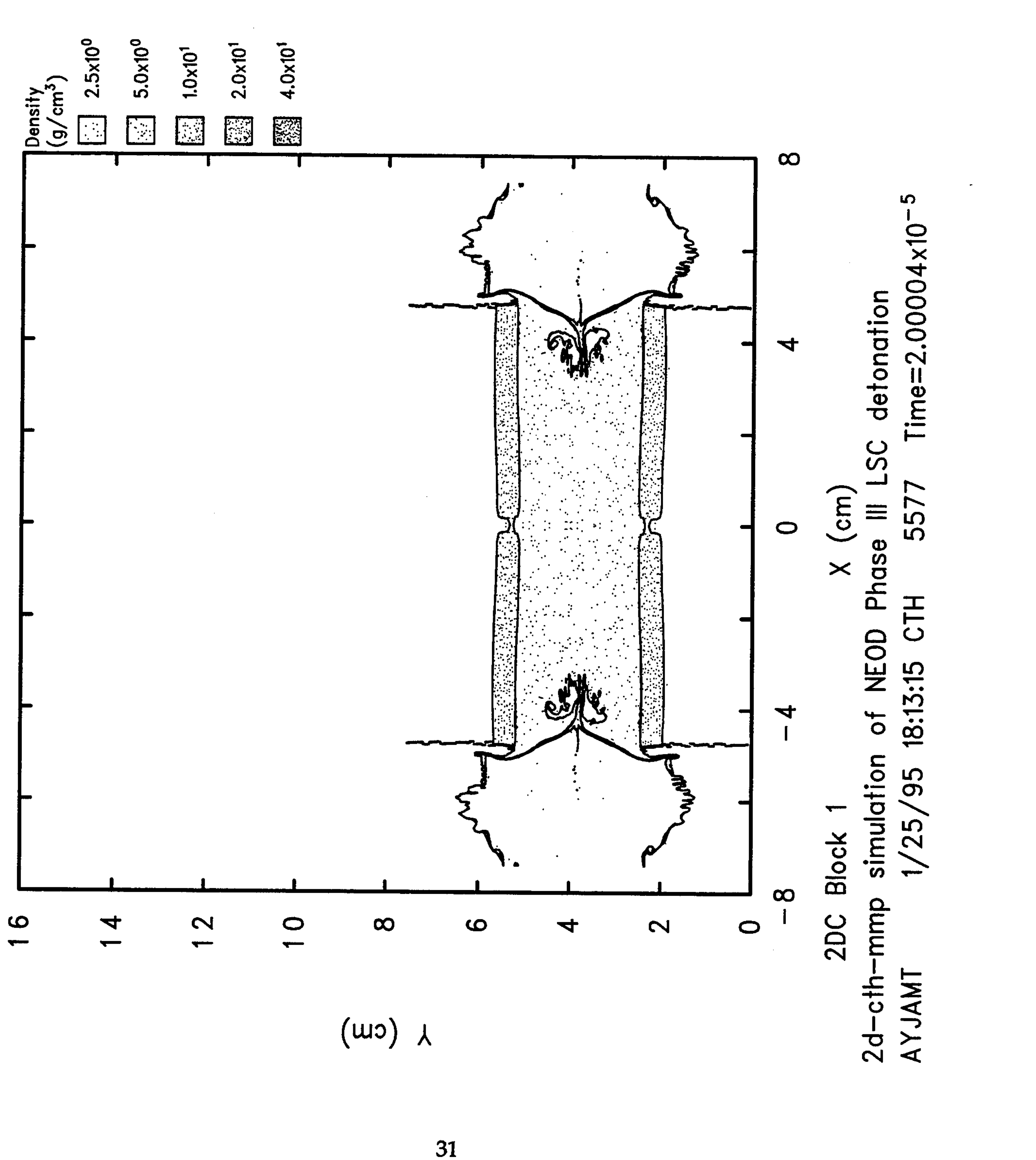
Density (g/cm3)
2.5x10^0
5.0x10^0
1.0x10^1
2.0x10^1
4.0x10^1
Y (cm)
X (cm)
2DC Block 1
2d-cth-mmp simulation of NEOD Phase III LSC detonation
AYJAMT 1/25/95 18:13:15 CTH 5577 Time=2.00004x10^-5

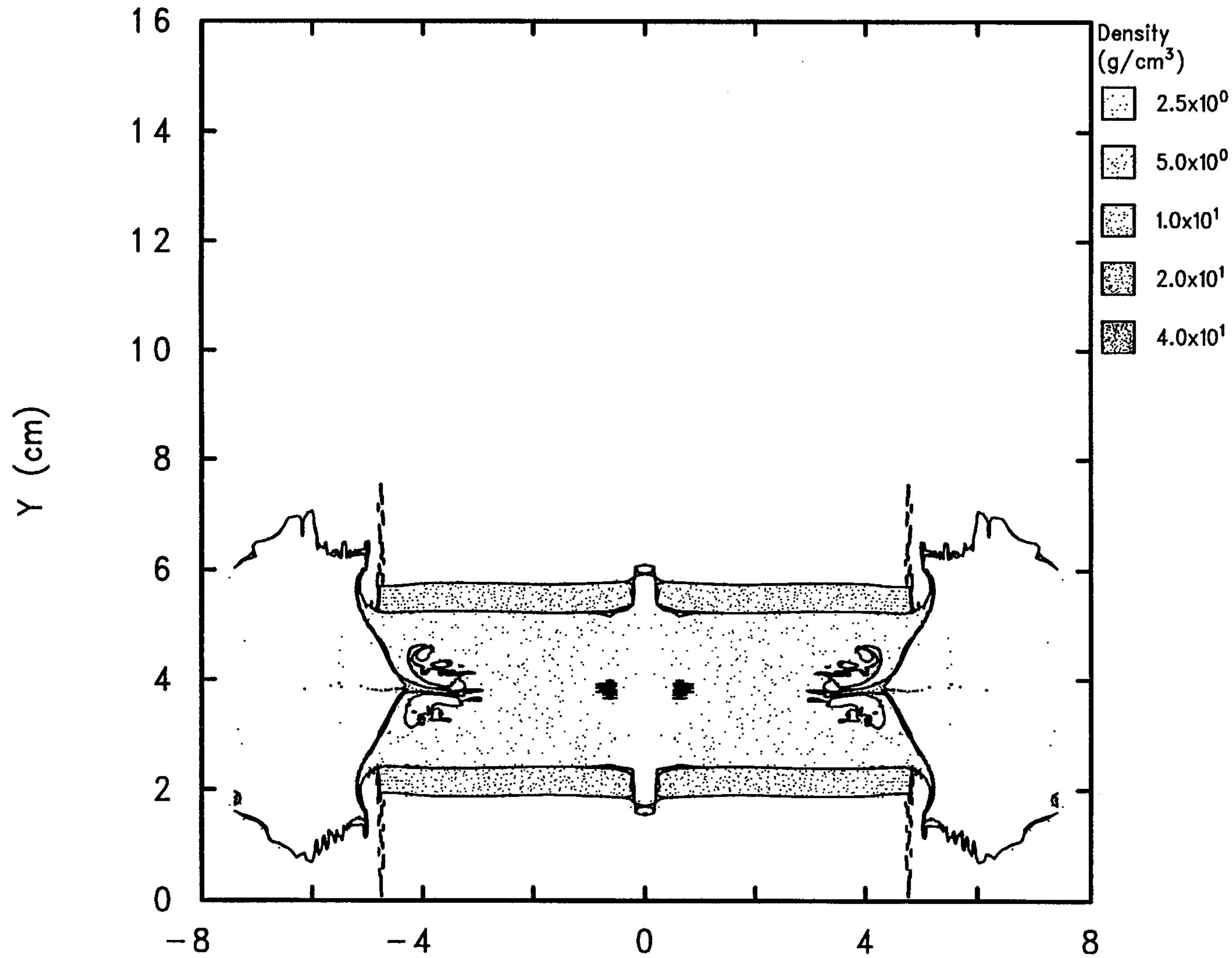

2DC Block 1 X (cm)

2d−cth−mmp simulation of NEOD Phase III LSC detonation

AYJAMT 1/26/95 00:39:35 CTH 6832 Time=2.48073×10^{-5}

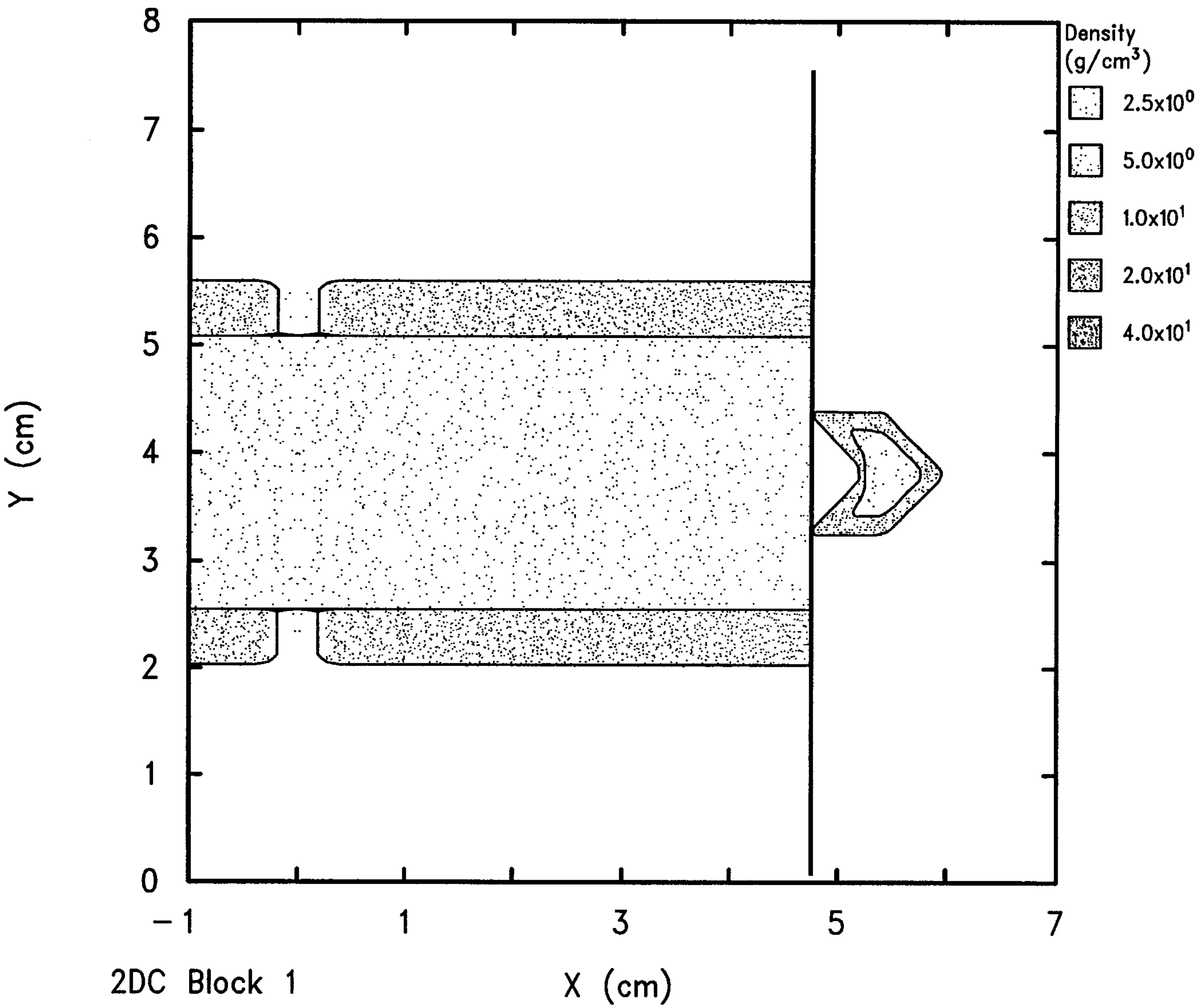

2d–cth–mmp simulation of NEOD Phase III LSC detonation
AXNATN G 1/24/95 13:08:27 CTH 0 Time=0.

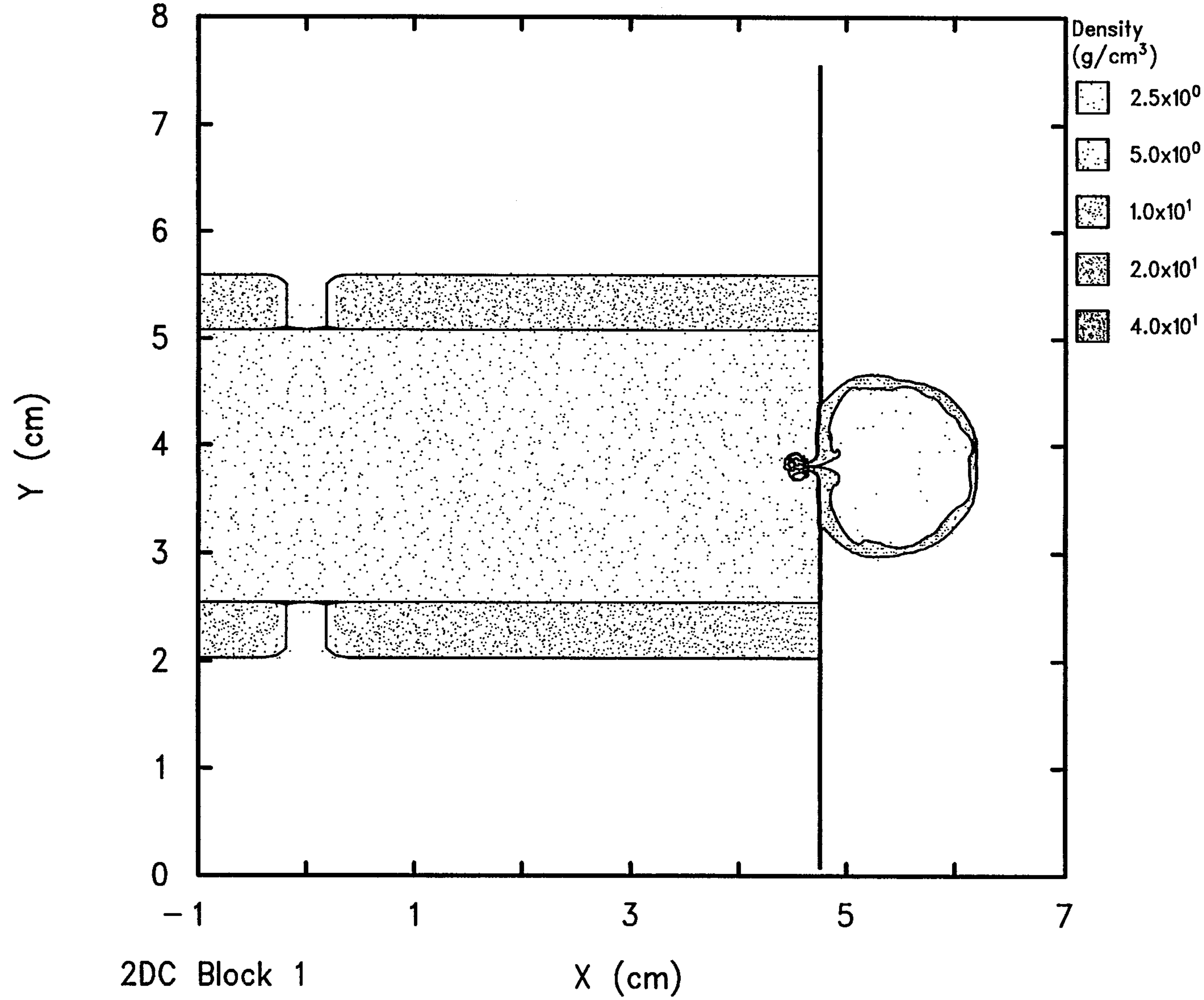

2d-cth-mmp simulation of NEOD Phase III LSC detonation

AXNCTT 1/24/95 19:45:27 CTH 1513 Time=5.00175×10^{-6}

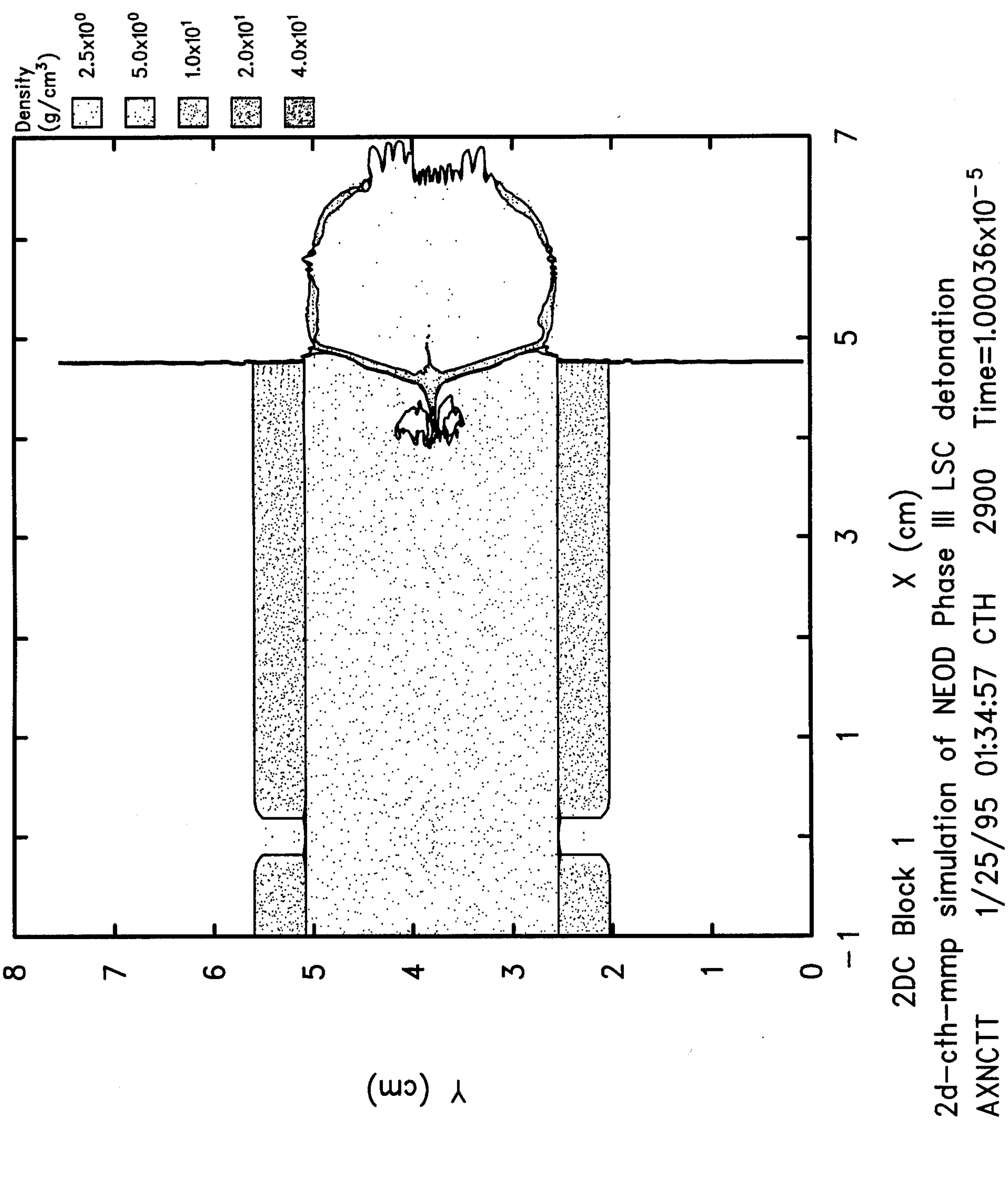
Density
(g/cm³)
2.5x10⁰
5.0x10⁰
1.0x10¹
2.0x10¹
4.0x10¹
Y (cm)
X (cm)
2DC Block 1
2d-cth-mmp simulation of NEOD Phase III LSC detonation
AXNCTT 1/25/95 01:34:57 CTH 2900 Time=1.00036x10⁻⁵

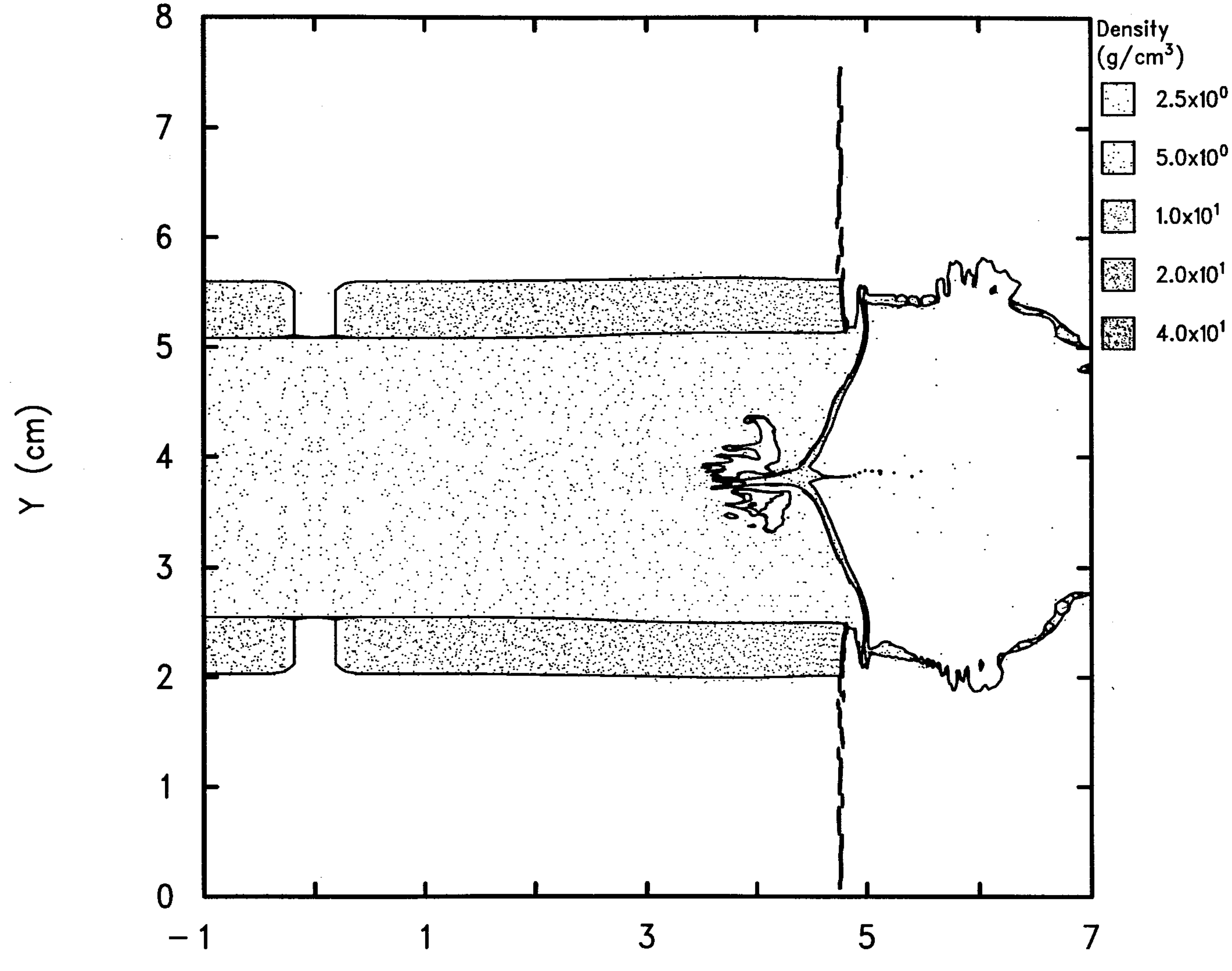

2DC Block 1

2d-cth-mmp simulation of NEOD Phase III LSC detonation

AYJAMT 1/25/95 10:03:14 CTH 4258 Time=1.50031×10^{-5}

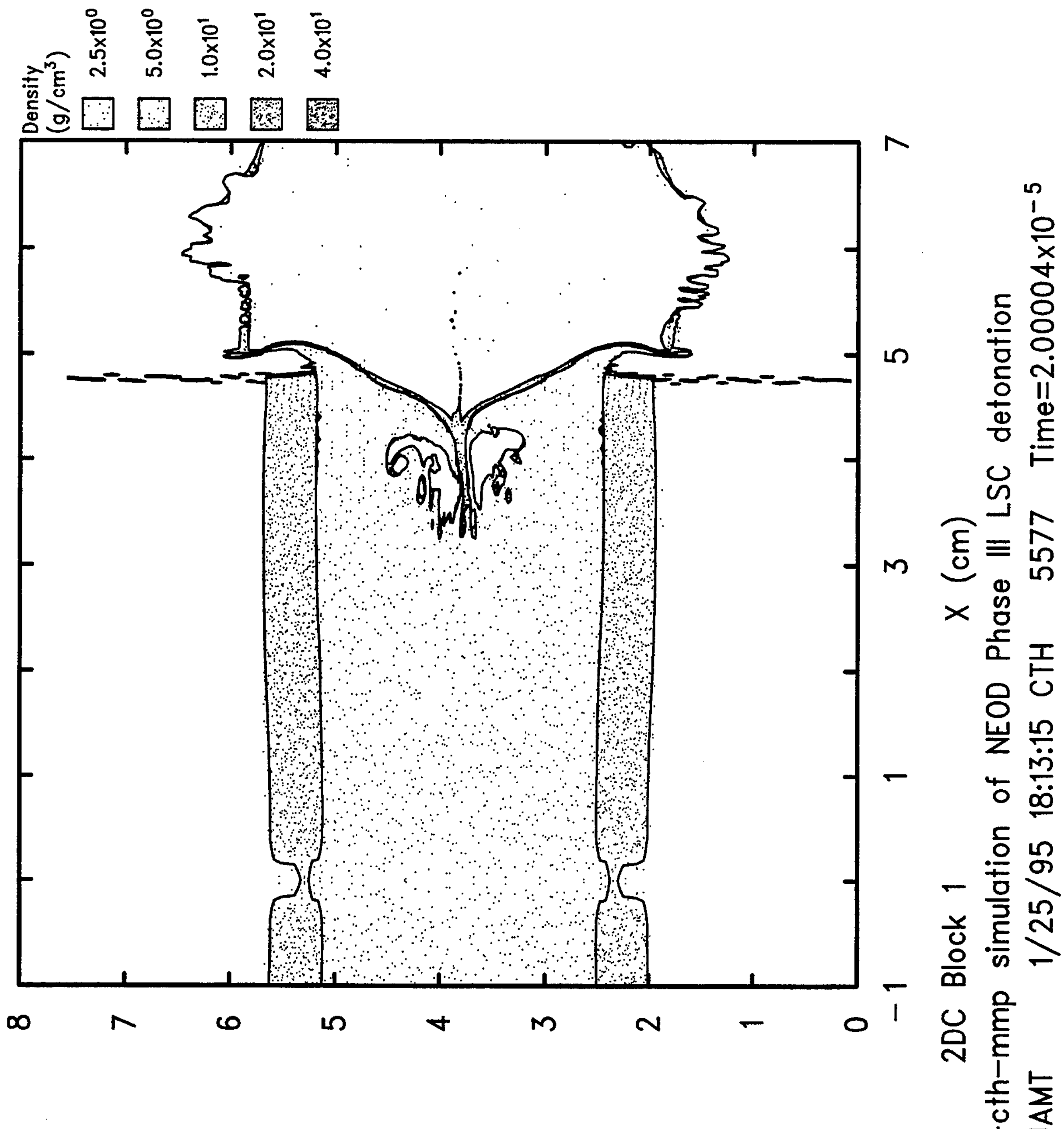
Density
(g/cm³)
2.5x10⁰
5.0x10⁰
1.0x10¹
2.0x10¹
4.0x10¹
Y (cm)
X (cm)
2DC Block 1
2d-cth-mmp simulation of NEOD Phase III LSC detonation
AYJAMT 1/25/95 18:13:15 CTH 5577 Time=2.00004x10⁻⁵

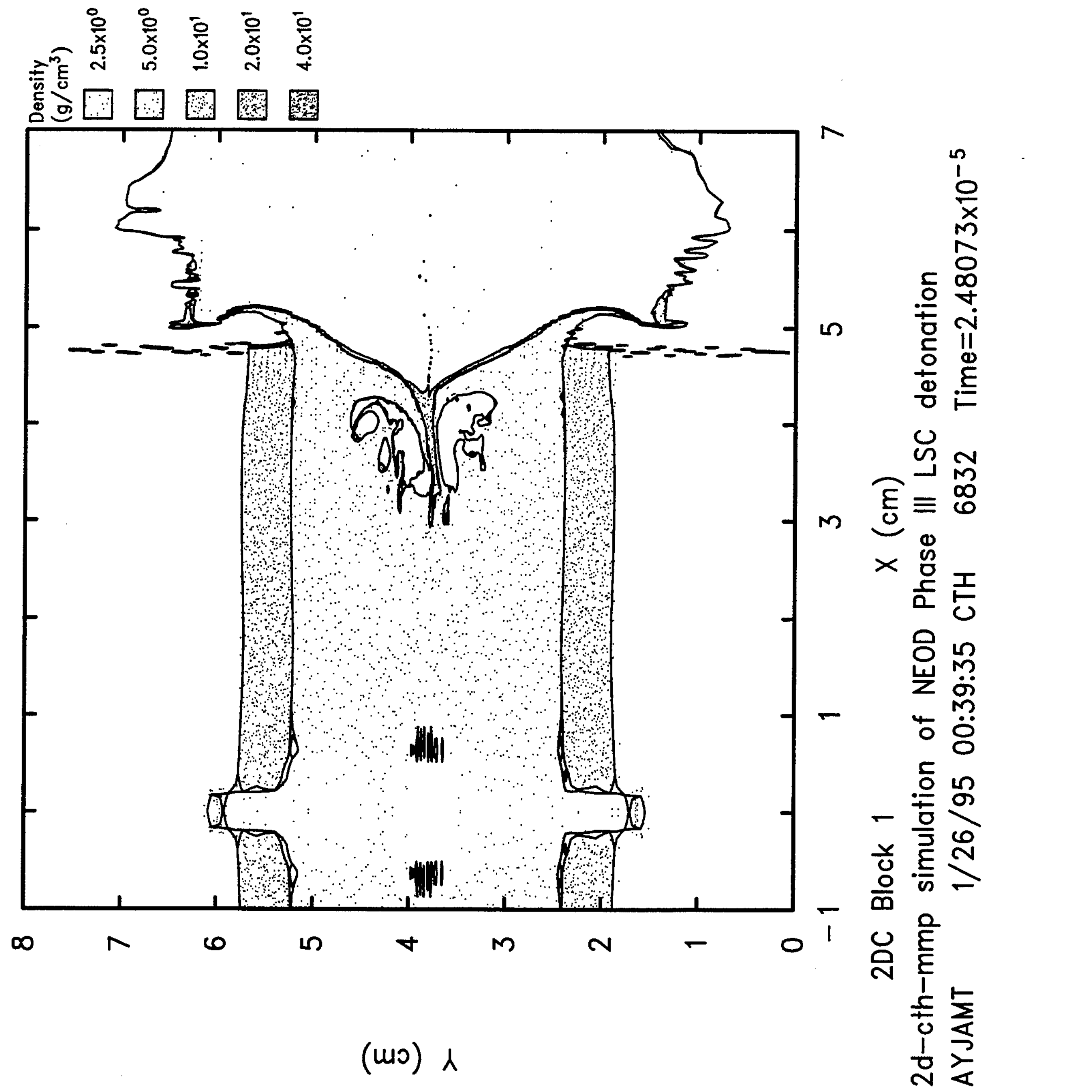

Density (g/cm³)
2.5x10⁰
5.0x10⁰
1.0x10¹
2.0x10¹
4.0x10¹
Y (cm)
X (cm)
2DC Block 1
2d-cth-mmp simulation of NEOD Phase III LSC detonation
AYJAMT 1/26/95 00:39:35 CTH 6832 Time=2.48073x10⁻⁵

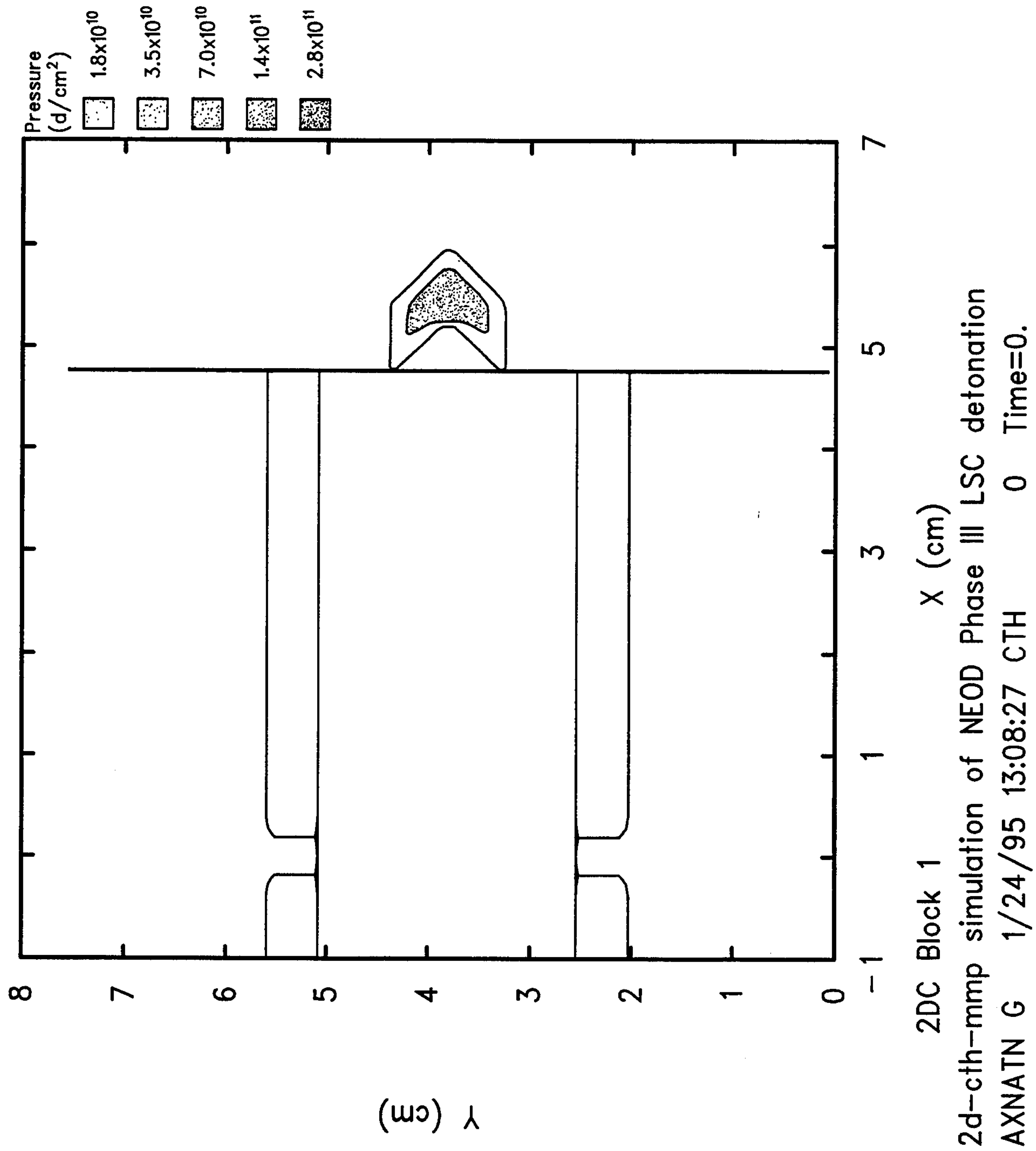

Pressure
(d/cm²)
1.8x10¹⁰
3.5x10¹⁰
7.0x10¹⁰
1.4x10¹¹
2.8x10¹¹
Y (cm)
X (cm)
2DC Block 1
2d-cth-mmp simulation of NEOD Phase III LSC detonation
AXNATN G 1/24/95 13:08:27 CTH 0 Time=0.

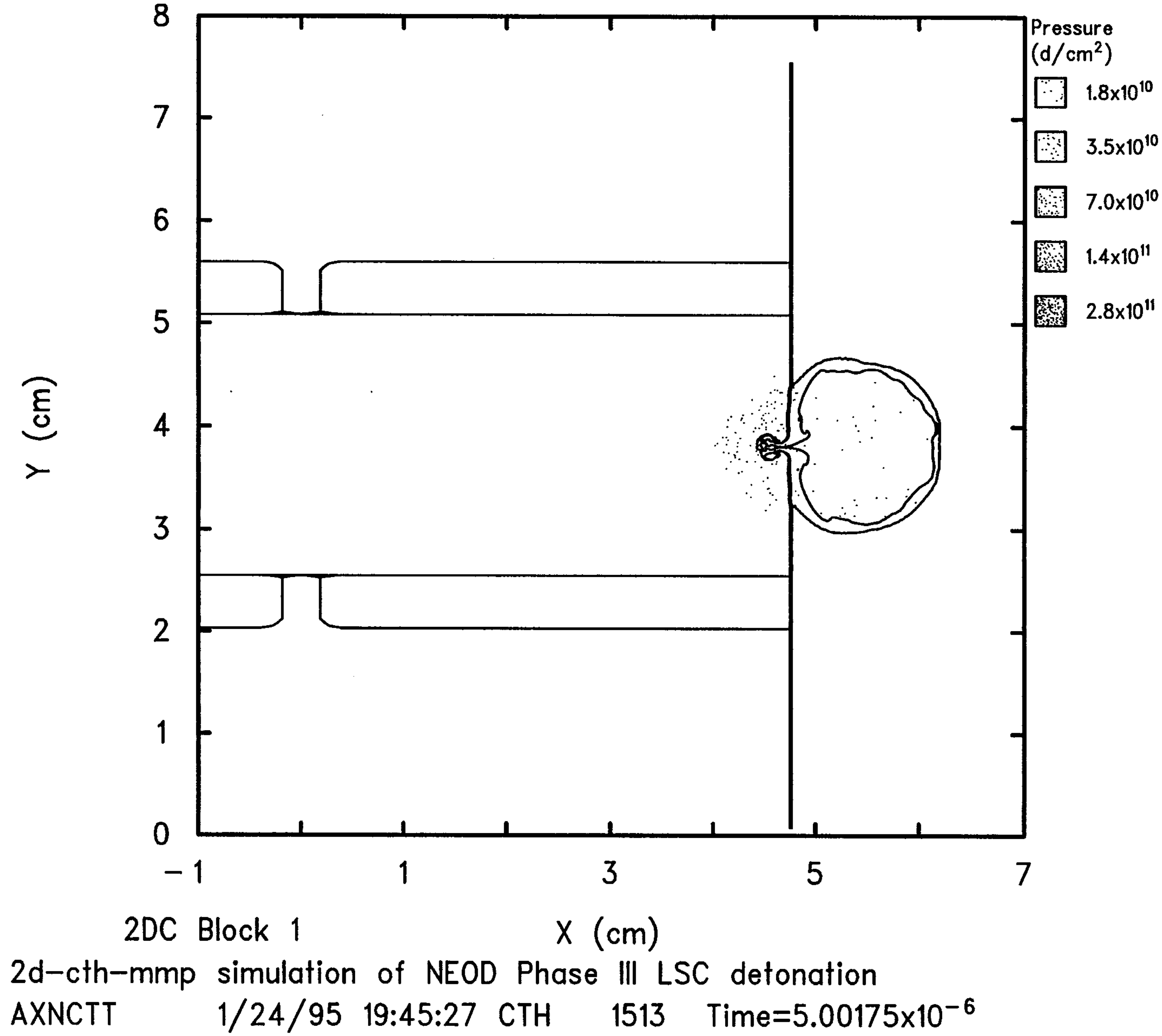
Pressure
(d/cm^2)
1.8x10^{10}
3.5x10^{10}
7.0x10^{10}
1.4x10^{11}
2.8x10^{11}
Y (cm)
X (cm)
2DC Block 1
2d-cth-mmp simulation of NEOD Phase III LSC detonation
AXNCTT 1/24/95 19:45:27 CTH 1513 Time=5.00175x10^{-6}

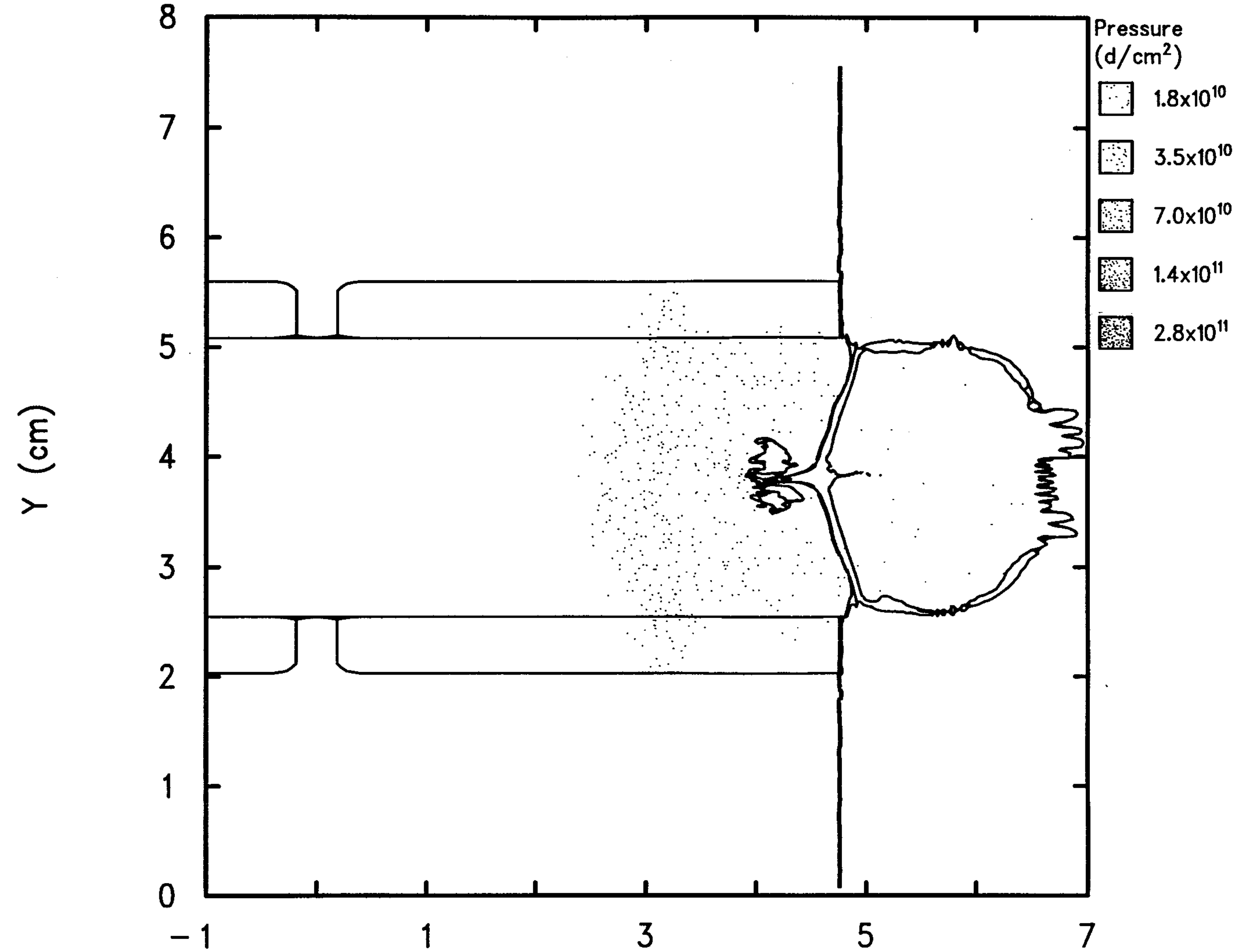

2DC Block 1 X (cm)

2d−cth−mmp simulation of NEOD Phase III LSC detonation

AXNCTT 1/25/95 01:34:57 CTH 2900 Time=1.00036×10^{-5}

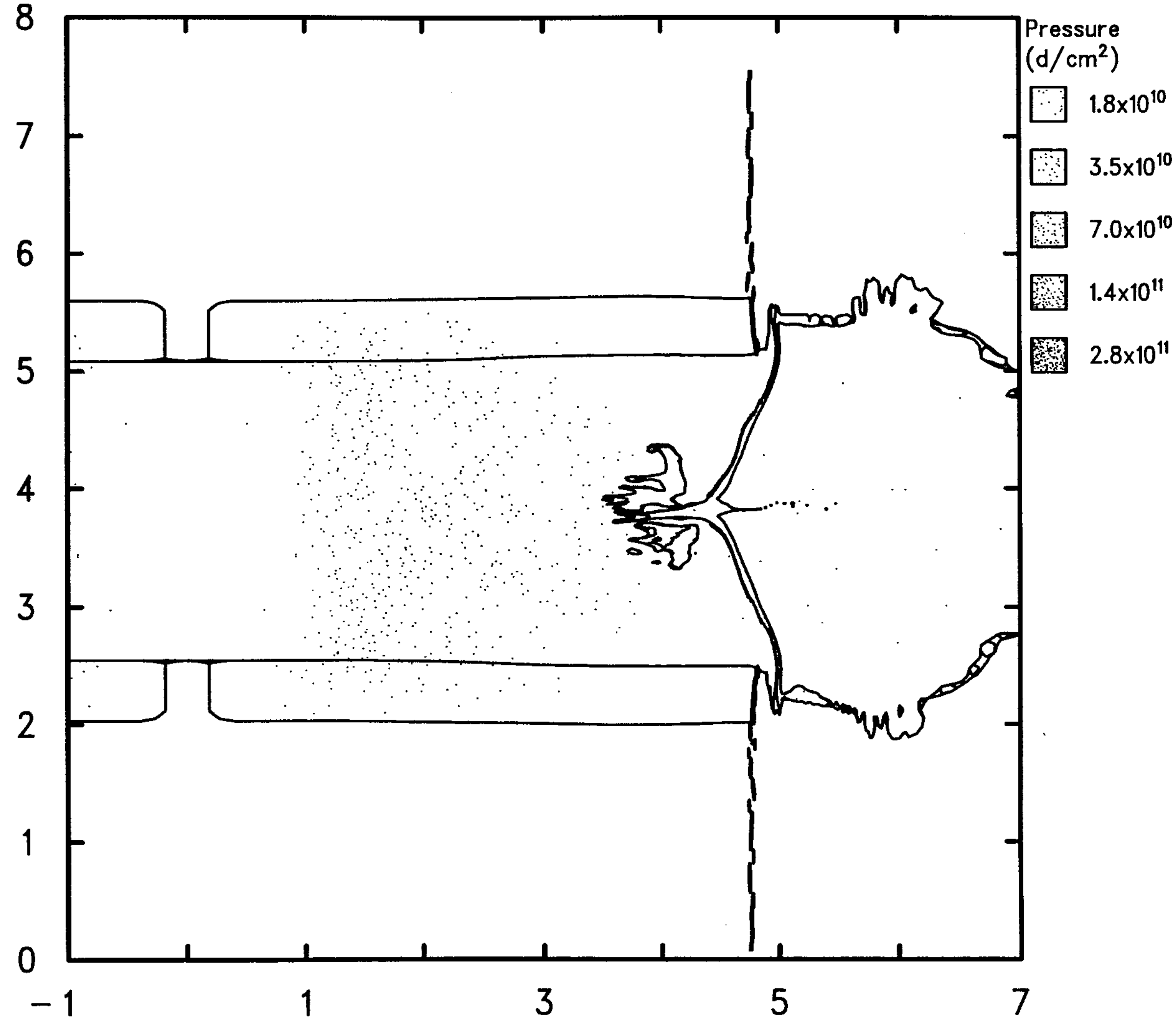

2DC Block 1

2d-cth-mmp simulation of NEOD Phase III LSC detonation

AYJAMT 1/25/95 10:03:14 CTH 4258 Time=1.50031×10^{-5}

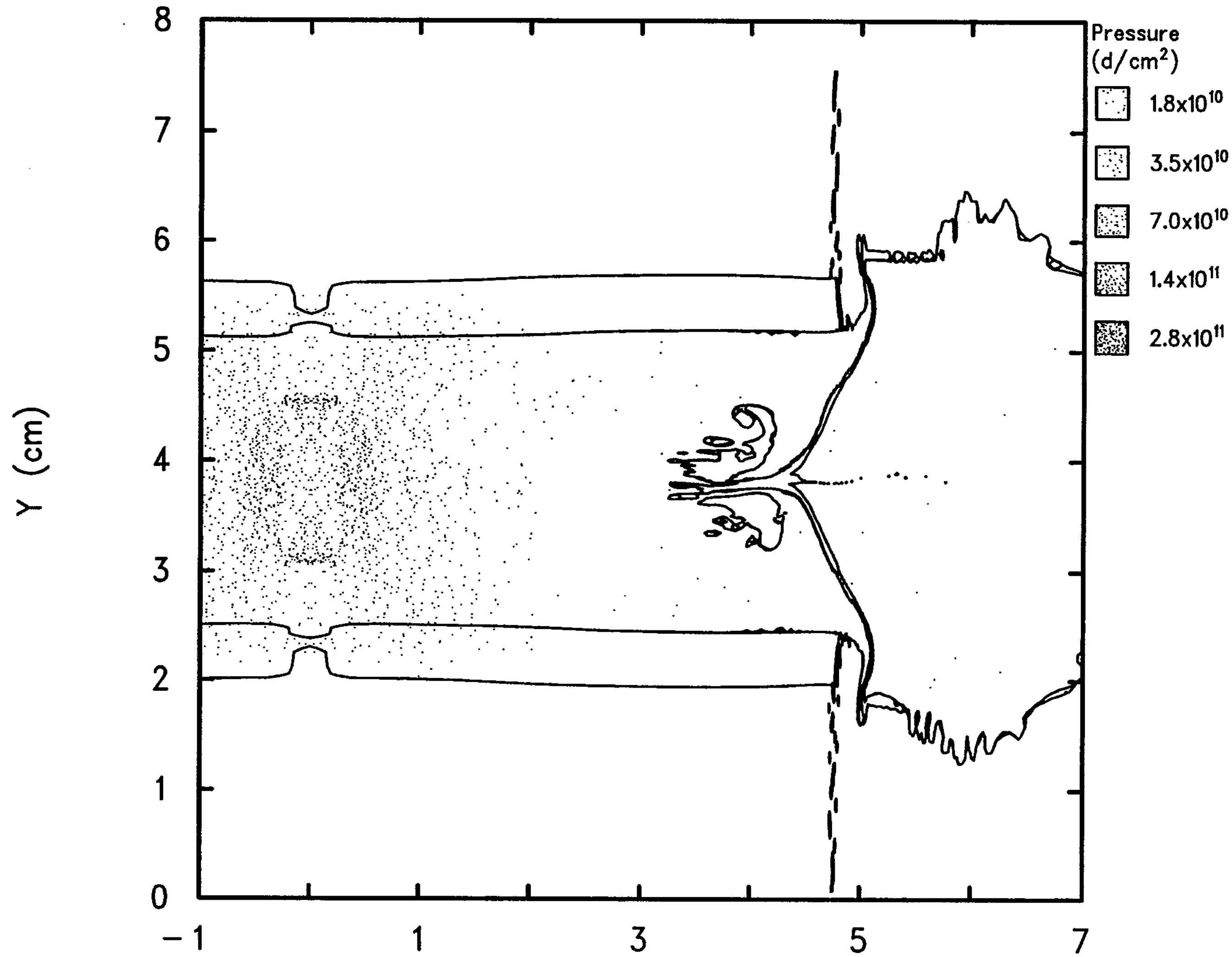

2DC Block 1 X (cm)
2d-cth-mmp simulation of NEOD Phase III LSC detonation
AYJAMT 1/25/95 18:13:15 CTH 5577 Time=2.00004×10^{-5}

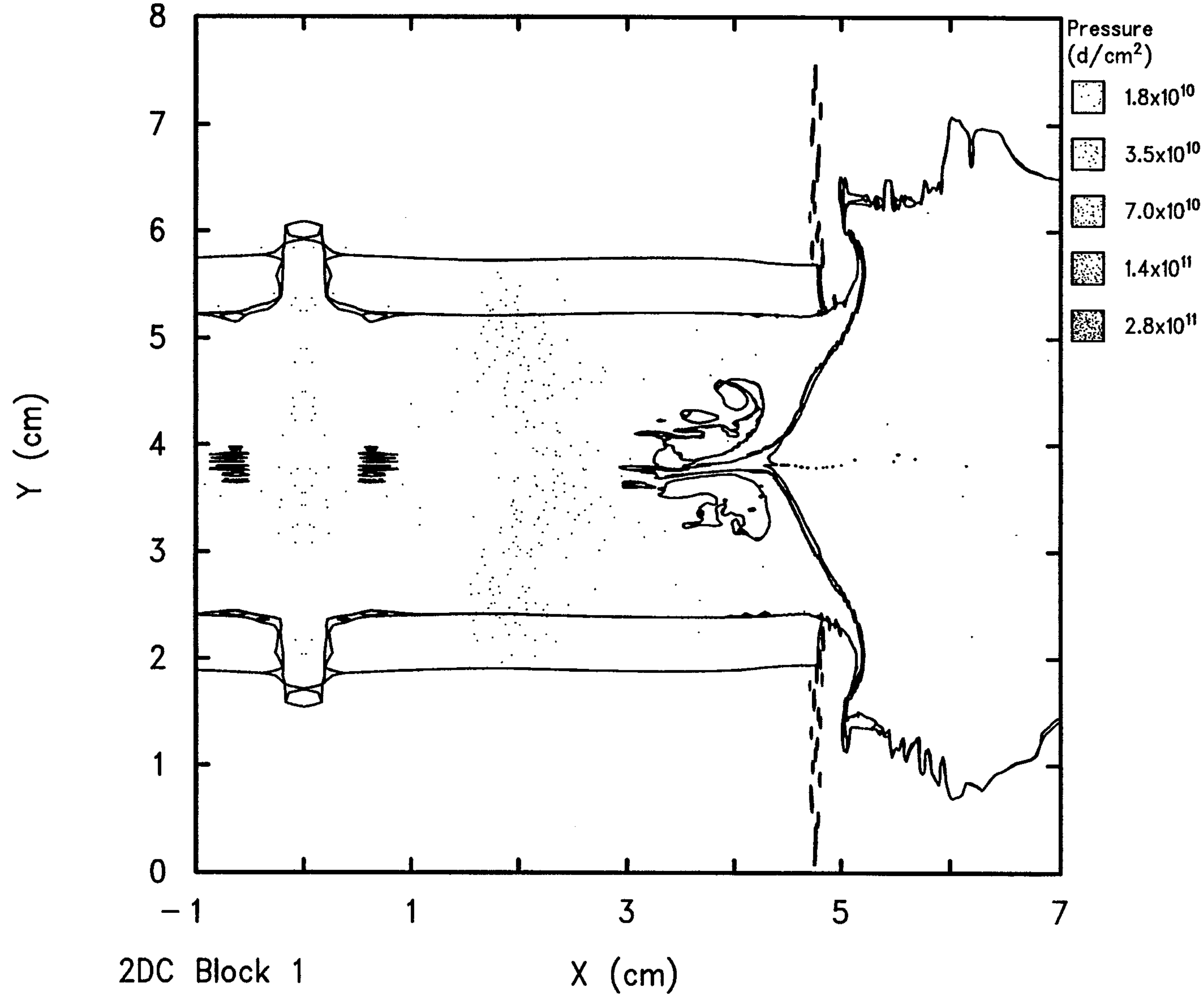

2DC Block 1

2d-cth-mmp simulation of NEOD Phase III LSC detonation

AYJAMT 1/26/95 00:39:35 CTH 6832 Time=2.48073×10^{-5}

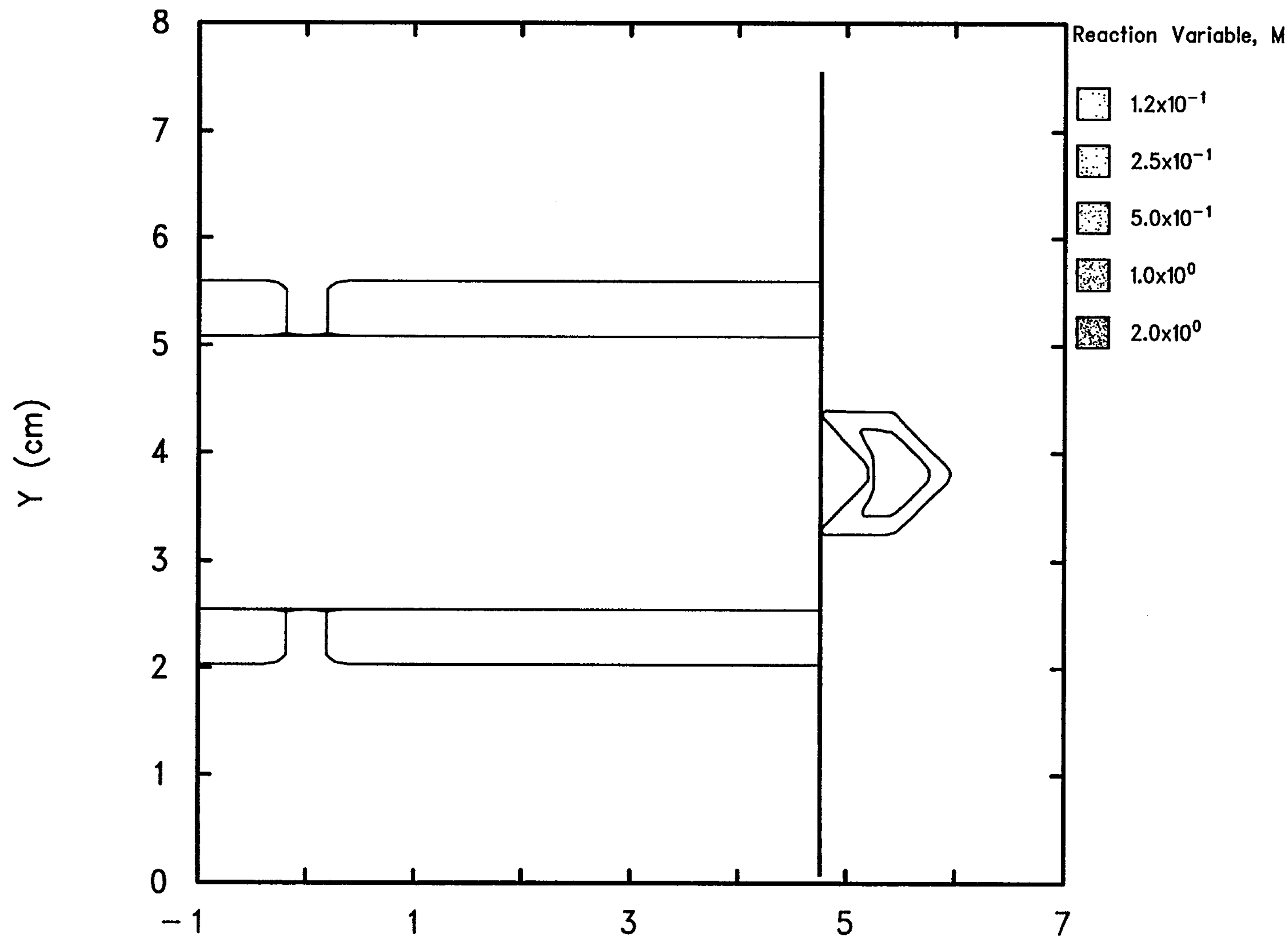

2DC Block 1

2d-cth-mmp simulation of NEOD Phase III LSC detonation

AXNATN G 1/24/95 13:08:27 CTH 0 Time=0.

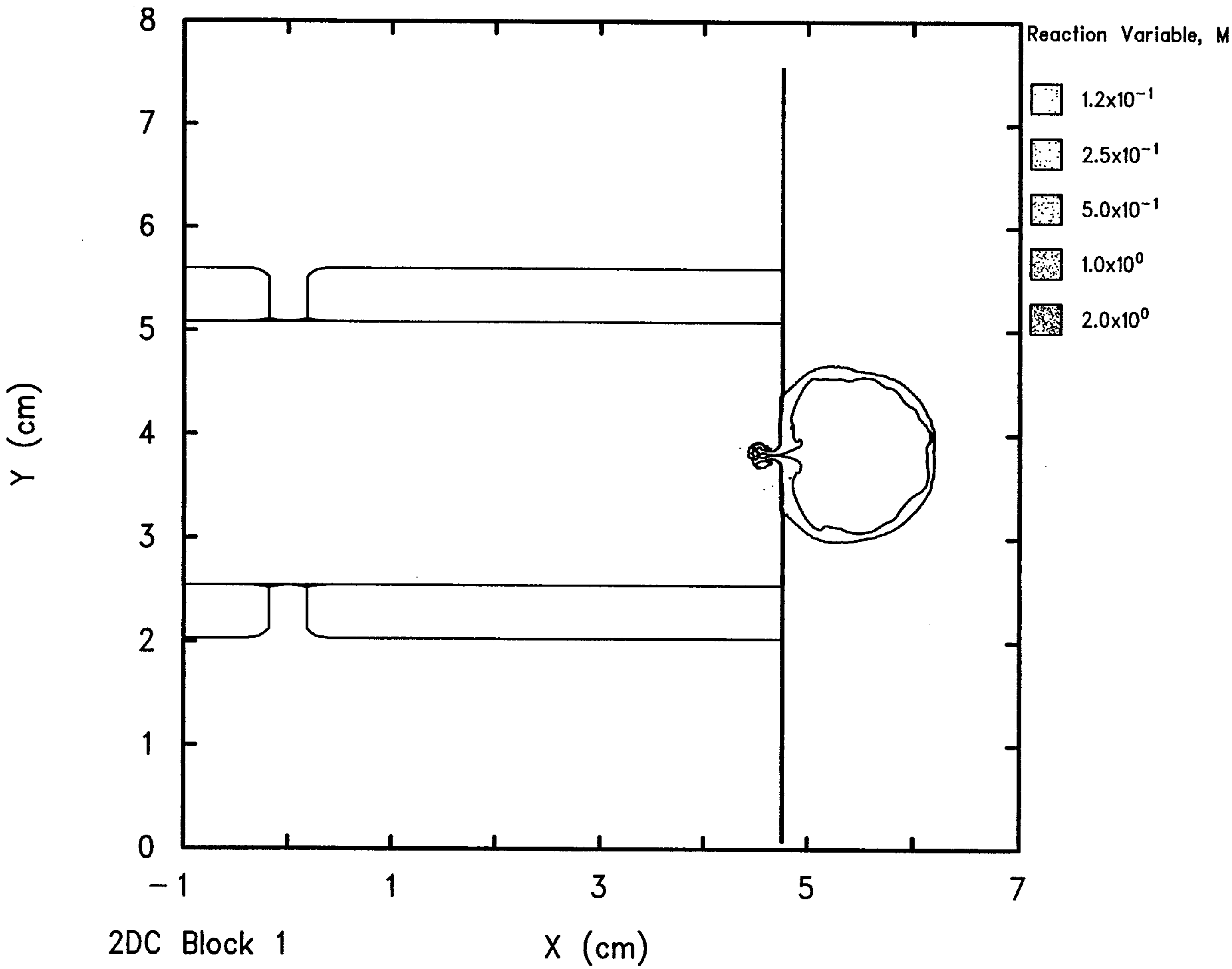

2DC Block 1

2d–cth–mmp simulation of NEOD Phase III LSC detonation

AXNCTT 1/24/95 19:45:27 CTH 1513 Time=5.00175x10^{-6}

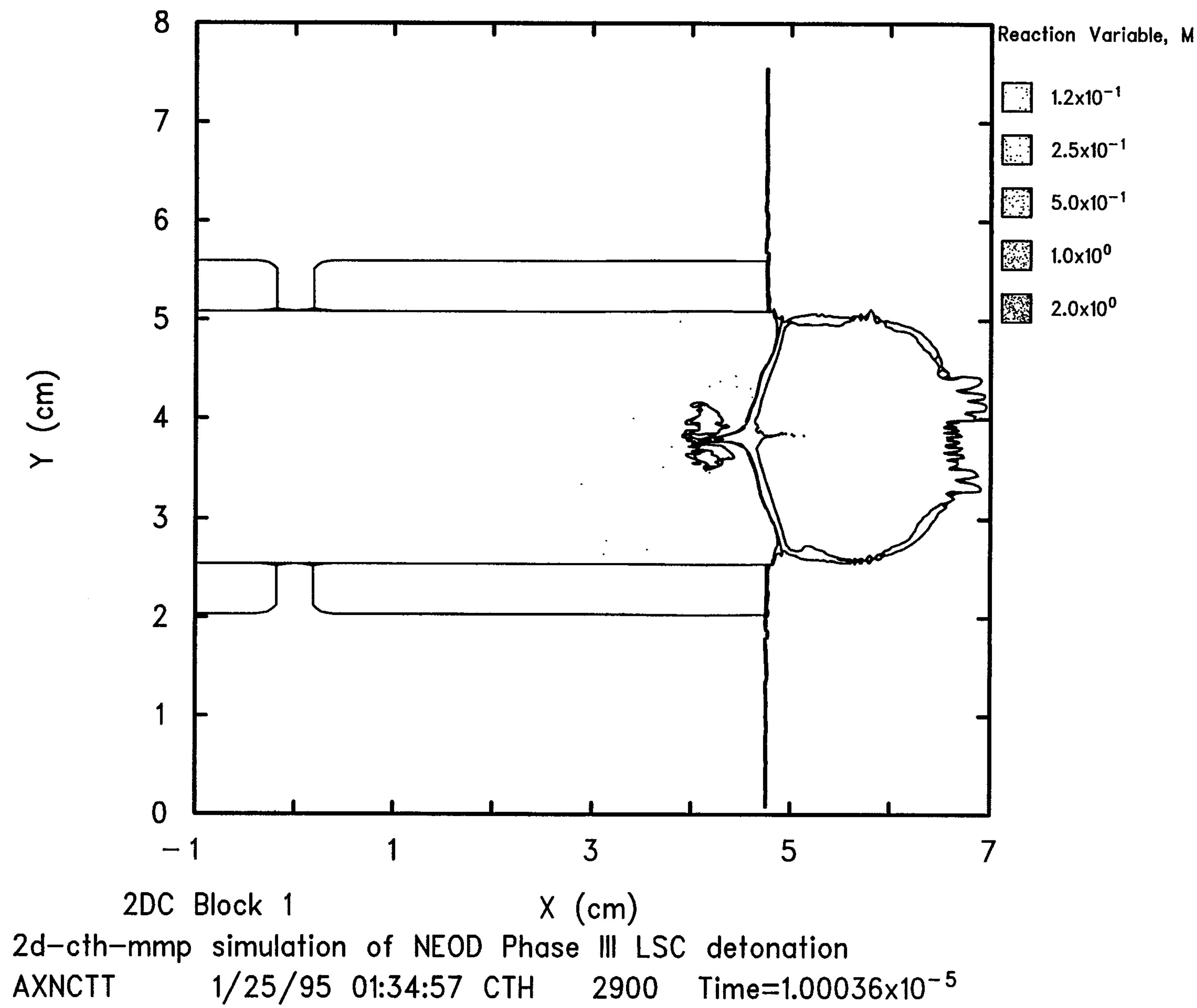
Reaction Variable, M
1.2x10⁻¹
2.5x10⁻¹
5.0x10⁻¹
1.0x10⁰
2.0x10⁰
Y (cm)
X (cm)
2DC Block 1
2d-cth-mmp simulation of NEOD Phase III LSC detonation
AXNCTT 1/25/95 01:34:57 CTH 2900 Time=1.00036x10⁻⁵

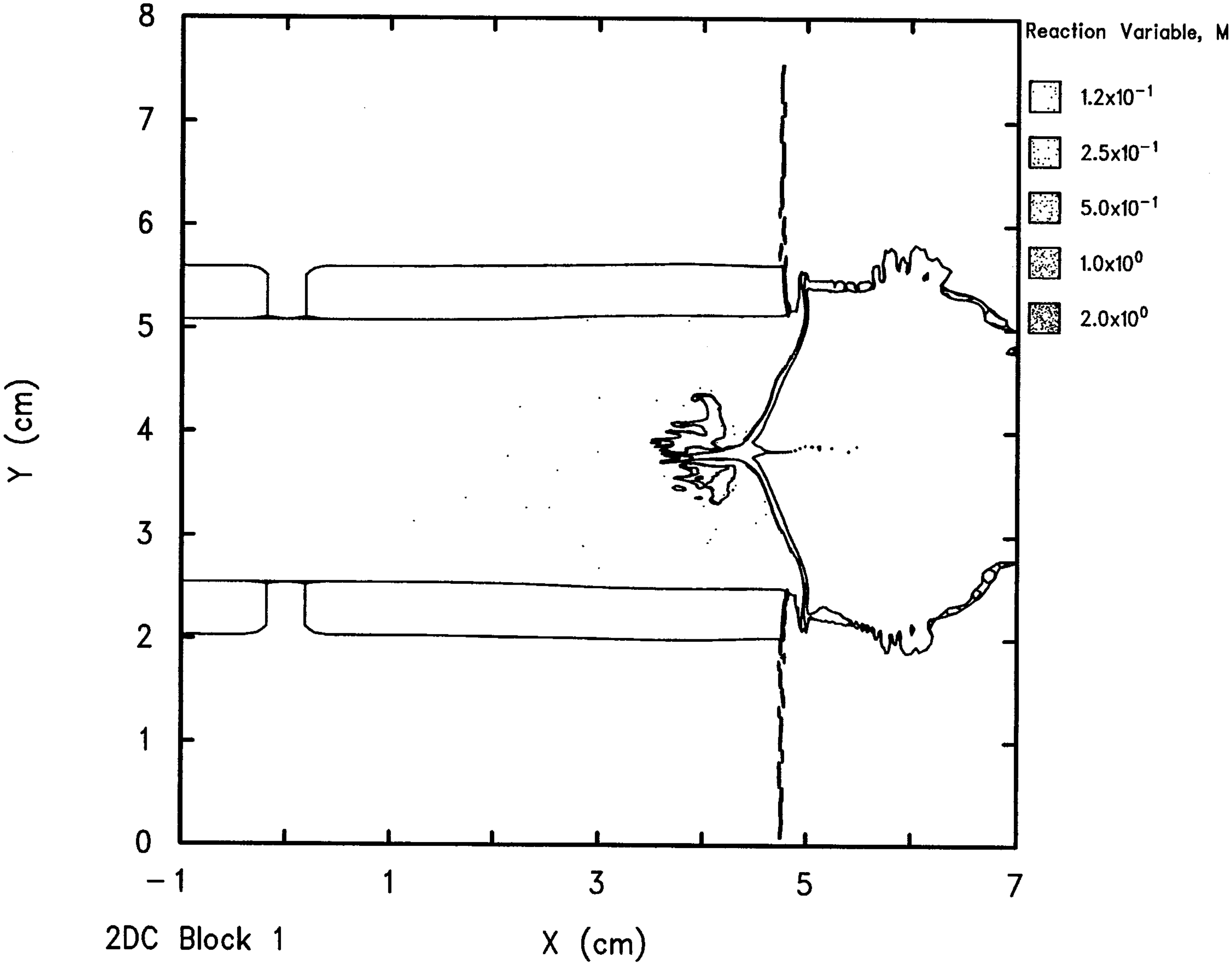

2d-cth-mmp simulation of NEOD Phase III LSC detonation

AYJAMT 1/25/95 10:03:14 CTH 4258 Time=1.50031×10^{-5}

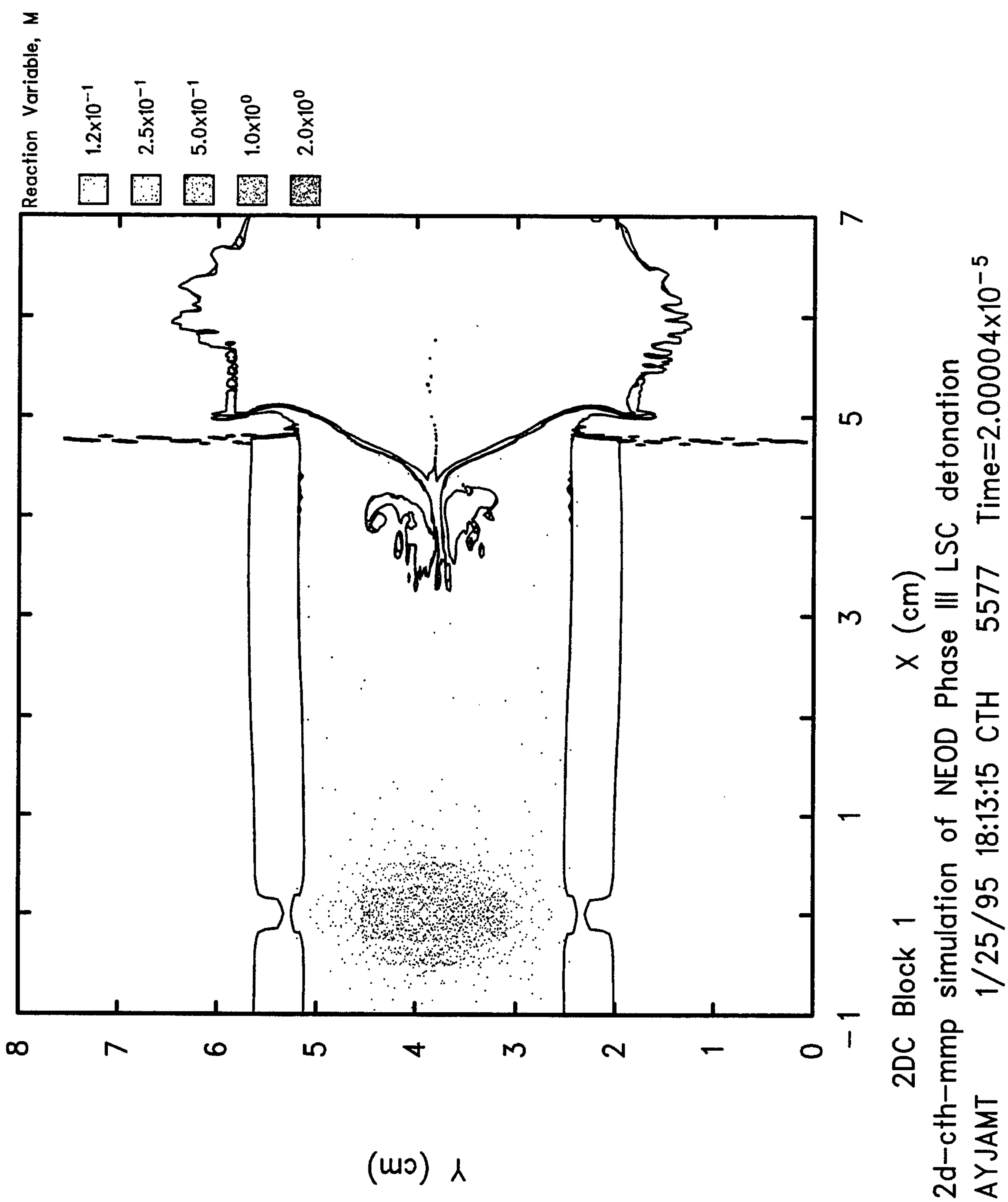

Reaction Variable, M
1.2x10^{-1}
2.5x10^{-1}
5.0x10^{-1}
1.0x10^{0}
2.0x10^{0}
Y (cm)
X (cm)
2DC Block 1
2d-cth-mmp simulation of NEOD Phase III LSC detonation
AYJAMT 1/25/95 18:13:15 CTH 5577 Time=2.00004x10^{-5}

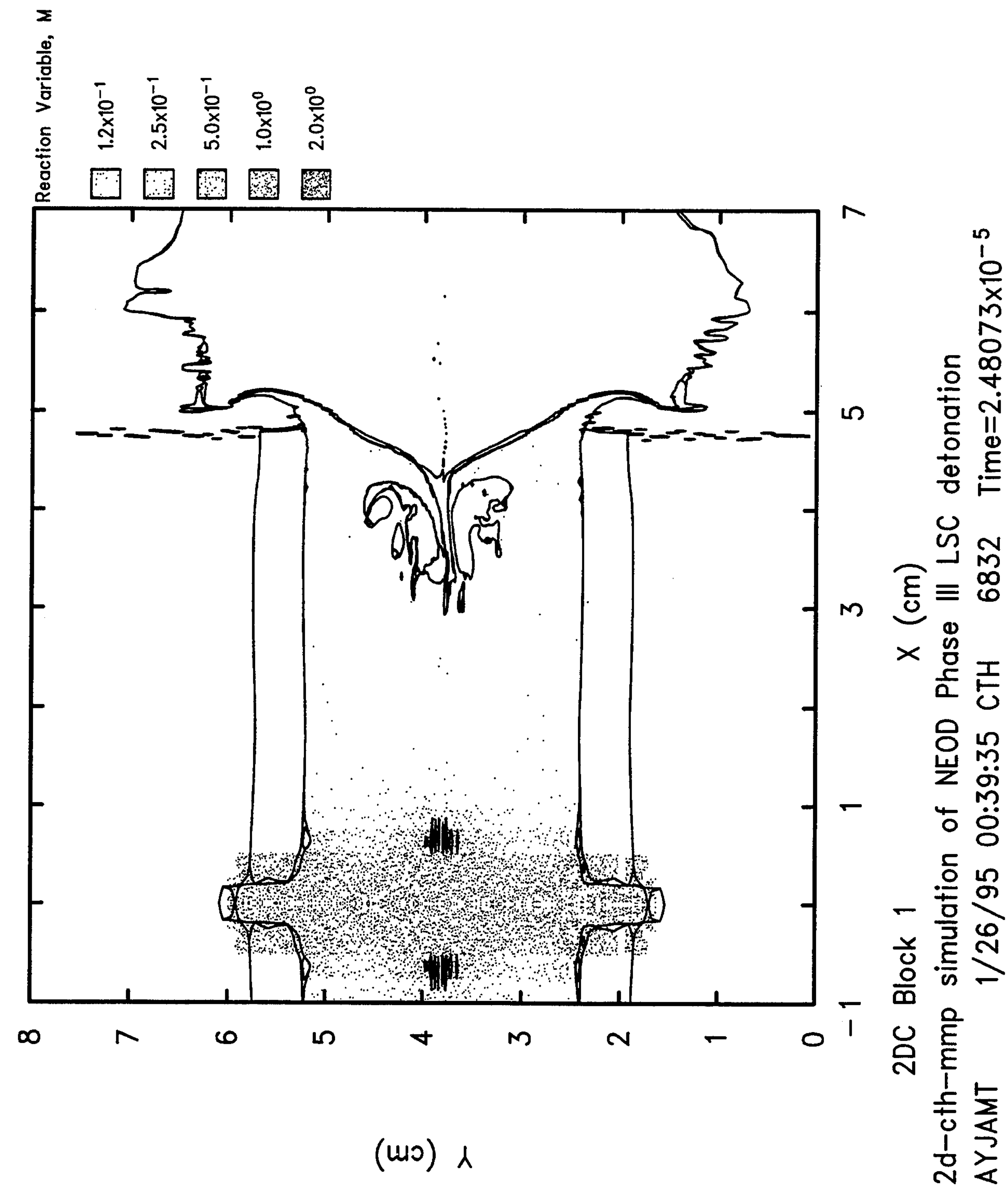
Reaction Variable, M
1.2×10^{-1}
2.5×10^{-1}
5.0×10^{-1}
1.0×10^{0}
2.0×10^{0}
Y (cm)
X (cm)
2DC Block 1
2d-cth-mmp simulation of NEOD Phase III LSC detonation
AYJAMT 1/26/95 00:39:35 CTH 6832 Time=2.48073×10^{-5}

APPENDIX C:

LX-14 SIMULATION INPUT DECK

INTENTIONALLY LEFT BLANK.

```
*
*eor*cgenin
*
2d-cth-mmp simulation of NEOD Phase III LSC detonation
*
control
 ep
 mmp
endcontrol
*
mesh
 block  geometry 2dc  type e
  x0=0.0
   x1  n=70  w=4.747  dxl=0.0055
   x2  n=3   w=0.0155 rat=1
   x3  n=110 w=1.252  dxf=0.0055
   x4  n=17  w=1.5    dxf=0.021
  endx
  y0=0.0
   y1  dyf 0.15    dyl 0.05     w 2.54
   y2  dyf 0.05    dyl 0.0055   w 1.27
   y3  dyf 0.0055  dyl 0.05     w 1.27
   y4  dyf 0.05    dyl 0.15     w 2.54
  endy
  xact=4.76,5.95
  yact=3.24,4.40
 endblock
endmesh
*
insertion of material
 block 1
*
  package 'AL Case - 1'
   material 1
   numsub 50
   pressure 1.0e6
   insert box
    x1  4.747    x2  4.76250
    y1  0.000    y2  15.24000
   endinsert
  endpackage
*
  package 'HE Patty - 1'
   material 2
   numsub 50
   pressure 1.0e6
```

```
  insert box
   x1  0.000    x2  4.74700
   y1  2.540    y2  5.08000
  endinsert
 endpackage
*
 package 'HE LSC - 1'
  material 3
  numsub 50
*   G. Kerley told me (12/1/94) that RDX @o=1.70 g/cc detonates at
*   T=3560K=0.30678eV; Po=13.8GPa.  This calculation was done with BCAT
*   or PANDA. Specifying the insert at this temp is equivalent to
*   detonating the whole mass at time=0.
  temperature 0.30678
  insert uds
   point  5.24615  3.81328
   point  5.24615  3.77718
   point  5.24615  3.71811
   point  5.23957  3.66561
   point  5.21983  3.60982
   point  5.20009  3.56716
   point  5.16719  3.51465
   point  5.14087  3.46543
   point  5.13758  3.44902
   point  5.14416  3.42933
   point  5.15403  3.41948
   point  5.17706  3.41292
   point  5.20338  3.41620
   point  5.25273  3.41620
   point  5.30538  3.41620
   point  5.35473  3.41620
   point  5.39421  3.42276
   point  5.42382  3.43589
   point  5.44685  3.45230
   point  5.48304  3.48183
   point  5.52253  3.51465
   point  5.56859  3.56388
   point  5.63768  3.63607
   point  5.69361  3.69186
   point  5.73639  3.73452
   point  5.75284  3.75749
   point  5.75613  3.77390
   point  5.75942  3.80344
   point  5.75613  3.82969
   point  5.75613  3.84938
   point  5.72652  3.88548
   point  5.67058  3.95111
```

```
    point  5.61465  4.00362
    point  5.51595  4.10535
    point  5.45672  4.15457
    point  5.43040  4.17755
    point  5.40737  4.19395
    point  5.37118  4.20052
    point  5.29551  4.21364
    point  5.20667  4.22021
    point  5.16390  4.22021
    point  5.13429  4.22021
    point  5.12113  4.21036
    point  5.11784  4.19724
    point  5.12113  4.18411
    point  5.13100  4.17098
    point  5.14087  4.14473
    point  5.15732  4.11191
    point  5.18035  4.07253
    point  5.20338  4.03643
    point  5.22641  3.99377
    point  5.23628  3.95439
    point  5.23957  3.91173
    point  5.24286  3.87563
    point  5.24286  3.83625
    point  5.24615  3.81656
  endinsert
endpackage
package 'Lead LSC - 1'
  material 4
  numsub 50
  pressure 1.0e6
  insert uds
    point  5.19022  3.81000
    point  5.19351  3.79031
    point  5.19351  3.76078
    point  5.18693  3.74437
    point  5.17706  3.73452
    point  5.13100  3.68202
    point  5.06519  3.60982
    point  4.93359  3.47527
    point  4.80527  3.34401
    point  4.77895  3.31775
    point  4.77237  3.31119
    point  4.76579  3.29478
    point  4.76579  3.27509
    point  4.77237  3.25868
    point  4.78553  3.24556
    point  4.80198  3.24227
```

point	4.82172	3.24227
point	4.87437	3.24227
point	5.12113	3.24556
point	5.29880	3.24227
point	5.33828	3.24556
point	5.39092	3.25212
point	5.43369	3.26196
point	5.46659	3.28494
point	5.52911	3.34072
point	5.66071	3.47199
point	5.79232	3.60326
point	5.91405	3.72468
point	5.93051	3.75093
point	5.94038	3.77390
point	5.94696	3.79359
point	5.94696	3.81656
point	5.94367	3.83625
point	5.93380	3.85266
point	5.92392	3.86579
point	5.89760	3.89532
point	5.83838	3.95767
point	5.76600	4.02659
point	5.70348	4.08894
point	5.63439	4.15457
point	5.55872	4.23333
point	5.46988	4.33178
point	5.45014	4.35147
point	5.43369	4.36788
point	5.41395	4.37444
point	5.38763	4.37773
point	5.30867	4.38101
point	5.20009	4.38101
point	5.03229	4.38429
point	4.84804	4.38757
point	4.80198	4.39085
point	4.78224	4.38101
point	4.77237	4.37116
point	4.76908	4.35804
point	4.76908	4.34819
point	4.77237	4.33178
point	4.78224	4.31537
point	4.81843	4.27928
point	4.88424	4.21036
point	4.95991	4.12504
point	5.05203	4.02987
point	5.11126	3.96424
point	5.15403	3.92486

```
      point  5.17377  3.89204
      point  5.18693  3.86579
      point  5.19022  3.83953
      point  5.19022  3.81656
    endinsert
  endpackage
*
  package 'Cu Damper - Bottom'
    material 5
    numsub 50
    pressure 1.0e6
    insert box
      x1  0.258    x2  4.747
      y1  2.032    y2  2.540
    endinsert
  endpackage
*
  package 'Cu Damper - Top'
    material 5
    numsub 50
    pressure 1.0e6
    insert box
      x1  0.258    x2  4.747
      y1  5.080    y2  5.588
    endinsert
  endpackage
*
 endblock
endinsertion
*
eos
*
* Aluminum Mie-Grüneisen
 mat1  mgrun  eos='7075-t6_al  feos='/b/scheffle/cth/MGR_data'
      ro=2.804    cs=0.5200E6  s=1.360    go=2.20   cv=1.07E11
*
* LX-14 Patty
*  Parameters estimated to be roughly halfway between RDX and TNT.
*  RP and R0 made identical per advice of G. Kerley, to avoid bug.
 MAT2  SESAME  EOS=8231  FEOS='/b/scheffle/cth/sesame'
      RP=1.850  R0=1.850  CS=2.9E5  S=2.0  G0=1.0  CV=1.35E11
      TYP=2.0  PR=8.8E10  ZR=2.36  MR=1.5  PI=0.5E10
      RMAX=5.0  RMIN=0.01  TMAX=5.0  PT=1.0E13
** CEQ(I),I=1,40
**  8.2310E+03  0.0000E+00  1.0000E+00  1.8500E+00  2.5680E-02
**  0.0000E+00  1.9166E+06  1.0000E+00  1.3500E+11  1.0000E-02
**  5.0000E+00  6.6667E-01  3.3333E-01  2.0000E-01  1.8889E-01
```

```
** 3.4120E+00 -1.7943E+12 4.2272E+12 1.3500E+09 2.0000E+00
** 5.0000E+00 1.5000E+00 2.3600E+00 8.8000E+10 6.8497E+10
** 2.9000E+05 2.0000E+00 5.0000E+09 1.8500E+00 1.2459E+01
** 0.0000E+00 0.0000E+00 0.0000E+00 0.0000E+00 0.0000E+00
** 0.0000E+00 0.0000E+00 0.0000E+00 5.1450E+01 1.0004E+02
*
* CH-6 (RDX=HMX) HE as LSC charge
 mat3 SESAME EOS=8012 FEOS='/b/scheffle/cth/sesame'
     RP=1.70 R0=1.70
*
* Lead (6% Antimony) Mie-Gru (modified from Library data)
 mat4 mgrun eos=lead_s feos='/b/scheffle/cth/MGR_data'
     ro=10.9    cs=0.2006E6 s=1.429    go=2.74    cv=1.5512E10
* Copper Mie-Grüneisen
 mat5 mgrun eos=copper feos='/b/scheffle/cth/MGR_data'
     ro=8.930    cs=3.940E5  s=1.489    go=1.99    cv=4.56E10
endeos
*
* heburn option not needed, with predetonated sesame option
**heburn
**endheburn
epdata
  vpsave
* Library 7075-T6 Al.
  matep 1 steinberg-guinan='7075-T6_ALUMINUM' fvp='/b/scheffle/cth/VP_data'
     poisson 0.16
 r0st=2.804   tm0st=0.105127 atmst=1.70 gm0st=2.20
 ast=6.52E-12 bst=7.148680  nst=0.10  c1st=0.00
 c2st=0.00    g0st=0.267E+12 btst=965.0 eist=0.00    ypst=0.00
 ukst=0.00    ysmst=0.00     yast=0.00 y0st=4.2E+09 ymst=8.1E+09
* Library Lead
  matep 4 steinberg-guinan='LEAD' fvp='/b/scheffle/cth/VP_data'
     poisson 0.43
 r0st=11.34   tm0st=0.065489 atmst=2.20 gm0st=2.74
 ast=11.63E-12 bst=13.461800 nst=0.52  c1st=0.00
 c2st=0.00    g0st=8.6E+10   btst=110.0 eist=0.00    ypst=0.00
 ukst=0.00    ysmst=0.00     yast=0.00 y0st=8.0E+07 ymst=1.0E+09
*
  matep 5 steinberg-guinan='COPPER' fvp='/b/scheffle/cth/VP_data'
     poisson 0.32
 r0st=8.93    tm0st=0.154244 atmst=1.50 gm0st=2.02
 ast=2.83E-12 bst=4.375085  nst=0.45  c1st=0.00
 c2st=0.00    g0st=0.477E+12 btst=36.0 eist=0.00    ypst=0.00
 ukst=0.00    ysmst=0.00     yast=0.00 y0st=1.2E+09 ymst=6.4E+09
*
  mix 3
endep
```

```
*
*
*eor*cthin
*
 2d-cth-mmp NEOD Phase III LSC detonation
*
control
 tstop=40.e-6
* cpshift=900.
* rdumpf=3600
* ntbad 1000000
endcontrol
restart
 cycle=0
* file='rs04h'
 newfile=all
endrestart
*
cellthermo
 mmp
endcell
*
convct
 convect=1
 nofrag=2
 interface=high
endc
*
discard
 material 3  density -0.01  pressure 5.0e6  ton 7.0e-6
endd
*
edit
 shortt
  tim=0.  dt=10000.
 ends
 longt
  tim=0.  dt=10000.
 endl
 plott
  time=0.  dtfreq=5.0e-6
 endp
endedit
*
mindt
 time=0.     dtmin=1.0e-13
endm
```

```
*
fracts
 stress
 pfrac1=-8.1E9
 pfrac3=-1.0E9
 pfmix =-5.0E6
 pfvoid=-5.0E6
endf
*
boundary
 bhydro
  block=1
   bxbot 0
   bxtop 2
   bybot 2
   bytop 2
  endb
 endh
endb
*
*eor*pltin
*
units cgsev
*
nlegend=off
*
time,0.0e-6,rest
color table 4
units cgsk
limits x=-8.0,8.0,1 y=0.0,16.0,1
*flegend=b
flegend=d
*2dplot,materials,mirror
2dplot,dots=density=10.,mirror,if
limits x=-1.0,7.0,1 y=0.0,8.0,1
*rbands, b1=1e9, b2=1e11, c1=236, c2=256, skip=2
*2dplot,materials
2dplot,dots=density=10.,mirror,if
nlegend=on
*2dplot bands=pressure, mirror, if
bands=1e9, 5e9, 1e10, 2e10, 4e10, 5e10, 6e10, 8e10, 1e11
2dplot dots=pressure=7e10 mirror if
*rbands, b1=0.0, b2=0.1, c1=236, c2=256, skip=2
*2dplot bands=hvb2, mirror if
bands=0.0, 0.01, 0.02, 0.03, 0.04, 0.05, 0.06, 0.07, 0.08, 0.09, 0.10
2dplot dots=hvb2=.50 mirror if
```

APPENDIX D:

LX-14 COMPUTATIONAL RESULTS

INTENTIONALLY LEFT BLANK.

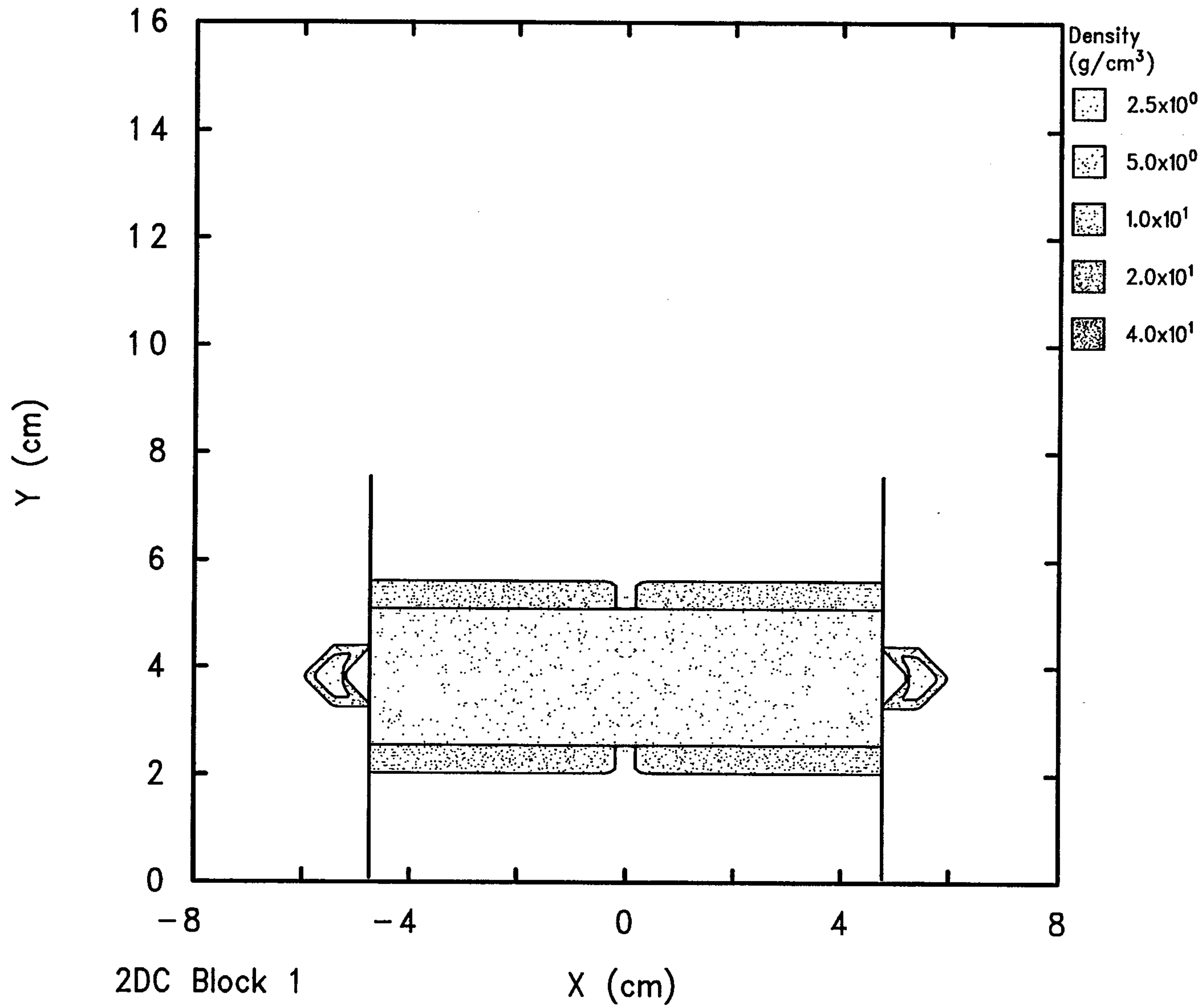

2DC Block 1
2d-cth-mmp simulation of NEOD Phase III LSC detonation
CTKCZY G 3/20/95 10:33:46 CTH 0 Time=0.

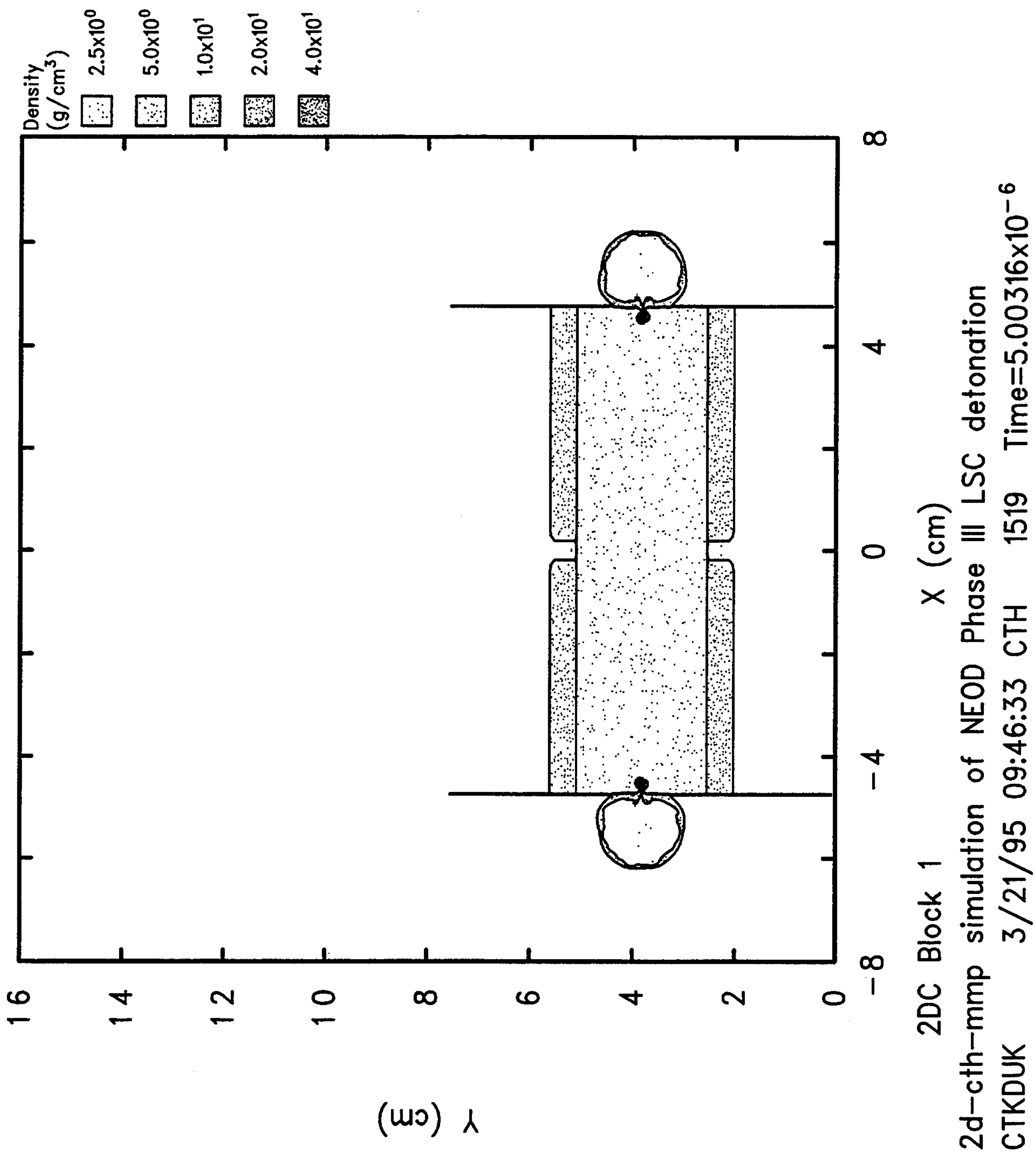
Density (g/cm3)
2.5x10^0
5.0x10^0
1.0x10^1
2.0x10^1
4.0x10^1
Y (cm)
X (cm)
2DC Block 1
2d-cth-mmp simulation of NEOD Phase III LSC detonation
CTKDUK 3/21/95 09:46:33 CTH 1519 Time=5.00316x10^-6

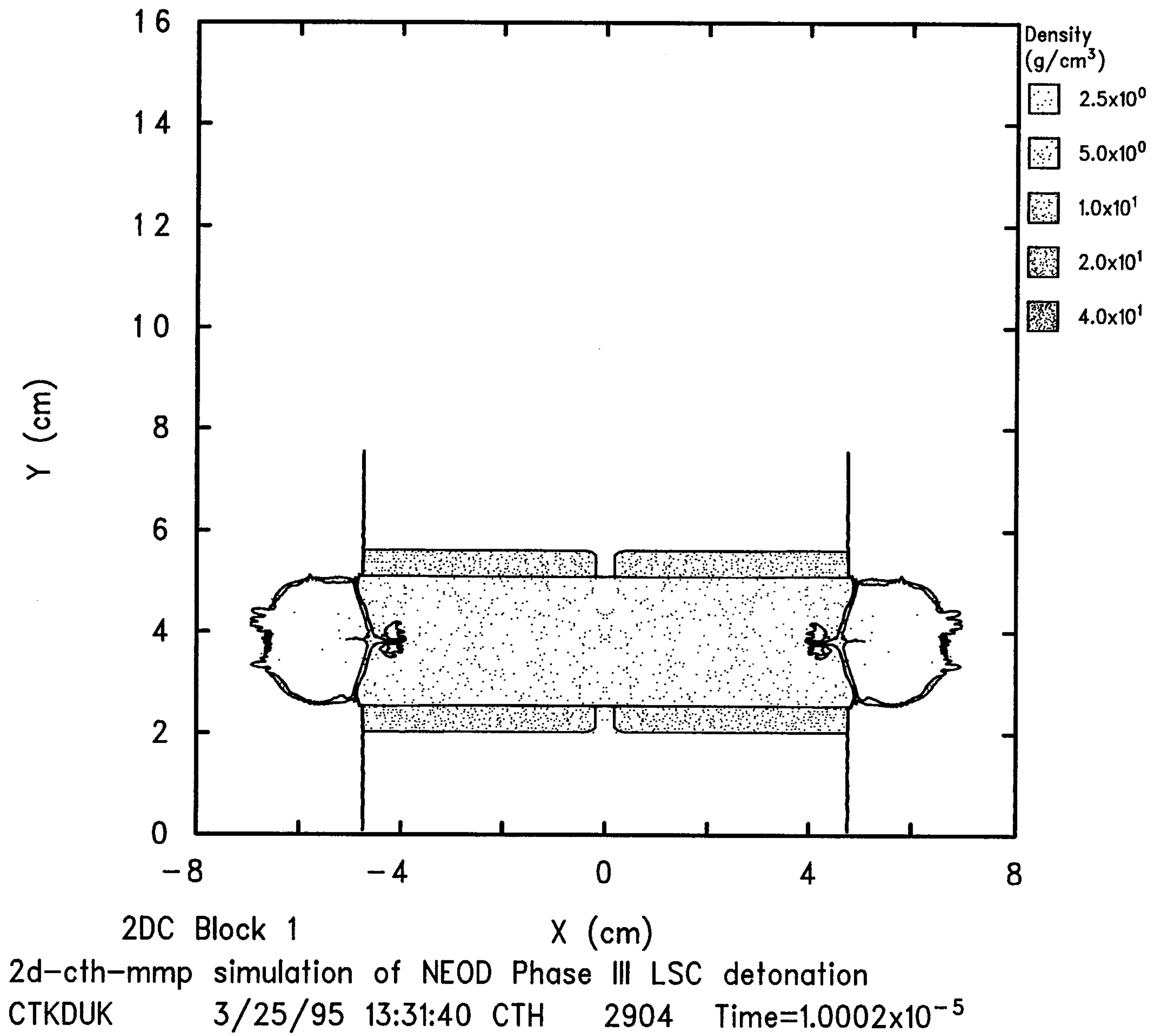
Density
(g/cm³)
2.5x10⁰
5.0x10⁰
1.0x10¹
2.0x10¹
4.0x10¹
Y (cm)
X (cm)
16
14
12
10
8
6
4
2
0
-8
-4
0
4
8
2DC Block 1
2d-cth-mmp simulation of NEOD Phase III LSC detonation
CTKDUK 3/25/95 13:31:40 CTH 2904 Time=1.0002x10⁻⁵

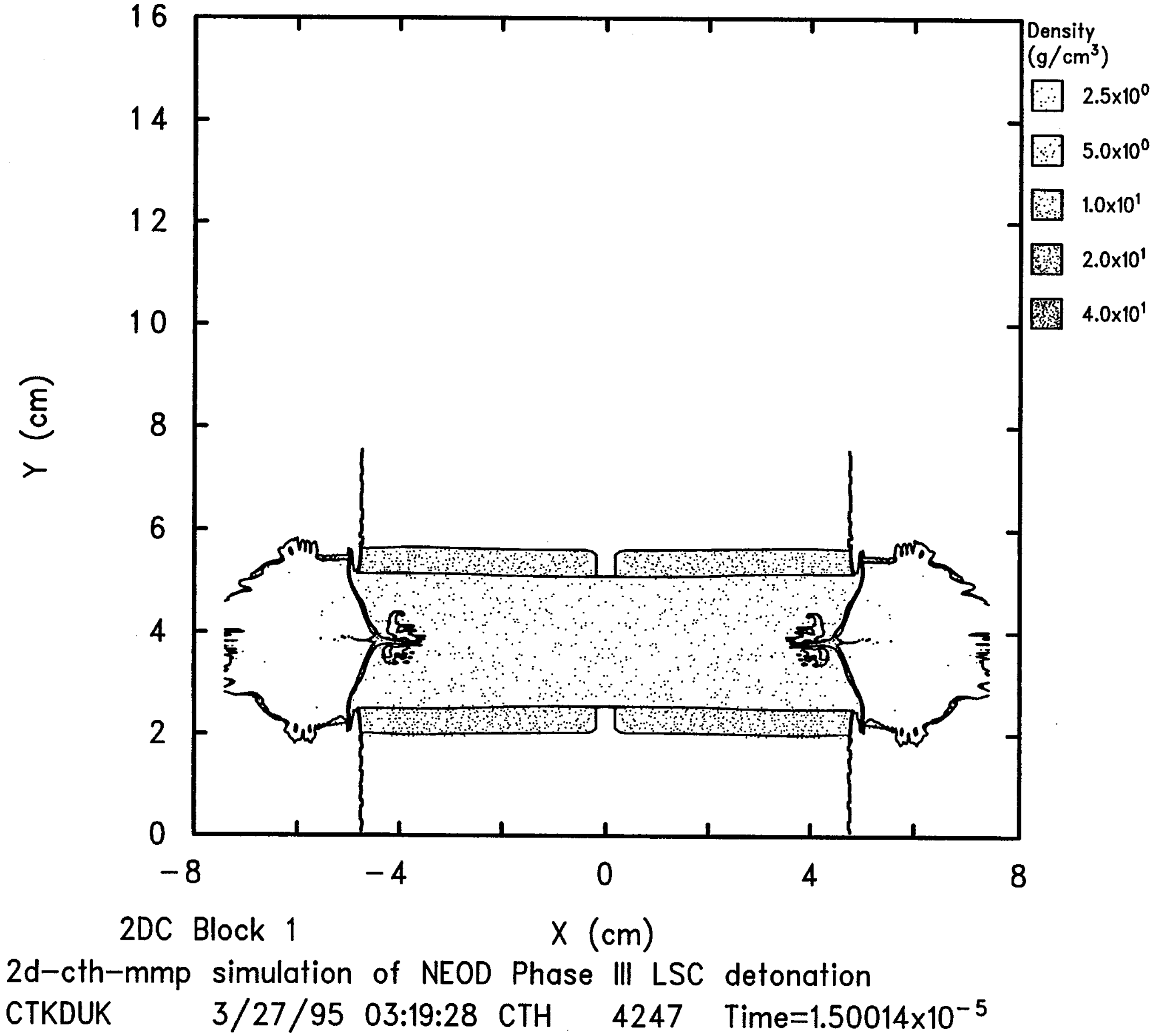

16
14
12
10
8
6
4
2
0
Y (cm)
−8
−4
0
4
8
X (cm)
Density
(g/cm³)
2.5x10⁰
5.0x10⁰
1.0x10¹
2.0x10¹
4.0x10¹
2DC Block 1
2d−cth−mmp simulation of NEOD Phase III LSC detonation
CTKDUK 3/27/95 03:19:28 CTH 4247 Time=1.50014x10⁻⁵

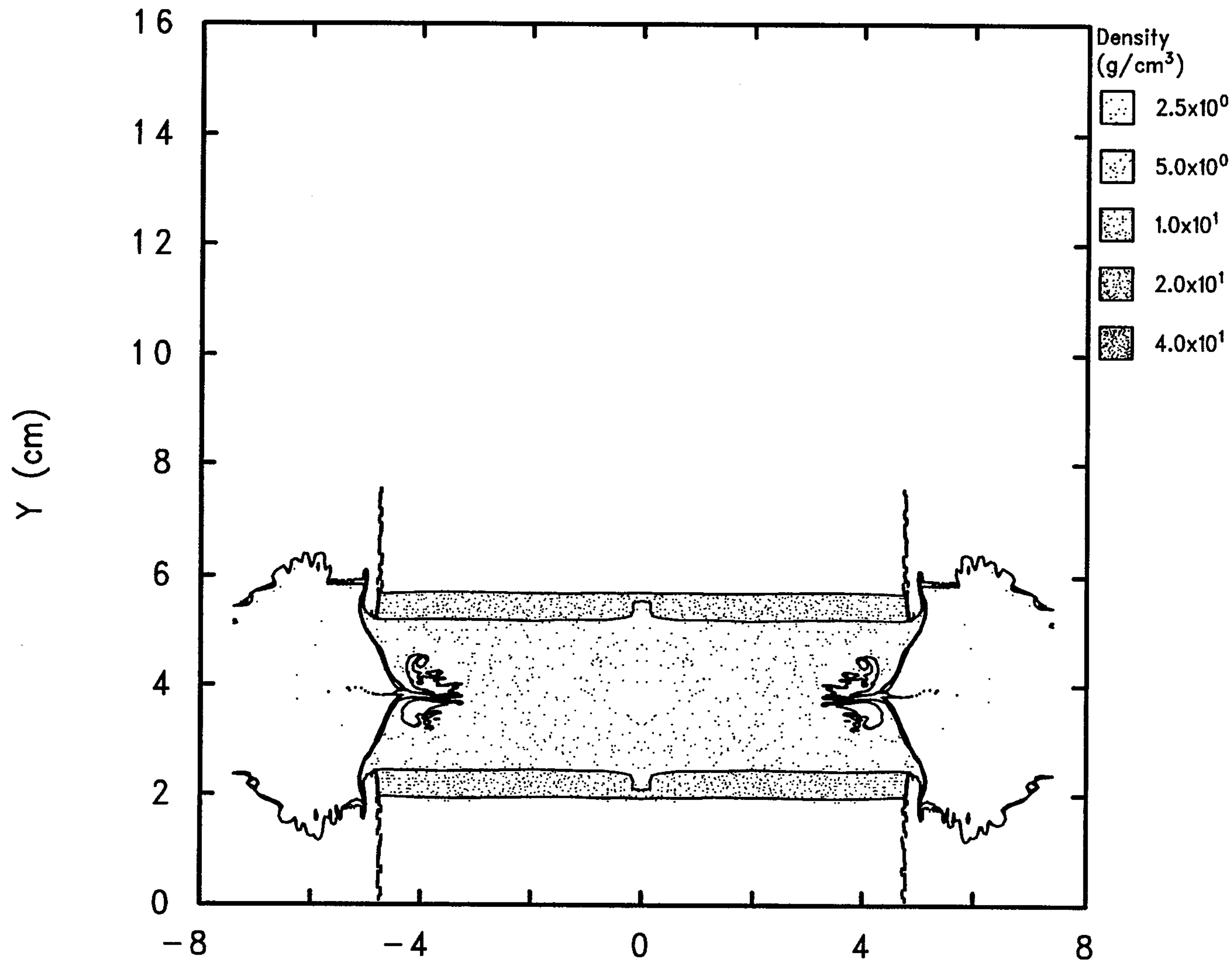

2DC Block 1
2d−cth−mmp simulation of NEOD Phase III LSC detonation
CTKDUK 3/28/95 11:40:25 CTH 5557 Time=2.00005x10^{-5}

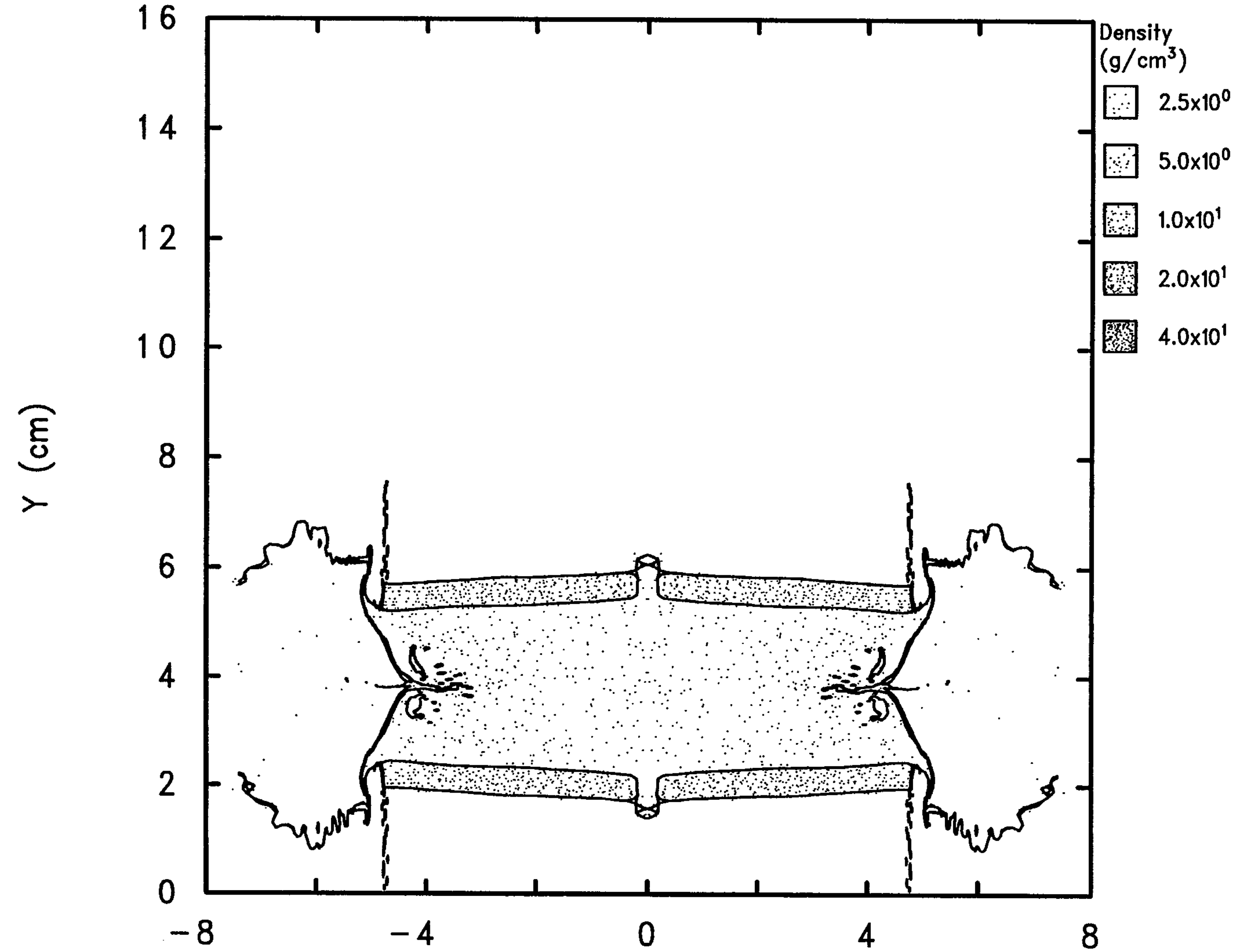

2DC Block 1

2d–cth–mmp simulation of NEOD Phase III LSC detonation

CTKDUK 4/03/95 01:39:30 CTH 12656 Time=2.27859×10^{-5}

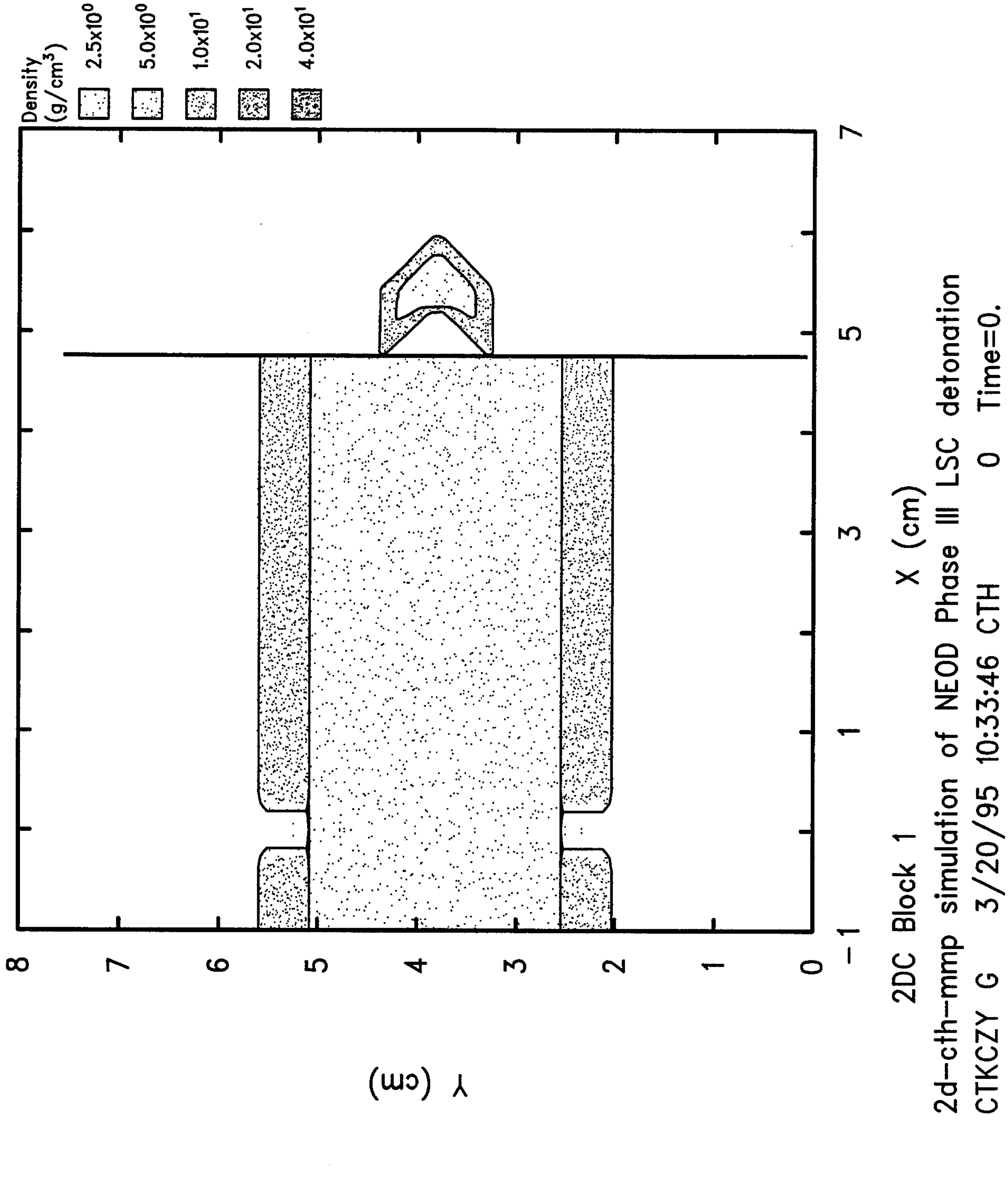

Density (g/cm³)
2.5x10⁰
5.0x10⁰
1.0x10¹
2.0x10¹
4.0x10¹
Y (cm)
X (cm)
2DC Block 1
2d-cth-mmp simulation of NEOD Phase III LSC detonation
CTKCZY G 3/20/95 10:33:46 CTH 0 Time=0.

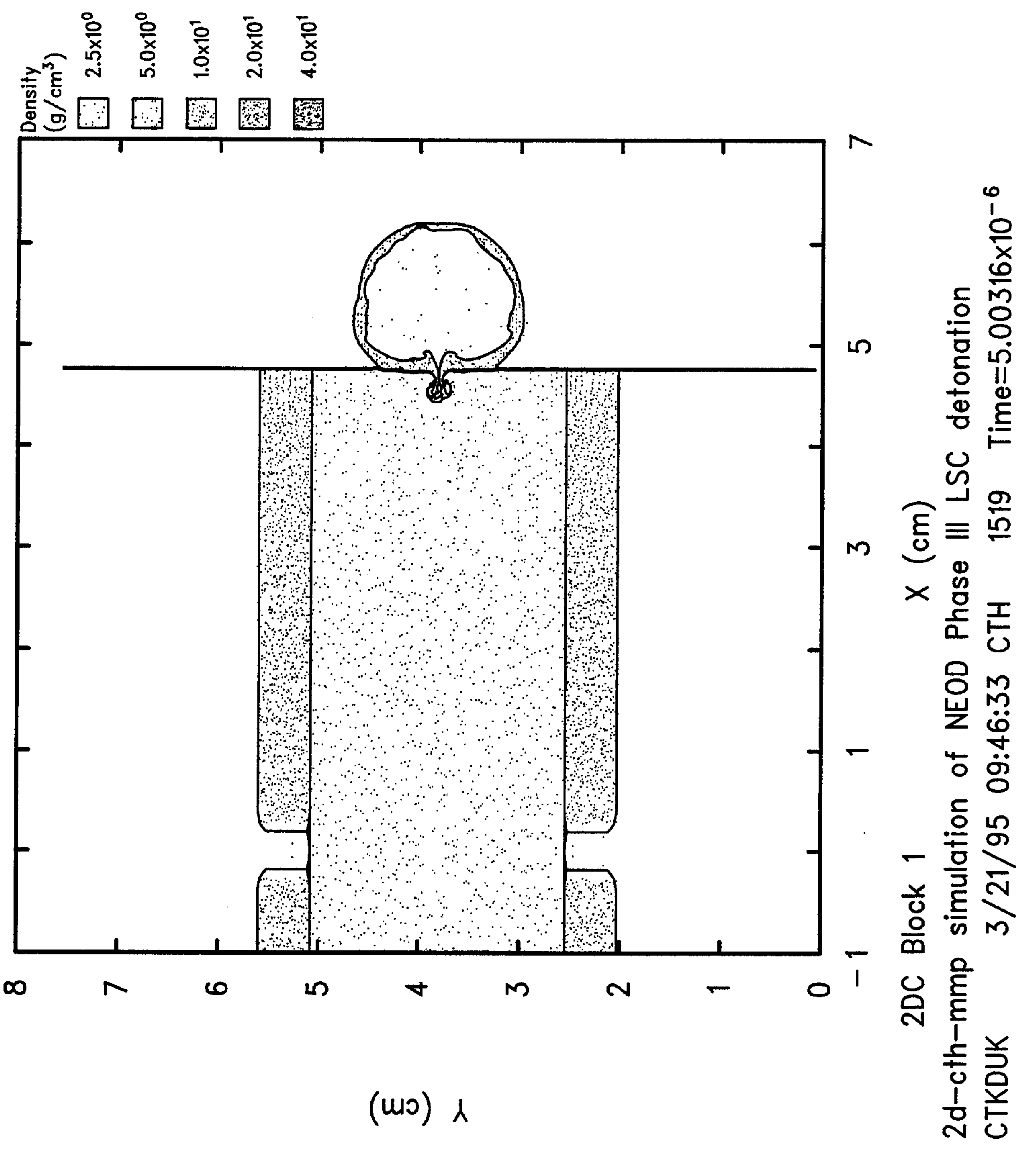
Density (g/cm³)
2.5x10⁰
5.0x10⁰
1.0x10¹
2.0x10¹
4.0x10¹
Y (cm)
X (cm)
2DC Block 1
2d-cth-mmp simulation of NEOD Phase III LSC detonation
CTKDUK 3/21/95 09:46:33 CTH 1519 Time=5.00316x10⁻⁶

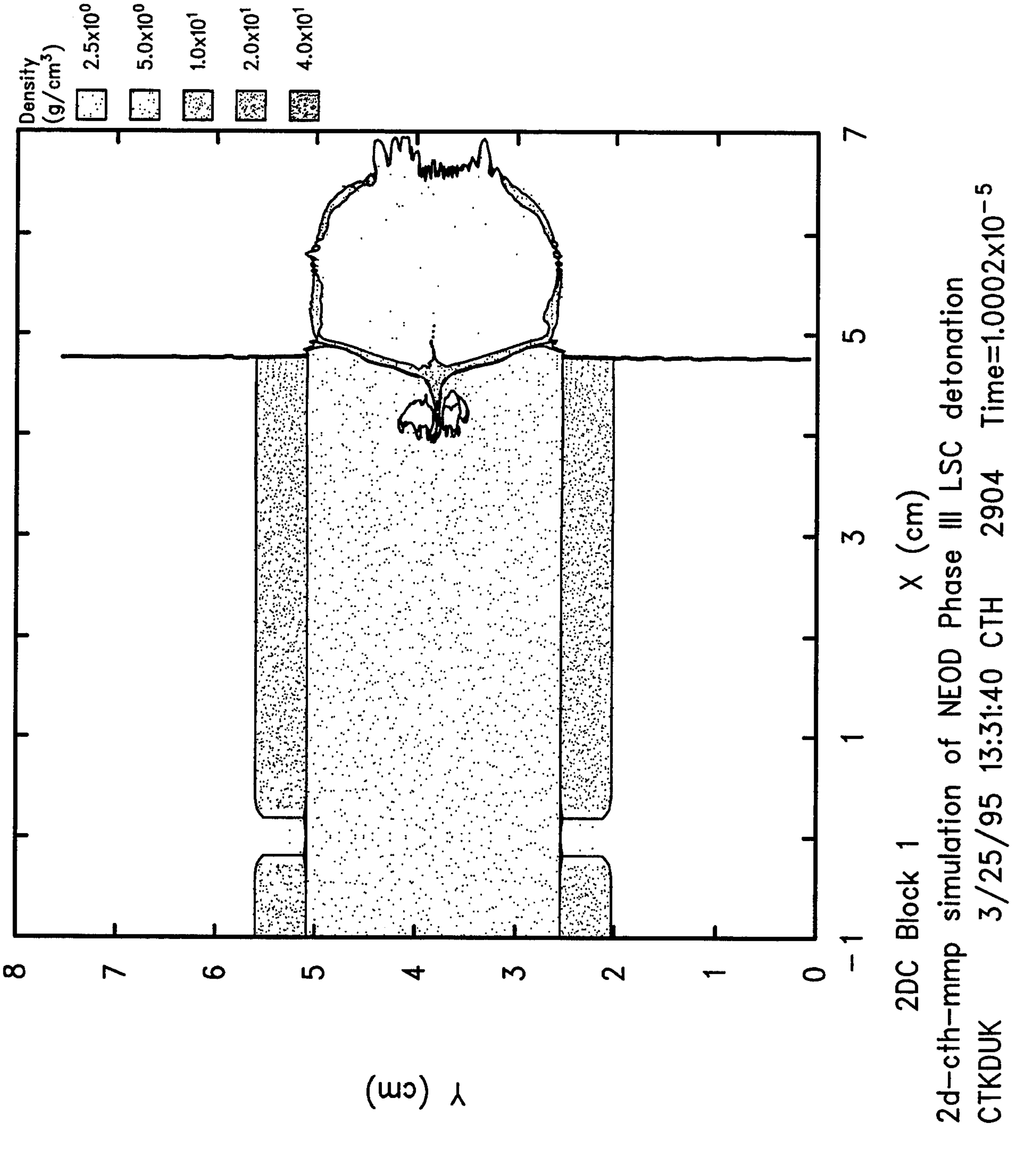
Density (g/cm³)
2.5x10⁰
5.0x10⁰
1.0x10¹
2.0x10¹
4.0x10¹
Y (cm)
X (cm)
2DC Block 1
2d-cth-mmp simulation of NEOD Phase III LSC detonation
CTKDUK 3/25/95 13:31:40 CTH 2904 Time=1.0002x10⁻⁵

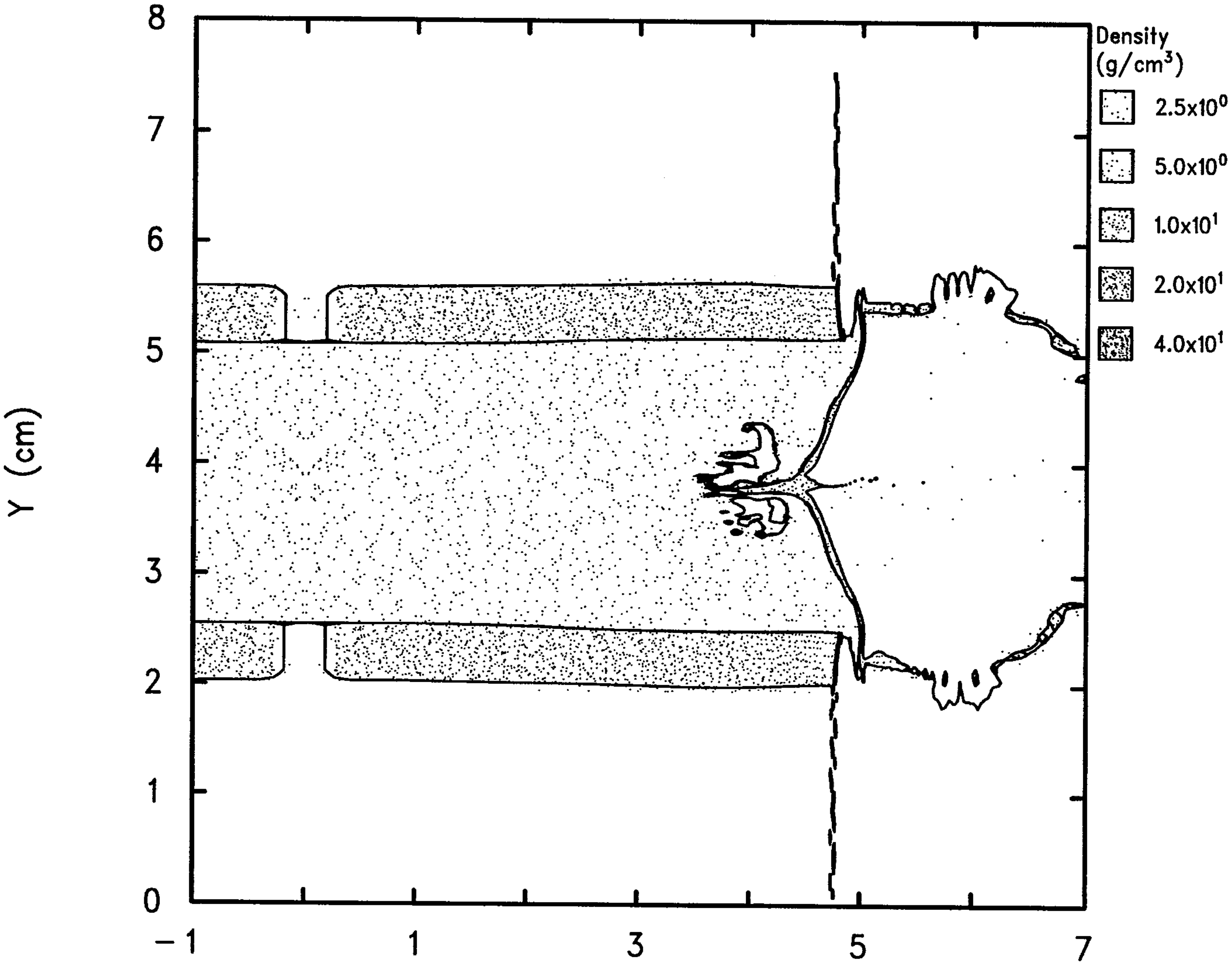

2DC Block 1 X (cm)

2d–cth–mmp simulation of NEOD Phase III LSC detonation

CTKDUK 3/27/95 03:19:28 CTH 4247 Time=1.50014×10^{-5}

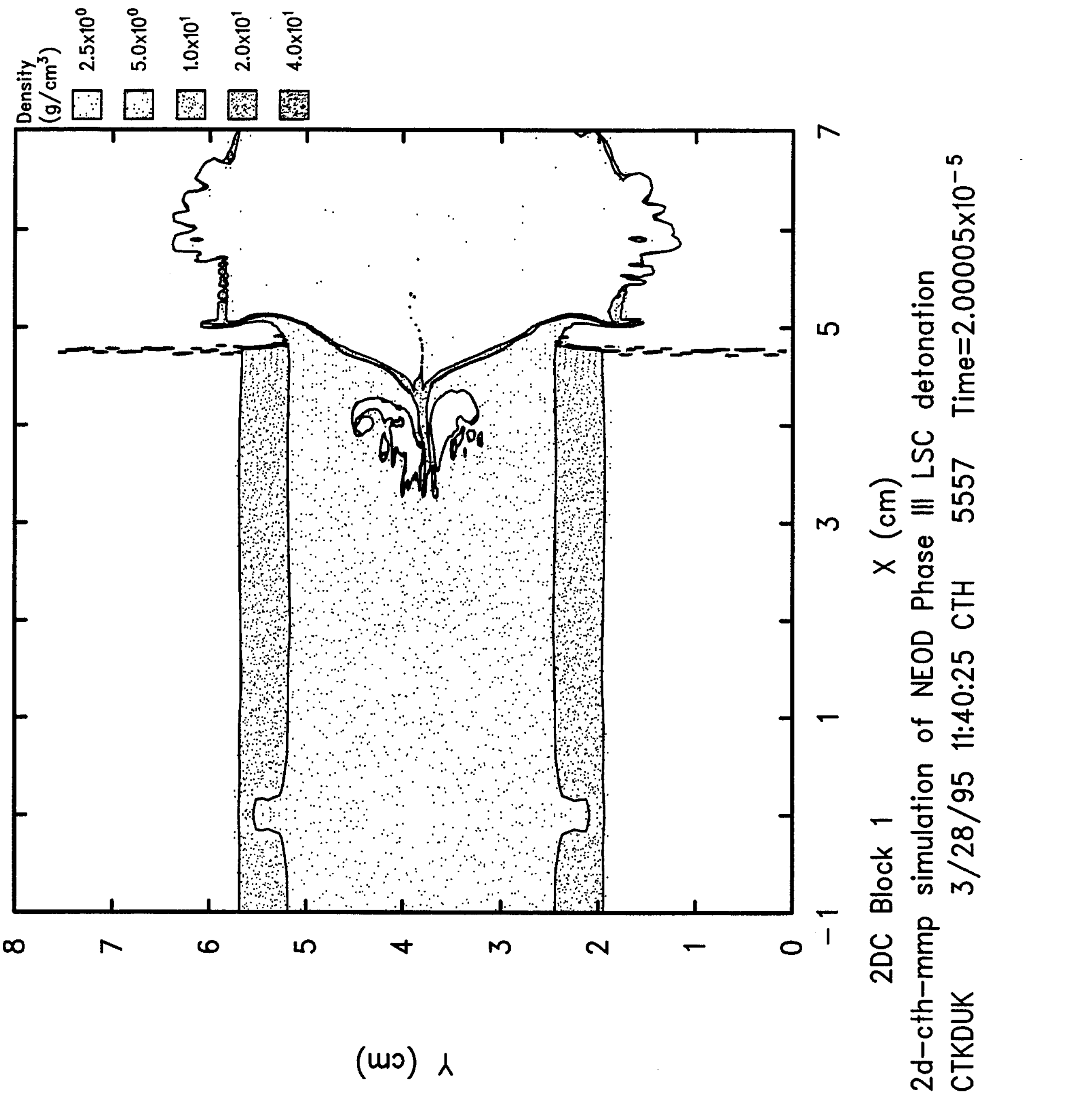

Density (g/cm³)
2.5x10⁰
5.0x10⁰
1.0x10¹
2.0x10¹
4.0x10¹
Y (cm)
X (cm)
2DC Block 1
2d-cth-mmp simulation of NEOD Phase III LSC detonation
CTKDUK 3/28/95 11:40:25 CTH 5557 Time=2.000005x10⁻⁵

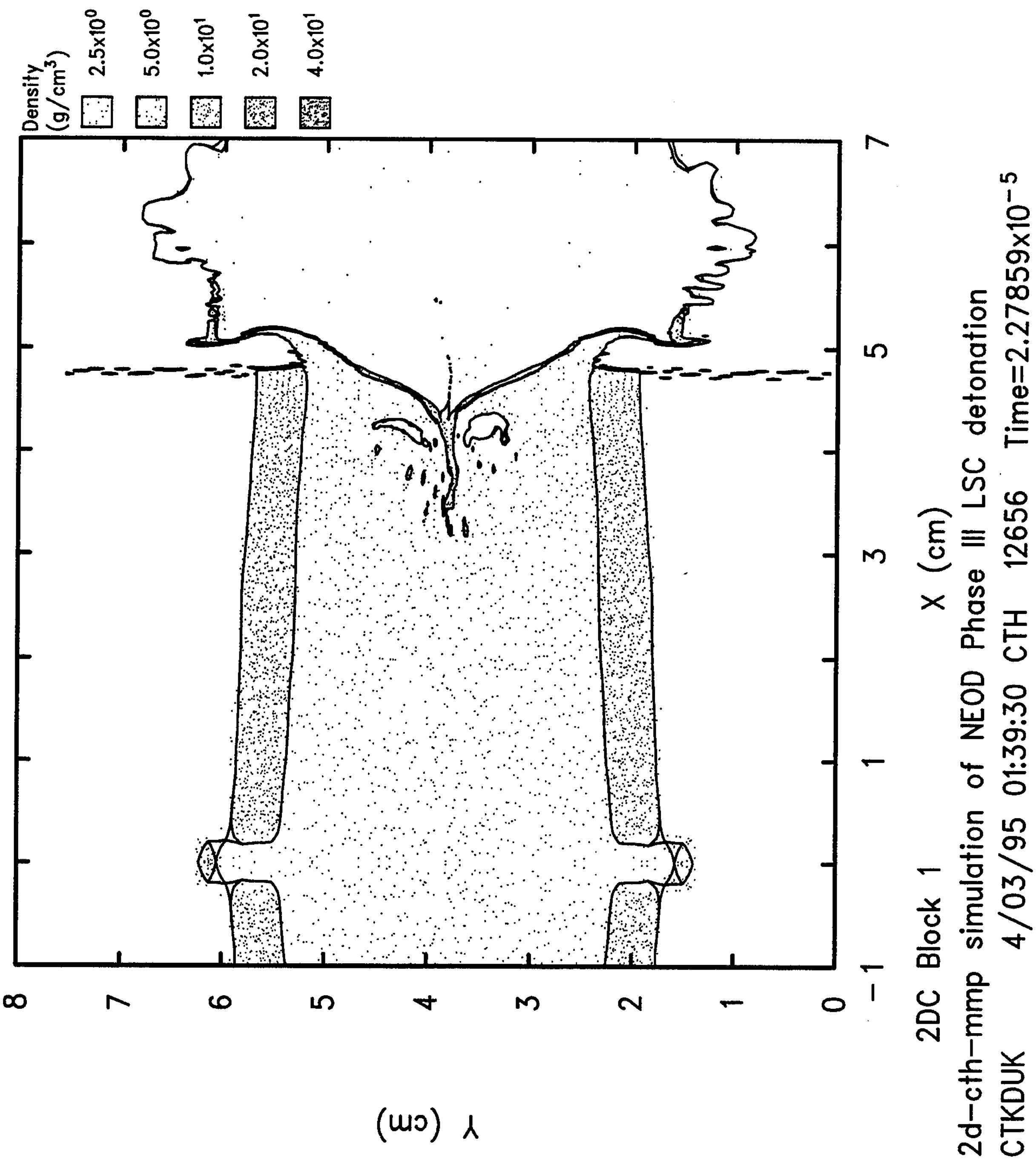
Density
(g/cm3)
2.5x10^0
5.0x10^0
1.0x10^1
2.0x10^1
4.0x10^1
Y (cm)
X (cm)
2DC Block 1
2d-cth-mmp simulation of NEOD Phase III LSC detonation
CTKDUK 4/03/95 01:39:30 CTH 12656 Time=2.27859x10^-5

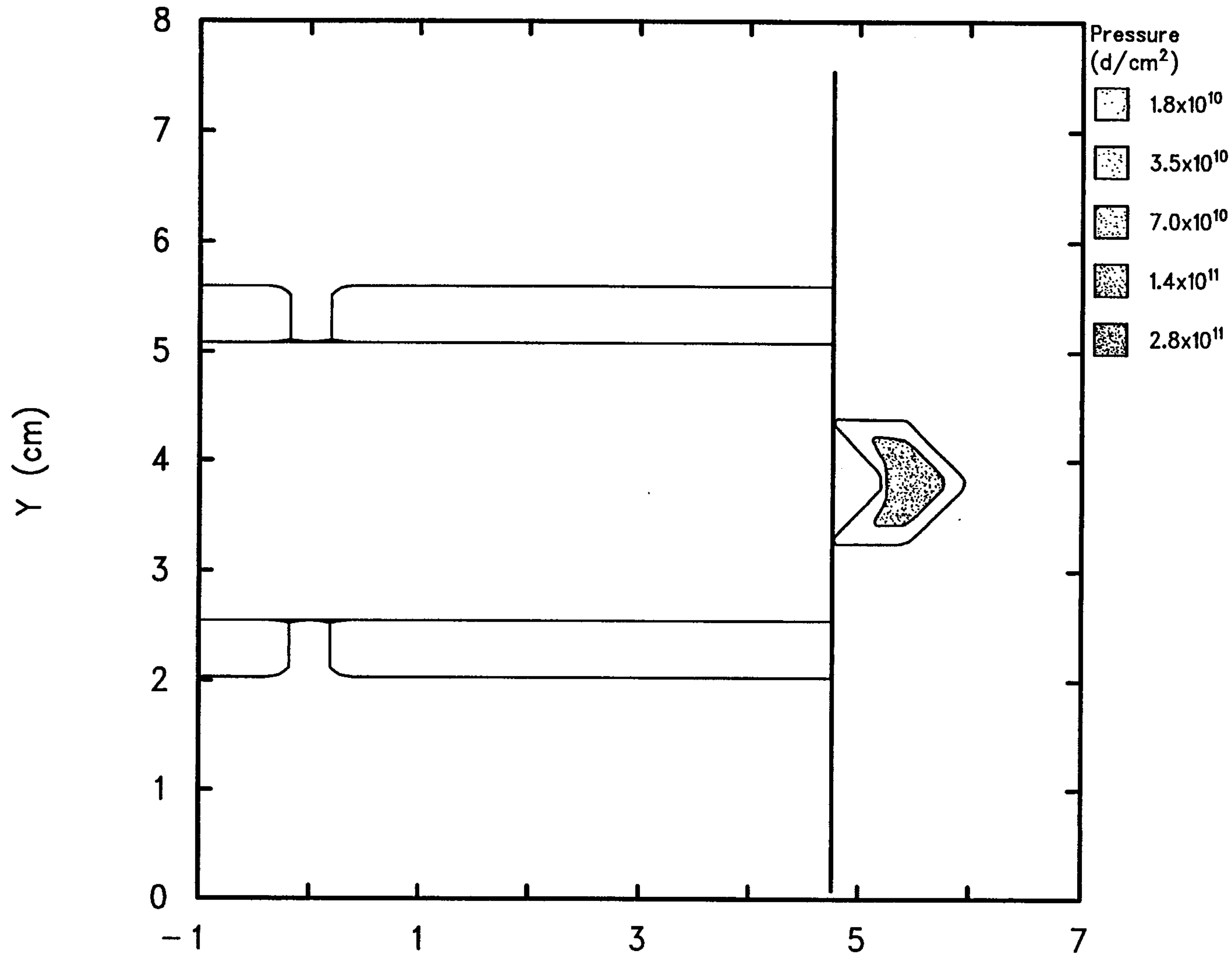

2DC Block 1

2d-cth-mmp simulation of NEOD Phase III LSC detonation

CTKCZY G 3/20/95 10:33:46 CTH 0 Time=0.

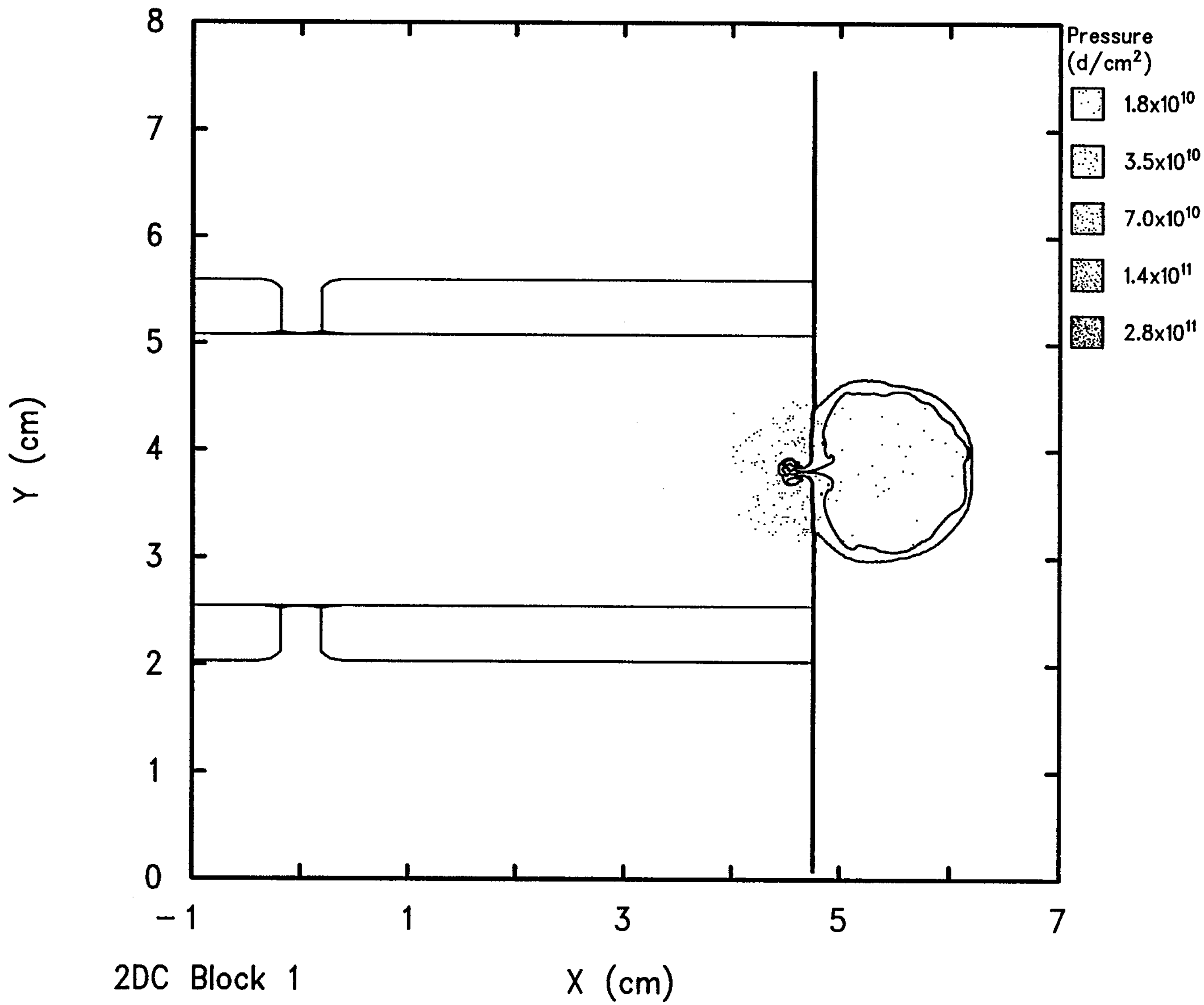

2d-cth-mmp simulation of NEOD Phase III LSC detonation

CTKDUK 3/21/95 09:46:33 CTH 1519 Time=5.00316×10^{-6}

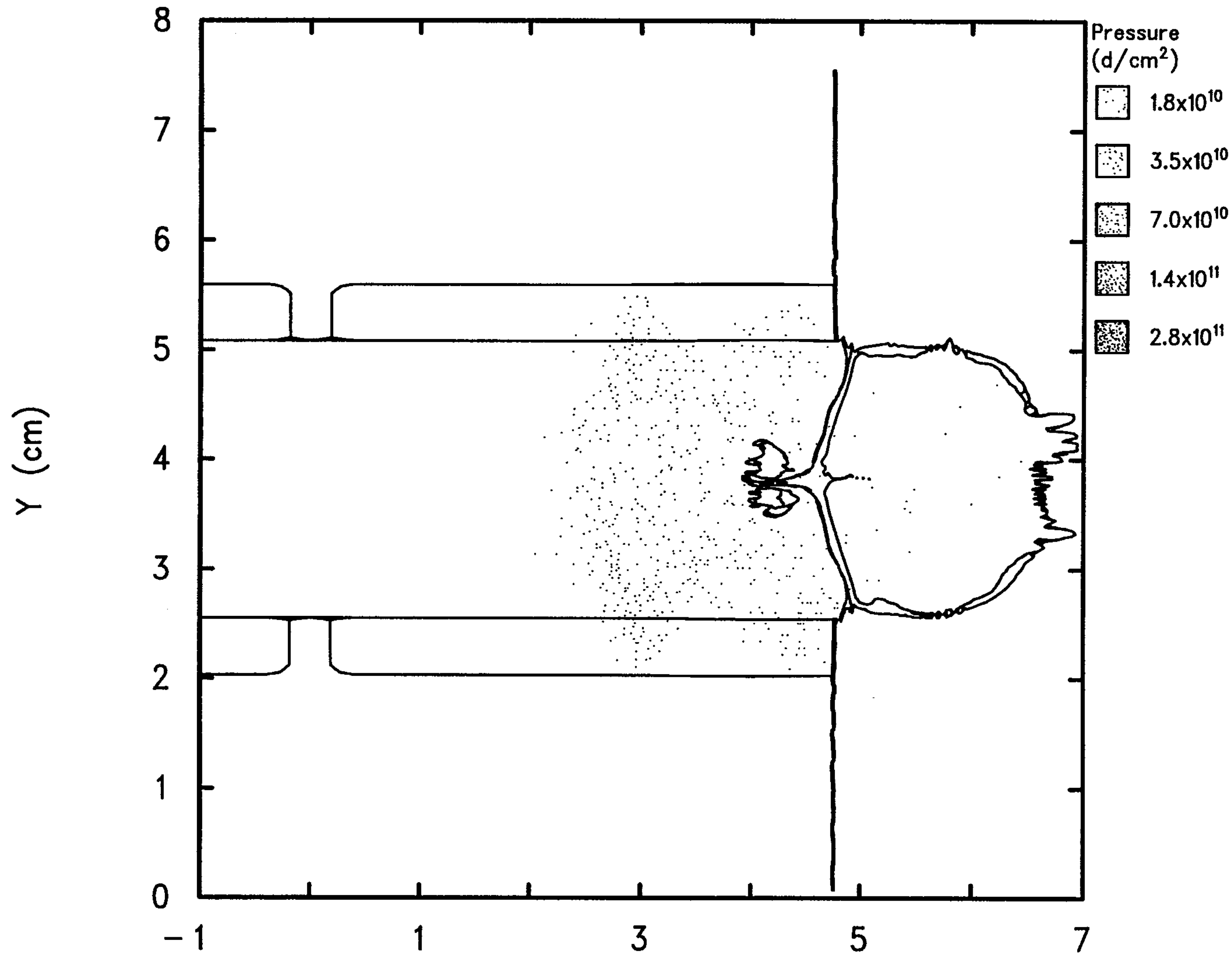

2DC Block 1

2d-cth-mmp simulation of NEOD Phase III LSC detonation

CTKDUK 3/25/95 13:31:40 CTH 2904 Time=1.0002×10^{-5}

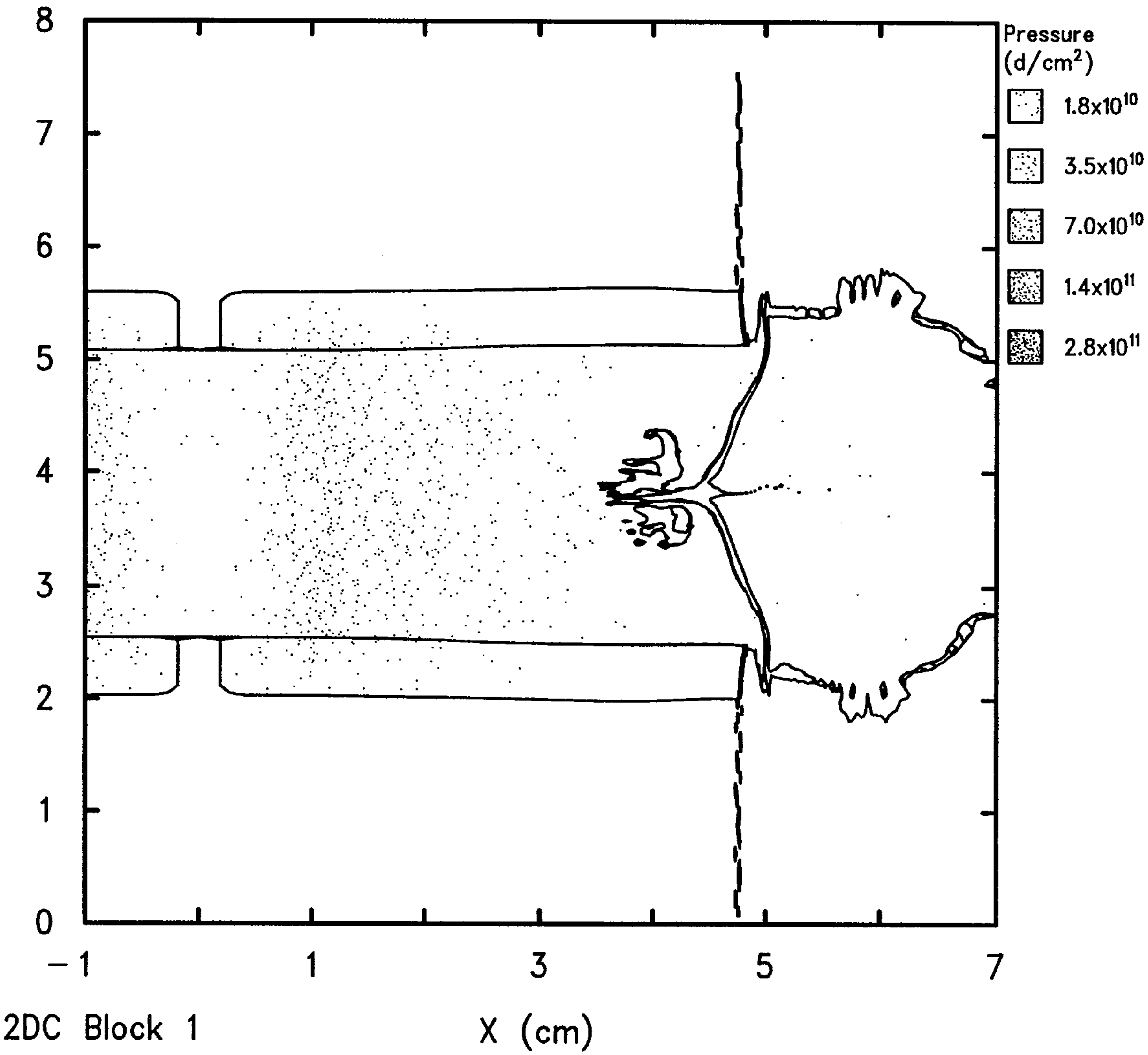

2DC Block 1

2d−cth−mmp simulation of NEOD Phase III LSC detonation

CTKDUK 3/27/95 03:19:28 CTH 4247 Time=1.50014×10^{-5}

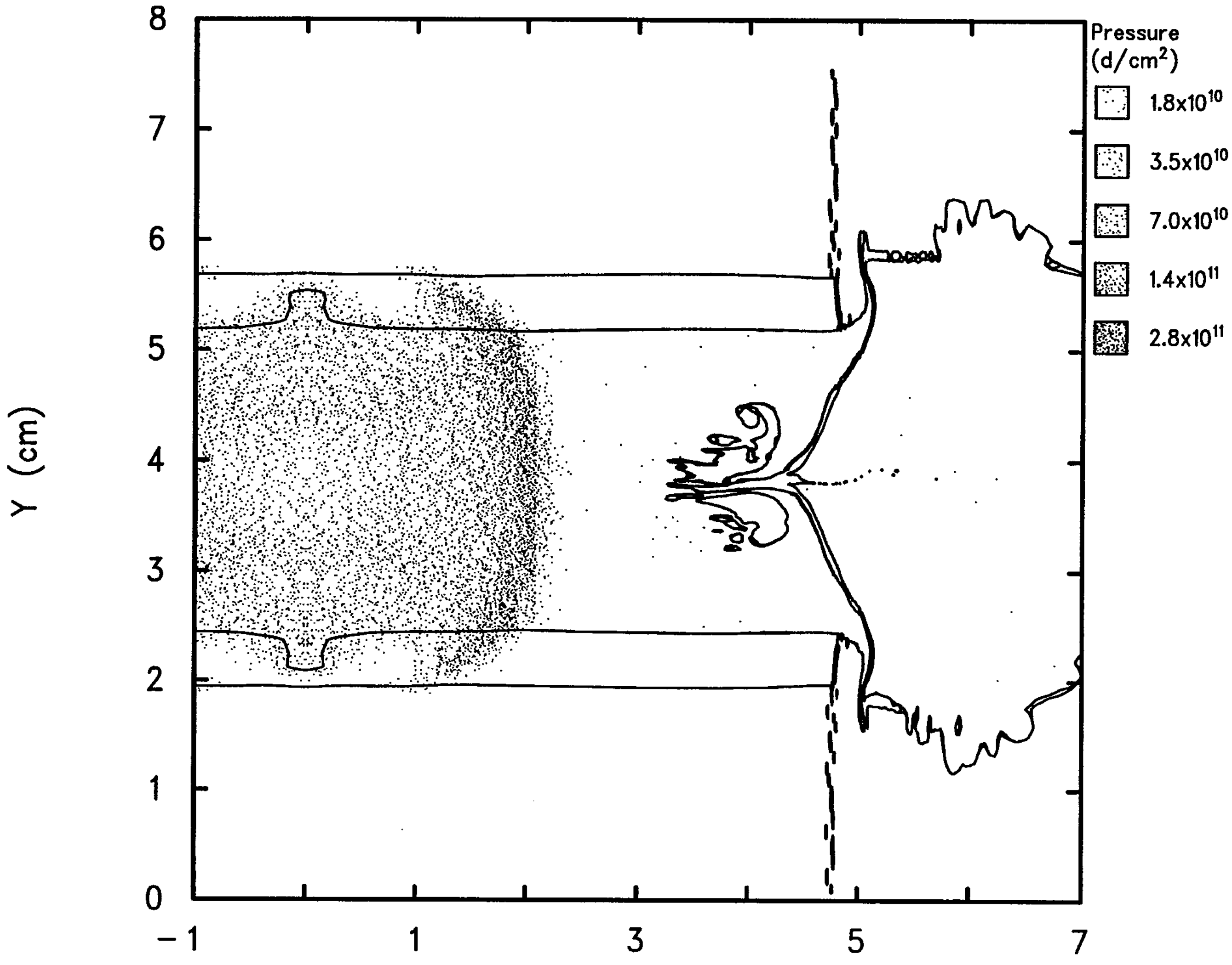

2DC Block 1

2d–cth–mmp simulation of NEOD Phase III LSC detonation

CTKDUK 3/28/95 11:40:25 CTH 5557 Time=2.00005×10^{-5}

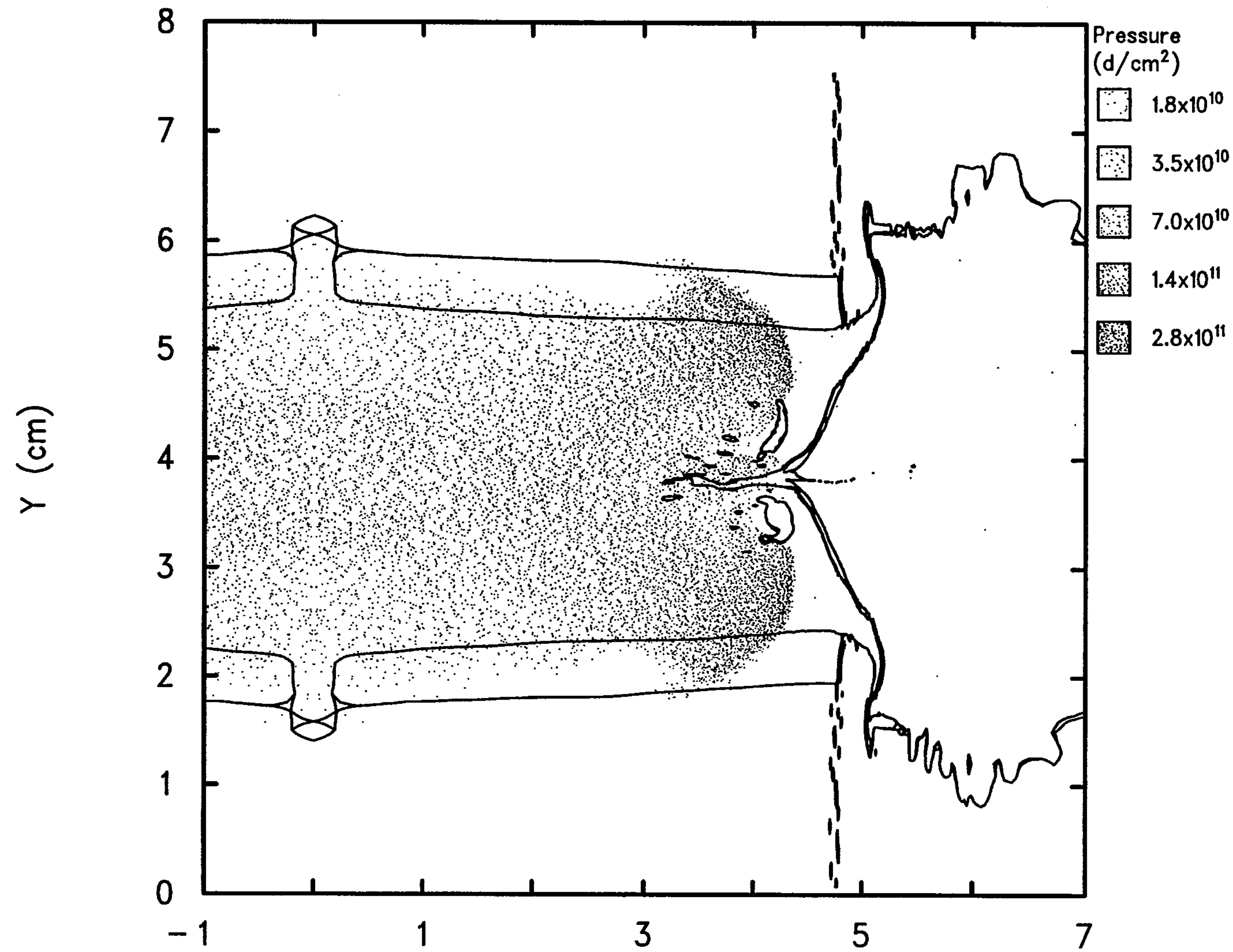

2DC Block 1

2d–cth–mmp simulation of NEOD Phase III LSC detonation

CTKDUK 4/03/95 01:39:30 CTH 12656 Time=2.27859×10^{-5}

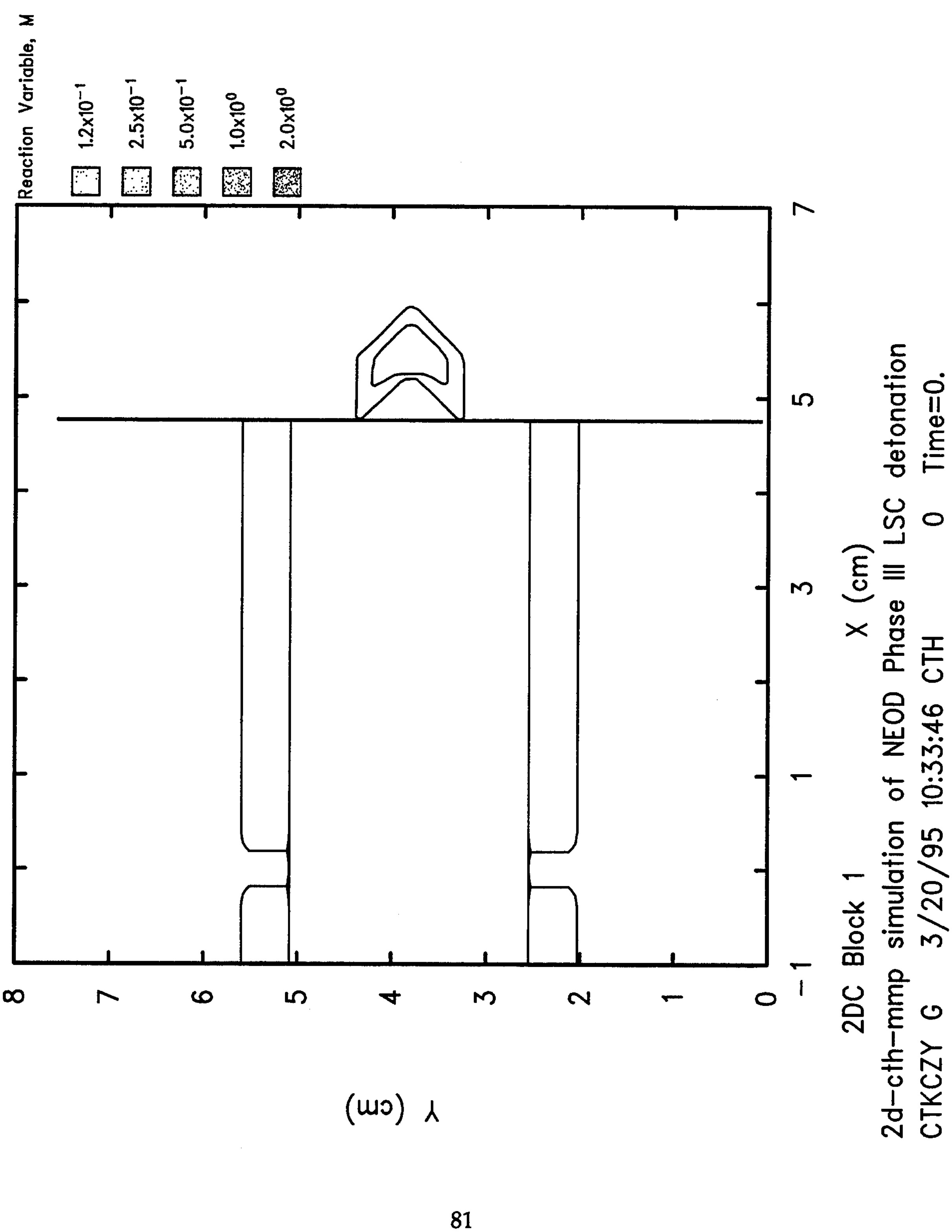
Reaction Variable, M
1.2x10^-1
2.5x10^-1
5.0x10^-1
1.0x10^0
2.0x10^0
8
7
6
5
4
3
2
1
0
Y (cm)
−1
1
3
5
7
X (cm)
2DC Block 1
2d−cth−mmp simulation of NEOD Phase III LSC detonation
CTKCZY G 3/20/95 10:33:46 CTH 0 Time=0.

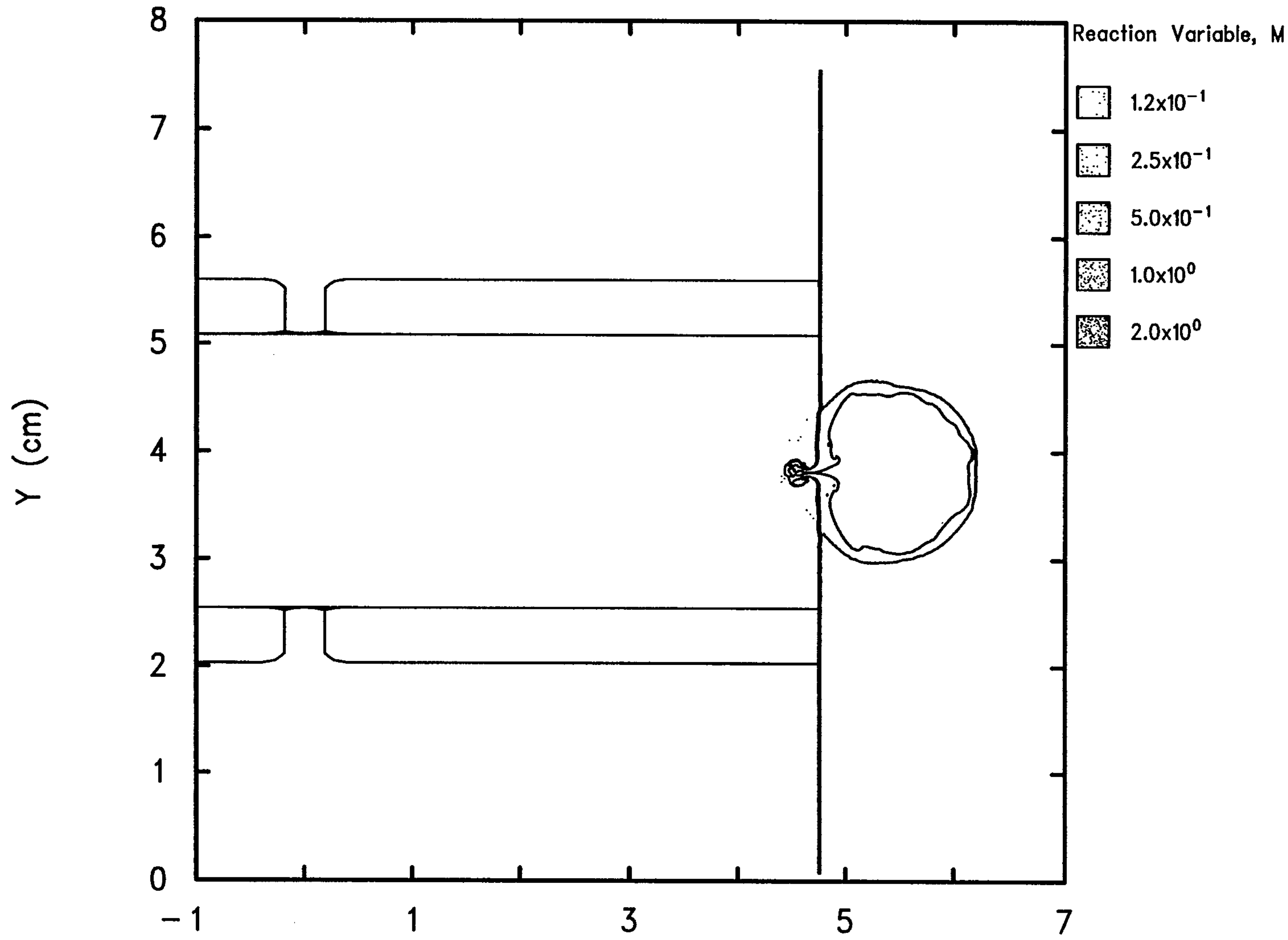

2d–cth–mmp simulation of NEOD Phase III LSC detonation
CTKDUK 3/21/95 09:46:33 CTH 1519 Time=5.00316×10^{-6}

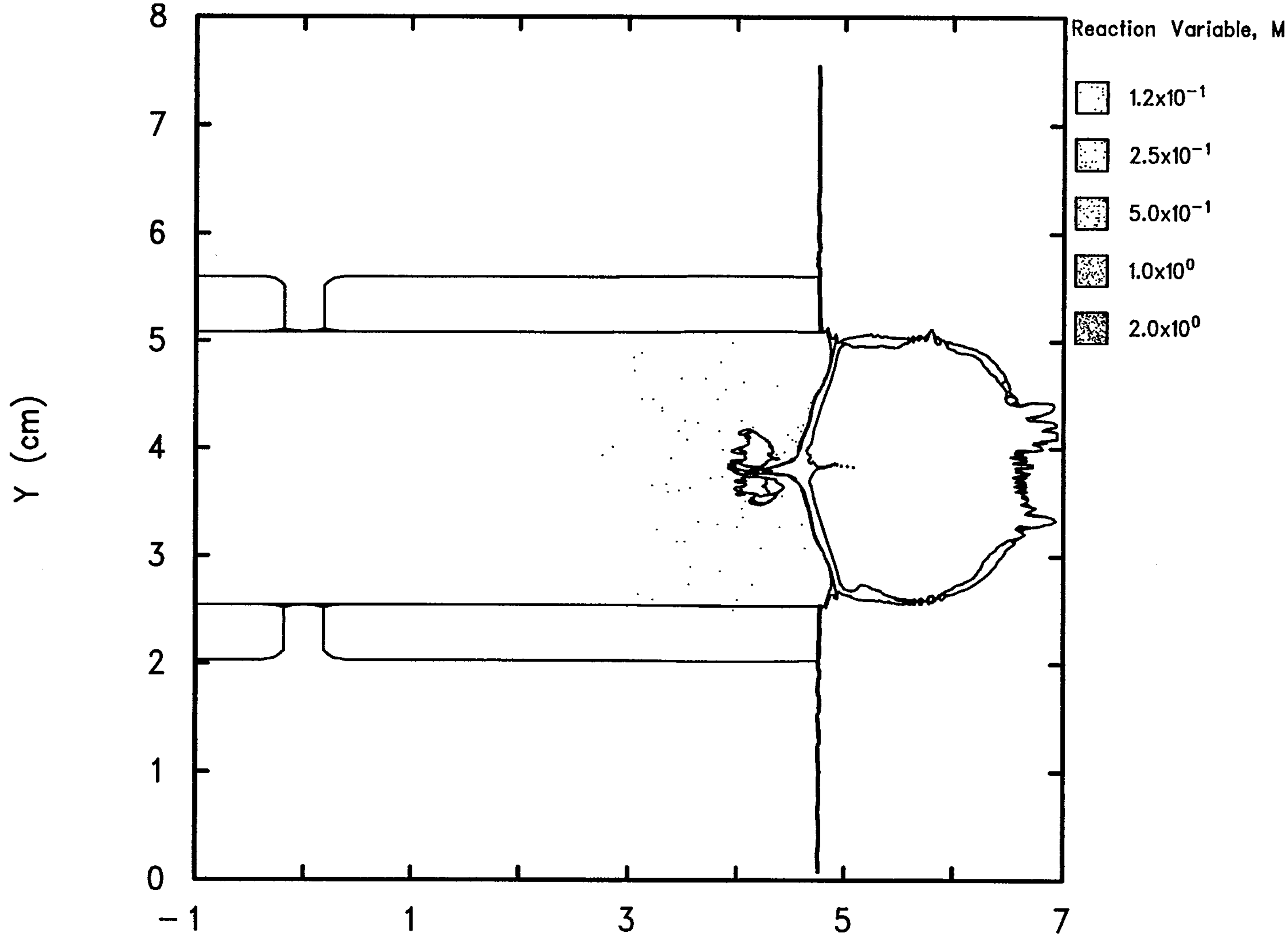

2DC Block 1

2d-cth-mmp simulation of NEOD Phase III LSC detonation

CTKDUK 3/25/95 13:31:40 CTH 2904 Time=1.0002×10^{-5}

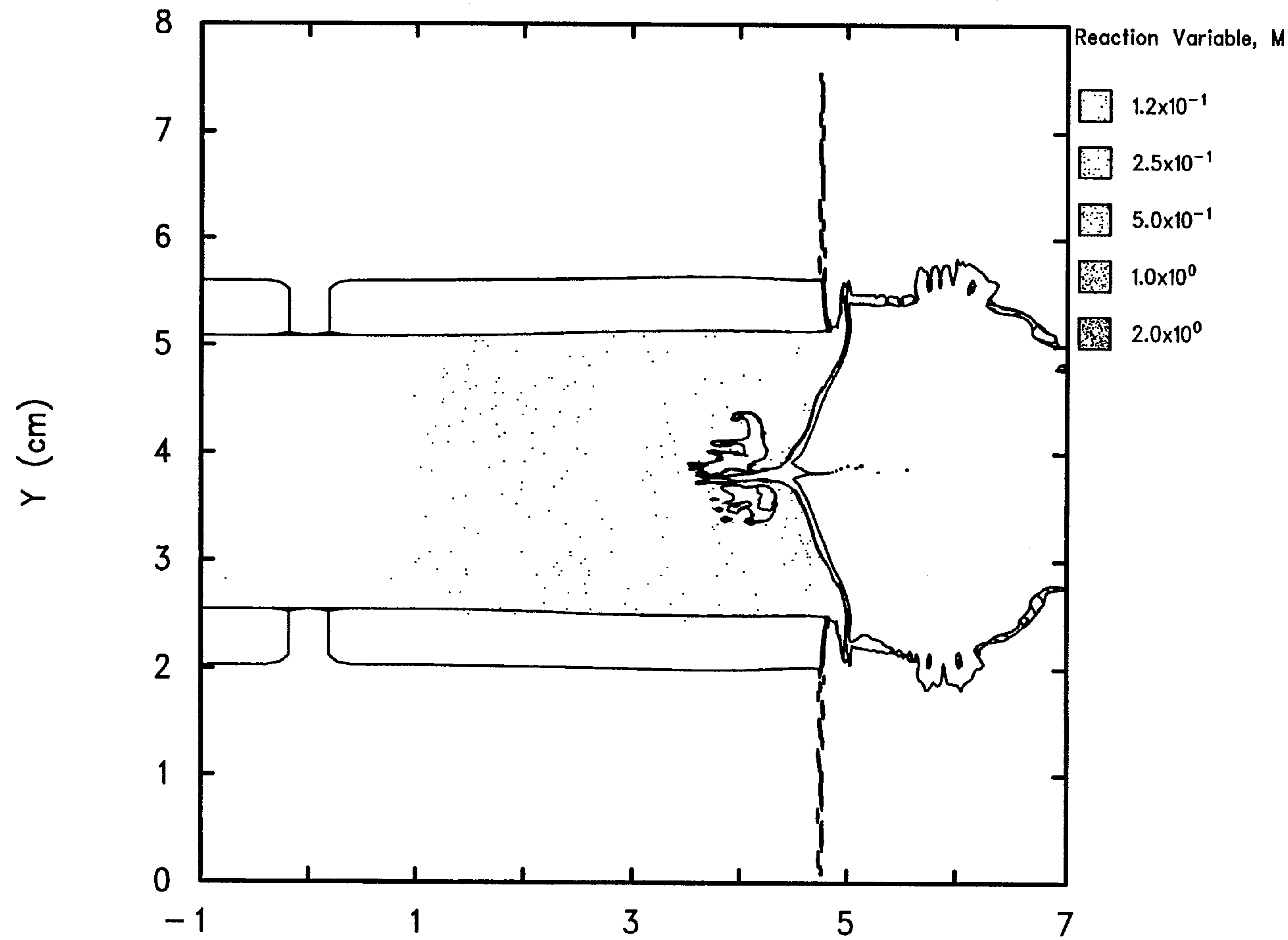

2DC Block 1

2d-cth-mmp simulation of NEOD Phase III LSC detonation

CTKDUK 3/27/95 03:19:28 CTH 4247 Time=1.50014×10^{-5}

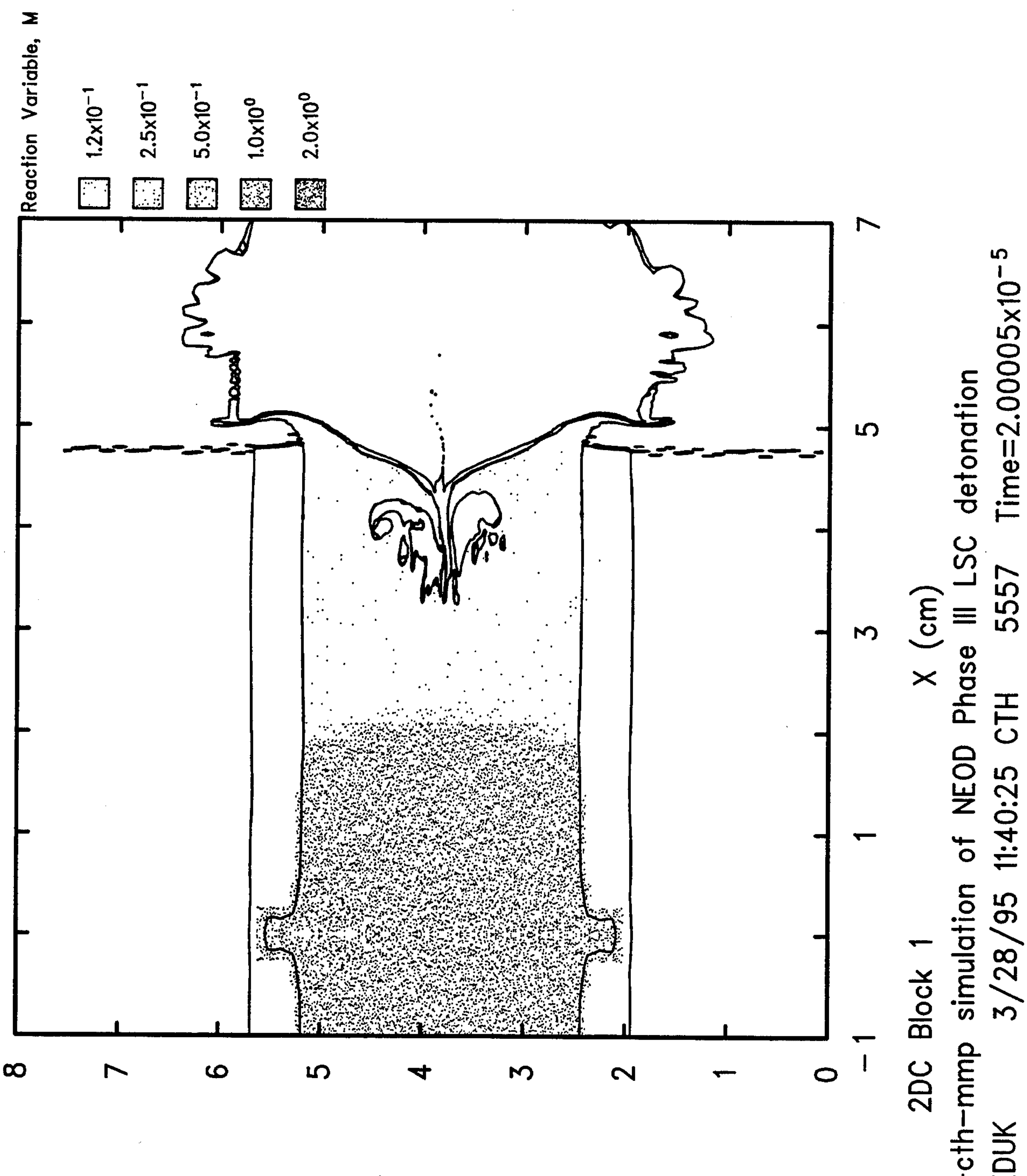
Reaction Variable, M
1.2x10^{-1}
2.5x10^{-1}
5.0x10^{-1}
1.0x10^{0}
2.0x10^{0}
Y (cm)
X (cm)
2DC Block 1
2d-cth-mmp simulation of NEOD Phase III LSC detonation
CTKDUK 3/28/95 11:40:25 CTH 5557 Time=2.00005x10^{-5}

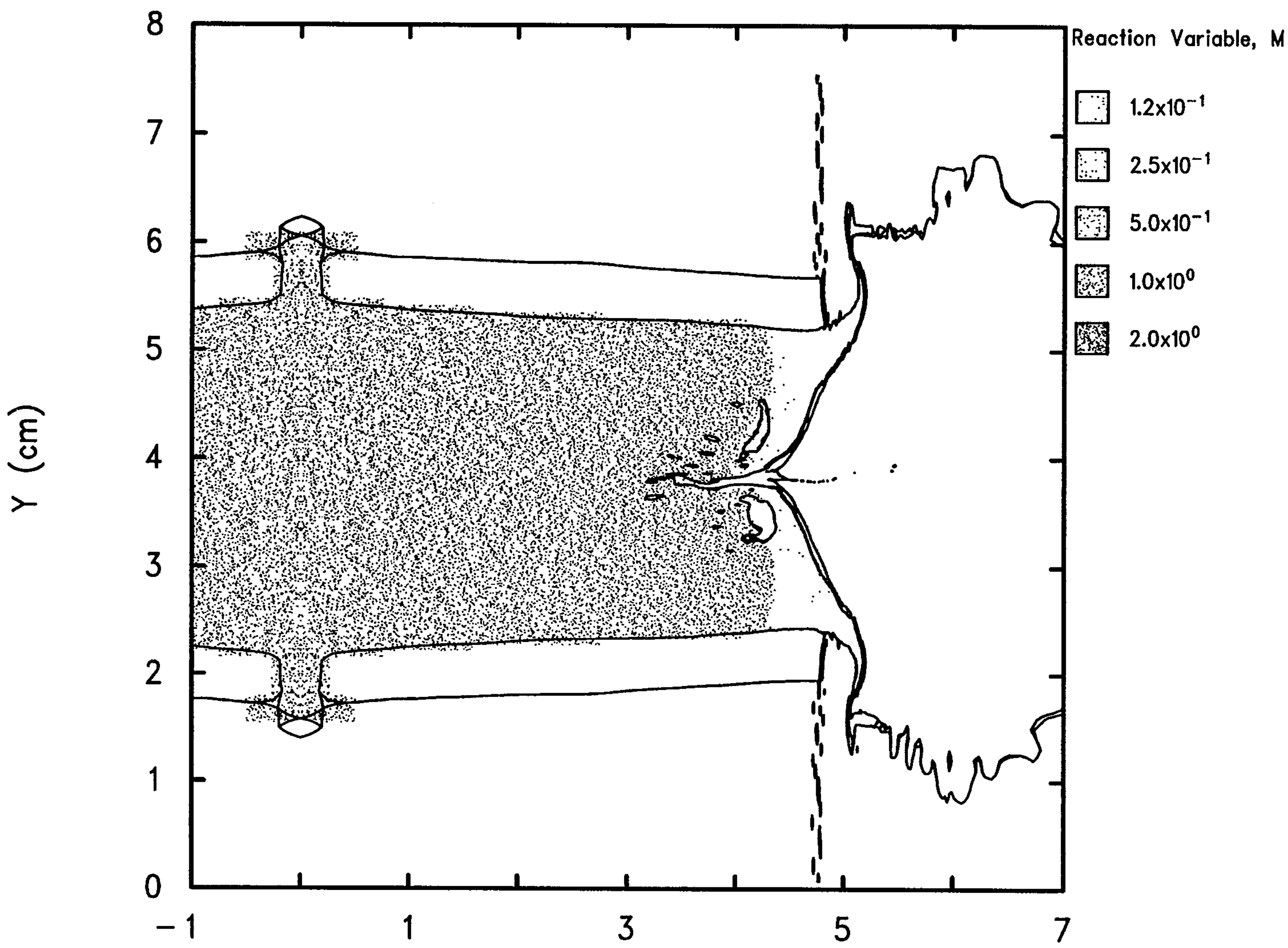

2DC Block 1

2d-cth-mmp simulation of NEOD Phase III LSC detonation

CTKDUK 4/03/95 01:39:30 CTH 12656 Time=2.27859×10^{-5}

NO. OF COPIES	ORGANIZATION
2	DEFENSE TECHNICAL INFO CTR ATTN DTIC DDA 8725 JOHN J KINGMAN RD STE 0944 FT BELVOIR VA 22060-6218
1	DIRECTOR US ARMY RESEARCH LAB ATTN AMSRL OP SD TA 2800 POWDER MILL RD ADELPHI MD 20783-1145
3	DIRECTOR US ARMY RESEARCH LAB ATTN AMSRL OP SD TL 2800 POWDER MILL RD ADELPHI MD 20783-1145
1	DIRECTOR US ARMY RESEARCH LAB ATTN AMSRL OP SD TP 2800 POWDER MILL RD ADELPHI MD 20783-1145
	ABERDEEN PROVING GROUND
5	DIR USARL ATTN AMSRL OP AP L (305)

NO. OF COPIES	ORGANIZATION
1	HEADQUARTERS ATTN SARD TT DR F MILTON PENTAGON WASHINGTON DC 20310-0103
1	HEADQUARTERS ATTN SARD TT MR J APPEL PENTAGON WASHINGTON DC 20310-0103
1	HEADQUARTERS ATTN SARD TT MS C NASH PENTAGON WASHINGTON DC 20310-0103
1	HEADQUARTERS ATTN SARD TR DR R CHAIT PENTAGON WASHINGTON DC 20310-0103
1	HEADQUARTERS ATTN SARD TR MS K KOMINOS PENTAGON WASHINGTON DC 20310-0103
1	DIRECTOR US ARMY RSRCH LAB ATTN AMSRL CP CA D SNIDER 2800 POWDER MILL RD ADELPHI MD 20783-1145
4	COMMANDER USA ARDEC ATTN SMCAR FSE T GORA E ANDRICOPOULOS B KNUTELSKY A GRAF PICATINNY ARSENAL NJ 07806-5000

NO. OF COPIES	ORGANIZATION
3	COMMANDER USA ARDEC ATTN SMCAR TD R PRICE V LINDER T DAVIDSON PICATINNY ARSENAL NJ 07806-5000
1	COMMANDER USA ARDEC ATTN F MCLAUGHLIN PICATINNY ARSENAL NJ 07806-5000
5	COMMANDER USA ARDEC ATTN SMCAR CCH T S MUSALLI P CHRISTIAN K FEHSAL N KRASNOW R CARR PICATINNY ARSENAL NJ 07806-5000
1	COMMANDER USA ARDEC ATTN SMCAR CCH V E FENNELL PICATINNY ARSENAL NJ 07806-5000
1	COMMANDER USA ARDEC ATTN SMCAR CCH J DELORENZO PICATINNY ARSENAL NJ 07806-5000
2	COMMANDER USA ARDEC ATTN SMCAR CC J HEDDERICH COL SINCLAIR PICATINNY ARSENAL NJ 07806-5000
1	COMMANDER USA ARDEC ATTN SMCAR CCH P J LUTZ PICATINNY ARSENAL NJ 07806-5000

NO. OF COPIES	ORGANIZATION
2	COMMANDER USA ARDEC ATTN SMCAR FSA M D DEMELLA F DIORIO PICATINNY ARSENAL NJ 07806-5000
1	COMMANDER USA ARDEC ATTN SMCAR FSA C SPINELLI PICATINNY ARSENAL NJ 07806-5000
11	DIRECTOR BENET LABORATORIES ATTN SMCAR CCB C KITCHENS J KEANE J SANTINI J VASILAKIS G FRIAR R FISCELLA V MONTVORI J WRZOCHALSKI J BATTAGLIA R HASENBEIN SMCAR CCB R S SOPOK WATERVLIET NY 12189-4050
1	COMMANDER WATERVLIET ARSENAL ATTN SMCWV QAE Q C HOWD BLDG 44 WATERVLIET NY 12189-4050
1	COMMANDER WATERVLIET ARSENAL ATTN SMCWV SPM T MCCLOSKEY BLDG 25 3 WATERVLIET NY 12189-4050
1	COMMANDER WATERVLIET ARSENAL ATTN SMCWV QA QS K INSCO WATERVLIET NY 12189-4050
1	COMMANDER USA ARDEC ATTN AMSMC PBM K PICATINNY ARSENAL NJ 07806-5000

NO. OF COPIES	ORGANIZATION
1	DIRECTOR USA CRREL ATTN P DUTTA 72 LYME RD HANOVER NH 03755
1	DIRECTOR US ARMY RSRCH LAB ATTN AMSRL WT L D WOODBURY 2800 POWDER MILL RD ADELPHI MD 20783-1145
1	COMMANDER USA MICOM ATTN AMSMI RD W MCCORKLE REDSTONE ARSENAL AL 35898-5427
1	COMMANDER USA MICOM AMSMI RD ST P DOYLE REDSTONE ARSENAL AL 35898-5427
1	COMMANDER USA MICOM AMSMI RD ST CN T VANDIVER REDSTONE ARSENAL AL 35898-5427
1	COMMANDER USA MICOM AMSMI RD ST WF M COLE REDSTONE ARSENAL AL 35898-5427
2	DIRECTOR USARO MATH & COMP SCI DIV ATTN A CROWSON J CHANDRA PO BOX 12211 RESEARCH TRIANGLE PK NC 27709-2211
2	DIRECTOR USARO ENGRNG SCI DIV ATTN G ANDERSON R SINGLETON PO BOX 12211 RESEARCH TRIANGLE PK NC 27709-2211

NO. OF COPIES	ORGANIZATION
2	PROJECT MANAGER SADARM PICATINNY ARSENAL NJ 07806-5000
2	PM TMAS ATTN SFAE AR TMA COL BREGARD C KIMKER PICATINNY ARSENAL NJ 07806-5000
3	PM TMAS ATTN SFAE AR TMA MD H YUEN J MCGREEN R KOWALSKI PICATINNY ARSENAL NJ 07806-5000
2	PM TMAS ATTN SFAE AR TMA MS R JOINSON D GUZIEWICZ PICATINNY ARSENAL NJ 07806-5000
1	PM TMAS ATTN SFAE AR TMA MP W LANG PICATINNY ARSENAL NJ 07806-5000
2	PEO ARMAMENTS ATTN SFAE AR PM D ADAMS T MCWILLIAMS PICATINNY ARSENAL NJ 07806-5000
1	PEO FIELD ARTILLERY SYSTEMS ATTN SFAE FAS PM H GOLDMAN PICATINNY ARSENAL NJ 07806-5000
4	PM AFAS ATTN LTC D ELLIS G DELCOCO J SHIELDS B MACHAK PICATINNY ARSENAL NJ 07806-5000
2	COMMANDER ATTN WL FIV A MAYER WL MLBM S DONALDSON WRIGHT PATTERSON AFB DAYTON OH 45433

NO. OF COPIES	ORGANIZATION
2	NASA LANGLEY RSRCH CTR ATTN AMSRL VS W ELBER AMSRL VS S F BARTLETT JR MAIL STOP 266 HAMPTON VA 23681-0001
2	NSWC CODE G33 DAHLGREN VA 22448
1	OFC OF NAVAL RSRCH ATTN YAPA RAJAPAKSE MECH DIV CODE 1132SM ARLINGTON VA 22217
1	NAVAL ORDNANCE STATION ADV SYS TECH BR ATTN D HOLMES CODE 2011 LOUISVILLE KY 40214-5245
1	DAVID TAYLOR RSRCH CTR SHIP STRUCTURES & PROT DEPT ATTN J CORRADO CODE 1702 BETHESDA MD 20054-5000
2	DAVID TAYLOR RSRCH CTR ATTN R ROCKWELL W PHYILLAIER BETHESDA MD 20054-5000
5	DIRECTOR LLNL ATTN R CHRISTENSEN S DETERESA W FENG F MAGNESS M FINGER PO BOX 808 LIVERMORE CA 94550
1	DIRECTOR LANL ATTN D RABERN MEE 13 MAIL STOP J 576 PO BOX 1633 LOS ALAMOS NM 87545
10	NAVAL EOD TECH CTR ATTN CODE 6012A A PATEL (5 CPS) R GOLD (5 CPS) INDIAN HEAD MD 20640-5070

NO. OF COPIES	ORGANIZATION
1	OAK RIDGE NATL LAB ATTN R M DAVIS PO BOX 2008 OAK RIDGE TN 37831-6195
2	BATTELLE PNL ATTN M SMITH M C C BAMPTON PO BOX 999 RICHLAND WA 99352
6	DIRECTOR SANDIA NATL LABS ATTN C ROBINSON G BENEDETTI W KAWAHARA K PERANO D DAWSON P NIELAN PO BOX 969 LIVERMORE CA 94550-0096
1	PENNSYLVANIA STATE UNIV ATTN R MCNITT 227 HAMMOND BLDG UNIVERSITY PK PA 16802
1	SOUTHWEST RSRCH INSTITUTE ATTN C ANDERSON 6220 CULEBRA RD SAN ANTONIO TX 78284
1	UCLA MAND DEPT ENGRNG IV ATTN H THOMAS HAHN LOS ANGELES CA 90024-1597
2	UNIV OF DAYTON RSRCH INST ATTN RAN Y KIM AJIT K ROY 300 COLLEGE PARK AVE DAYTON OH 45469-0168
2	UNIV OF DELAWARE CTR FOR COMPOSITE MATLS ATTN J GILLESPE M SANTARE 201 SPENCER LABORATORY NEWARK DE 19716

NO. OF COPIES	ORGANIZATION
1	UNIV OF TEXAS AT AUSTIN CTR FOR ELECTROMECHANICS ATTN J PRICE 10100 BURNET RD AUSTIN TX 78758-4497
1	AAI CORPORATION ATTN TECH LIBRARY PO BOX 126 HUNT VALLEY MD 21030-0126
1	ARMTEC DEFENSE PRODUCTS ATTN S DYER PO BOX 848 COACHELLA CA 92236
3	ALLIANT TECHSYSTEMS INC ATTN J BODE C CANDLAND K WARD 5901 LINCOLN DR MINNEAPOLIS MN 55346-1674
2	ALLIANT TECHSYSTEMS INC ATTN T HOLMQUIST G R JOHNSON 600 SECOND ST NE HOPKINS MN 55343
1	BALLISTIC IMPACT DYNAMICS ATTN R RECHT 3650 S CHEROKEE 2 ENGLEWOOD CO 80110
1	CALIFORNIA RSRCH & TECH ATTN D ORPHAL 5117 JOHNSON DR PLEASANTON CA 94566
1	CHAMBERLAIN MFG CORP R&D DIV ATTN M TOWNSEND PO BOX 2545 WATERLOO IA 50704
1	COMPUTNL MECH ASSOC ATTN J A ZUKAS PO BOX 11314 BALTIMORE MD 21239-0314

NO. OF COPIES	ORGANIZATION
1	CUSTOM ANALYTICAL ENGRNG SYS INC ATTN A ALEXANDER STAR RTE BOX 4A FLINTSTONE MD 21530
1	GDLS DIV ATTN D BARTLE PO BOX 1901 WARREN MI 48090
1	IAP RSRCH INC ATTN A CHALLITA 2763 CULVER AVE DAYTON OH 45429
5	INSTITUTE FOR ADV TECH ATTN T KIEHNE H FAIR P SULLIVAN S BLESS R SUBRAMANIAN 4030 2 W BRAKER LN AUSTIN TX 78759
1	INTERFEROMETRICS INC ATTN R LARRIVA VP 8150 LEESBURG PK VIENNA VA 22100
3	KAMAN SCI CORP ATTN D ELDER T HAYDEN N ARI PO BOX 7463 COLORADO SPRINGS CO 80933
1	DR KENNEDY & ASSOC INC ATTN D KENNEDY PO BOX 4003 MOUNTAIN VIEW CA 94040
1	LIVERMORE SOFTWARE TECH CORP ATTN J O HALLQUIST 2876 WAVERLY WAY LIVERMORE CA 94550
2	LORAL VOUGHT SYS CORP ATTN G JACKSON K COOK 1701 W MARSHALL DR GRAND PRAIRIE TX 75051

NO. OF COPIES	ORGANIZATION
1	LORAL VOUGHT SYS CORP ATTN K HAVENS MS EM 36 PO BOX 650003 DALLAS TX 75265-0003
2	MARTIN MARIETTA CORP ATTN P DEWAR L SPONAR 230 E GODDARD BLVD KING OF PRUSSIA PA 19406
2	OLIN CORP FLINCHBAUGH DIV ATTN E STEINER B STEWART PO BOX 127 RED LION PA 17356
1	OLIN CORP ATTN L WHITMORE 10101 9TH ST N ST PETERSBURG FL 33702
2	UNIV OF MINNESOTA AHPCRC ATTN G SELL D AUSTIN 1100 WASHINGTON AVE S MINNEAPOLIS MN 55415

NO. OF COPIES	ORGANIZATION
	ABERDEEN PROVING GROUND
45	DIR, USARL ATTN: AMSRL-CI, C. MERMAGEN (394) W. STUREK (1121) AMSRL-CI-CB, R. KASTE (394) AMSRL-CI-S, A. MARK (309) AMSRL-SL-B, P. DIETZ (328) AMSRL-SL-BA, J. WALBERT (1068) AMSRL-SL-BL, D. BELY (328) AMSRL-SL-I, D. HASKILL (1065) AMSRL-WT-P, A. HORST (390A) AMSRL-WT-PA, T. MINOR (390) C. LEVERITT (390) D. KOOKER (390A) AMSRL-WT-PB, E. SCHMIDT (120) P. PLOSTINS (120) AMSRL-WT-PC, R. FIFER (390A) AMSRL-WT-PD, B. BURNS (390) W. DRYSDALE (390) T. BOGETTI (390) J. BENDER (390) R. MURRAY (390) AMSRL-WT-PD, R. KIRKENDALL (390) T. ERLINE (390) D. HOPKINS (390) S. WILKERSON (390) D. HENRY (390) R. KASTE (390) L. BURTON (390) J. TZENG (390) R. LIEB (390) G. GAZONAS (390) (5 CPS) M. LEADORE (390) AMSRL-WT-PD-ALC, A. ABRAHAMIAN K. BARNES M. BERMAN H. DAVISON A. FRYDMAN T. LI W. MCINTOSH E. SZYMANSKI AMSRL-WT-T, W. MORRISON (309) T. WRIGHT (309)

NO. OF COPIES	ORGANIZATION
52	DIR, USARL ATTN: AMSRL-WT-TA, W. GILLICH (390) W. BRUCHEY (390) J. DEHN (390) AMSRL-WT-TB, K. BENJAMIN (309) T. DORSEY (309) R. FREY (309) F. GREGORY (309) W. HILLSTROM (309) W. LAWRENCE (309) O. LYMAN (1185) J. STARKENBERG (309) L. VANDE KIEFT (309) J. WATSON (309) V. BOYLE (309) S. STEGALL (1185) AMSRL-WT-TC, K. KIMSEY (309) R. COATES (309) W. DE ROSSET (309) F. GRACE (309) M. LAMPSON (309) D. SCHEFFLER (309) AMSRL-WT-TC, B. SORENSEN (309) R. SUMMERS (309) E. WALKER (309) W. WALTERS (309) AMSRL-WT-TD, D. DIETRICH (309) G. RANDERS-PEHRSON (309) J. HUFFINGTON (309) A. DAS GUPTA (309) J. SANTIAGO (309) K. FRANK J. HARRISON M. SCHEIDLER S. SEGLETES (5 CPS) J. WALTER C. PAXTON (5 CPS) J. GARDINER AMSRL-WT-NC, R. LOTTERO (309) R. PEARSON (309) S. SCHRAML (309) AMSRL-WT-W, C. MURPHY (120) AMSRL-WT-WA, H. ROGERS (394) B. MOORE (394) A. BARAN (394)

NO. OF COPIES	ORGANIZATION
8	DIR, USARL ATTN: AMSRL-WT-WB, F. BRANDON (120) W. D'AMICO (120) AMSRL-WT-WC, J. ROCCHIO (120) AMSRL-WT-WD, A. ZIELINSKI (120) J. POWELL (120) A. PRAKASH (120) AMSRL-WT-WE, J. TEMPERLEY (120) J. THOMAS (394)
7	DIR, USARL ATTN: AMSRL-MA-P L. JOHNSON T. CHOU C. WHITE J. MCLAUGHLIN AMSRL-MA-PA D. GRANVILLE W. HASKELL AMSRL-MA-MA, G. HAGNAUER

USER EVALUATION SHEET/CHANGE OF ADDRESS

This Laboratory undertakes a continuing effort to improve the quality of the reports it publishes. Your comments/answers to the items/questions below will aid us in our efforts.

1. ARL Report Number ARL-TR-976 Date of Report March 1996

2. Date Report Received ______

3. Does this report satisfy a need? (Comment on purpose, related project, or other area of interest for which the report will be used.) ______

4. Specifically, how is the report being used? (Information source, design data, procedure, source of ideas, etc.) ______

5. Has the information in this report led to any quantitative savings as far as man-hours or dollars saved, operating costs avoided, or efficiencies achieved, etc? If so, please elaborate. ______

6. General Comments. What do you think should be changed to improve future reports? (Indicate changes to organization, technical content, format, etc.) ______

CURRENT ADDRESS

Organization

Name

Street or P.O. Box No.

City, State, Zip Code

7. If indicating a Change of Address or Address Correction, please provide the Current or Correct address above and the Old or Incorrect address below.

OLD ADDRESS

Organization

Name

Street or P.O. Box No.

City, State, Zip Code

(Remove this sheet, fold as indicated, tape closed, and mail.)

(DO NOT STAPLE)

DEPARTMENT OF THE ARMY

OFFICIAL BUSINESS

NO POSTAGE NECESSARY IF MAILED IN THE UNITED STATES

BUSINESS REPLY MAIL

FIRST CLASS PERMIT NO 0001,APG,MD

POSTAGE WILL BE PAID BY ADDRESSEE

DIRECTOR
U.S. ARMY RESEARCH LABORATORY
ATTN: AMSRL-WT-PD
ABERDEEN PROVING GROUND, MD 21005-5066